

ON TWO SPECIAL RIVLIN-ERICKSEN FLUID MODELS  
GENERALIZING GLEN'S FLOW LAW FOR POLYCRYSTALLINE ICE

BY

QUAN-XIN SUN

A Dissertation

Presented to The University of Manitoba  
in Partial Fulfillment of the Requirements  
for the Degree of Doctor of Philosophy

Winnipeg, Manitoba, Canada

1987



Permission has been granted to the National Library of Canada to microfilm this thesis and to lend or sell copies of the film.

The author (copyright owner) has reserved other publication rights, and neither the thesis nor extensive extracts from it may be printed or otherwise reproduced without his/her written permission.

L'autorisation a été accordée à la Bibliothèque nationale du Canada de microfilmer cette thèse et de prêter ou de vendre des exemplaires du film.

L'auteur (titulaire du droit d'auteur) se réserve les autres droits de publication; ni la thèse ni de longs extraits de celle-ci ne doivent être imprimés ou autrement reproduits sans son autorisation écrite.

ISBN 0-315-37412-8

ON TWO SPECIAL RIVLIN-ERICKSEN FLUID MODELS  
GENERALIZING GLEN'S FLOW LAW FOR POLYCRYSTALLINE ICE

BY

QUAN-XIN SUN

A thesis submitted to the Faculty of Graduate Studies of  
the University of Manitoba in partial fulfillment of the requirements  
of the degree of

DOCTOR OF PHILOSOPHY

© 1987

Permission has been granted to the LIBRARY OF THE UNIVER-  
SITY OF MANITOBA to lend or sell copies of this thesis, to  
the NATIONAL LIBRARY OF CANADA to microfilm this  
thesis and to lend or sell copies of the film, and UNIVERSITY  
MICROFILMS to publish an abstract of this thesis.

The author reserves other publication rights, and neither the  
thesis nor extensive extracts from it may be printed or other-  
wise reproduced without the author's written permission.

**CONTENTS**

=====

ABSTRACT.....(1)

ACKNOWLEDGMENTS.....(3)

**CHAPTER 1 Introduction**

- 1.1 A review of some constitutive relations for creep of polycrystalline ice.....(4)
- 1.2 Two special Rivlin-Ericksen fluid models.....(7)

**CHAPTER 2 Constitutive restrictions on the two models**

- 2.1 Introduction.....(12)
- 2.2 Effect of the exponent  $m$  on the regularity of solution of steady isothermal channel-flow.....(15)
- 2.3 Thermodynamic restrictions.....(22)
- 2.4 Cannister flows for models compatible with thermodynamics: stability implies asymptotic stability...(35)
- 2.5 What happens if  $\alpha_1 < 0$  ? Some consequences.....(42)

**CHAPTER 3 Evaluation of material parameters by fitting creep data of pressuremeter tests**

- 3.1 Initial-boundary value problem pertaining to pressuremeter tests.....(48)
- 3.2 Effect of the material parameters on the predicted creep rate.....(55)
- 3.3 Evaluation of the material parameters  $\mu$  and  $m$  by fitting data of secondary creep.....(63)
- 3.4 Evaluation of the material parameter  $\alpha_1$  by fitting data of primary creep.....(69)
- 3.5 Discussion.....(75)  
Tables and figures.....(79)

**CHAPTER 4 Evaluation of material parameters by fitting data of triaxial tests**

- 4.1 Initial-value problem pertaining to triaxial tests.....(89)
- 4.2 Evaluation of material parameters.....(95)  
Tables and figures.....(104)

CHAPTER 5 Evaluation of material parameters by fitting  
short-term creep data of pressuremeter tests

5.1 Introduction.....(109)  
5.2 Evaluation of material parameters by fitting  
short-term data of a single-stage creep test.....(112)  
5.3 Evaluation of material parameters by simultaneously  
fitting short-term data of two single-stage  
creep tests.....(117)  
Tables and figures.....(120)

CHAPTER 6 Applications of the two models

6.1 Application to glacier flows.....(127)  
6.2 Heat and mass transfer in a pipe.....(133)

CONCLUSION.....(140)

APPENDICES

A.1 Least squares fitting with constraints.....(142)  
A.2 Nonlinear least squares optimization by the  
Levenberg-Marquardt method.....(145)  
A.3 Procedure of fitting creep data of ice by nonlinear  
optimization.....(148)

REFERENCES.....(152)

PROGRAMS

MUM: Evaluation of  $\mu$  and  $m$  by fitting the secondary  
creep data of pressuremeter tests.....(157)  
ALPHA1: Evaluation of  $\alpha_1$  for model (I) by fitting  
primary creep data of pressuremeter tests  
with  $\mu$  and  $m$  fixed.....(160)  
X31: Evaluation of  $\mu$ ,  $\alpha_1$  and  $m$  for model (I) by  
fitting creep data of triaxial tests.....(167)

**ABSTRACT**

The main objective of this dissertation is to study whether the constitutive models proposed by Man, namely (I) "the modified second-order fluid" and (II) "the power-law fluid of grade 2", are applicable for describing the creeping flow of polycrystalline ice. Both models (I) and (II) are the special instances of Rivlin-Ericksen fluids of complexity 2, and both of them can be regarded as simple generalization of Glen's flow law. Since the models are meant only for the slow creeping flow of ice, they are supposed to have constitutive domains for which the first Rivlin-Ericksen tensor  $A_1$  and its material derivative are restricted to some neighbourhoods of  $0$  in  $\text{Sym}_0$ , the space of symmetric tensors with zero trace.

To see whether the two models can represent empirical data, they are employed to fit the experimental data of pressuremeter and triaxial creep tests provided by Kjartanson and Jones, respectively. The nonlinear second-order ordinary differential equations which govern the creeping flows of specimens in pressuremeter and triaxial tests are derived for both models (I) and (II). These creep equations contain unknown material parameters which pertain to the specimens. By drawing on what is known about Glen's flow law and after a sensitivity analysis, a fitting procedure is worked out to estimate the values of the material parameters from the available data for the

pressuremeter and the triaxial tests, respectively. The procedure includes an iterative least-squares fitting scheme using the Levenberg-Marquardt algorithm; at each iteration the creep equation in question is solved numerically by using the fifth-order Runge-Kutter-Nyström method. While both models give good fits to the data of Kjartanson and Jones, model (II) is found to give consistently better fits to the pressuremeter data.

Constitutive restrictions imposed by thermodynamics (i.e., the Clausius-Duhem inequality) are derived for both models (I) and (II) under the assumptions that the free energy assumes a minimum value at the rest state and is a convex function of  $\mathbf{A}_1$  in a neighbourhood of  $\mathbf{0}$  in  $\text{Sym}_0$ . The restrictions on the material coefficients are consistent with the numerical values obtained by fitting data of the pressuremeter and the triaxial creep tests. Some stability problems related to cannister flows and triaxial homogeneous motions are discussed, both for models which obey the thermodynamic restrictions and for models which violate them.

Some possible applications of the models are also discussed. Among them are: (i) flows of glaciers, (ii) heat and mass transfer in a pipe, (iii) a preliminary investigation on devising a short-term in-situ pressuremeter test which will deliver the material parameters of polycrystalline ice in models (I) and (II).

## ACKNOWLEDGMENTS

3

I wish to thank all those who helped me through this work. I am particularly grateful to Dr. Chi-Sing Man, my advisor of the dissertation, for his guidance, encouragement and support of my study. It would be impossible for me to complete this work without his help. I thank Dr. H. Cohen, Dr. E.V. Wilms and Dr. P.N. Shivakumar, who are the members of my dissertation examining committee. I am grateful to Dr. R. L. Fosdick, who is the external examiner of my dissertation. I am obliged to Drs. S.J. Jones and B. Kjartanson, who provided me with data of triaxial and pressuremeter tests, respectively. I also wish to express my gratitude to Dr. T.T. Loo, who kindly led me into the field of applied mechanics.

My wife Ching-Mei and daughter Tina have spent endless hours on their own. They deserve my gratitude.

Part of this work was supported by a graduate studies fellowship of The University of Manitoba, Canada.

Q.-X. Sun

## CHAPTER 1 Introduction

### Section 1.1 A brief review of some constitutive relations for creep of polycrystalline ice

Ice, as a natural substance, is widely distributed over cold regions of the world. In particular, it is significant to reveal the mechanical properties of ice for establishment of foundation of structures, development of natural resources at cold regions, prediction of motion of glaciers and icebergs, and treatment of ice sheets on the sea and lakes. It is recognized from observation (Michel, 1978; Hutter, 1983) that any ice body is composed of ice crystals which appear in the form of hexagonal structures and have anisotropic mechanical properties. But when an ice body contains a great deal of randomly oriented ice crystals, we could approximately regard it as a material which has isotropic mechanical properties. Such an ice body is usually called polycrystalline. In this dissertation, we shall be mainly concerned with the creep behaviour of homogeneous bodies of polycrystalline ice for the reason that many ice problems involve phenomenon of creep (for instance, flow of glaciers and settlement of foundations).

An often used simple equation that describes polycrystalline ice in uniaxial creep is

$$\dot{\epsilon} = b\sigma^n \quad (1.1.1)$$

(cf. Glen, 1952, 1955); here  $\epsilon$  is the uniaxial engineering strain,  $\sigma$  is the uniaxial stress,  $b$  and  $n$  are material coefficients. Equation (1.1.1) is usually called Glen's flow law. Nye (1952, 1957) generalized Glen's flow law to a full constitutive equation. Nye's generalization is usually called "the generalized flow law" (Paterson, 1981, p. 30); it in effect models ice as an incompressible power-law fluid (Bird and others, 1977, p.208). But since the thirties, (1.1.1) and the power-law fluid model have been used in metallurgy to describe metals at high temperatures (Norton, 1929; Odqvist, 1966). In the current literature, Glen's flow law is often expressed in the form

$$\dot{\xi} = (\tau/B)^n, \quad (1.1.2)$$

where

$$\dot{\xi} \equiv (\text{tr}D^2/3)^{1/2}, \quad \tau \equiv [\text{tr}(\mathbf{T}')^2/3]^{1/2} \quad (1.1.3)$$

are the octahedral strain rate and shear stress, respectively;  $D$  is the stretching tensor,  $\mathbf{T}'$  is the deviator of the Cauchy stress tensor  $\mathbf{T}$  (Hooke, 1981). It is well known from tests in laboratory and measurements in glacier that Glen's flow law and its generalization by Nye are adequate for describing the secondary (i.e. steady) creep of

polycrystalline ice (Hooke, 1981; Mellor & Cole, 1983; Ashby, 1985). For instance, it will be shown in Sec. 6.1 that the velocity profile in shearing flows predicted by the power-law fluid model is corroborated by measurements in glaciers. But this model cannot describe the primary creep of ice. Besides, it fails to show any normal stress effect in shear flows. After noticing the preceding defects of Glen's flow law, McTigue and others (1985) suggested to use the second-order fluid model as a constitutive relation for the creep of polycrystalline ice. However, the second-order fluid model has its own two shortcomings, namely, inability to describe adequately the secondary creep of ice and to show the appropriate velocity profile in the shearing flow of glaciers. For details, see Secs.5.3 and 6.1 below, and Man & Sun (1986). It is interesting to notice that the merits of Glen's flow law may just be used to remedy the defects of the second order fluid model, and vice versa.

In the literature there are also many other constitutive relations proposed for creep of polycrystalline ice, which mostly are empirical or semi-empirical, (cf. Szyzekewski & Glockner, 1985; Spring & Morland, 1983; Hutter, 1983). In what follows, however, we shall concentrate on two special Rivlin-Ericksen fluid models to be introduced in the next section.

## Section 1.2 Two special Rivlin-Ericksen fluid models

Man (1984) has proposed the following two constitutive relations for the creep of polycrystalline ice:

$$(I) \quad \mathbf{T} + p\mathbf{I} = \mu\mathbb{I}\mathbf{A}_1 + \alpha_1\mathbf{A}_2 + \alpha_2\mathbf{A}_1^{\otimes 2}, \quad (1.2.1)$$

$$(II) \quad \mathbf{T} + p\mathbf{I} = \mathbb{I}(\mu\mathbf{A}_1 + \alpha_1\mathbf{A}_2 + \alpha_2\mathbf{A}_1^{\otimes 2}), \quad (1.2.2)$$

$$\text{where } \text{tr}\mathbf{A}_1 = 0, \quad (1.2.3)$$

$$\mathbb{I} = (\text{tr}\mathbf{A}_1^{\otimes 2}/2)^{m/2}. \quad (1.2.4)$$

Here (1.2.3) indicates the incompressibility of ice;  $\mathbf{T}$  is the Cauchy stress tensor;  $-p\mathbf{I}$  is the indeterminate spherical stress due to incompressibility,  $\mu$ ,  $\alpha_1$ ,  $\alpha_2$  and  $m$  are material parameters which in general depend on the material point and the temperature;  $\mathbf{A}_1$  and  $\mathbf{A}_2$  are the first and second Rivlin-Ericksen tensors defined through the rate of the relative right Cauchy-Green tensor  $\mathbf{C}_t(\tau)$  (Truesdell and Noll, 1965):

$$\mathbf{A}_i = d^i \mathbf{C}_t(\tau) / d\tau^i \Big|_{\tau=t}, \quad i=1,2,\dots \quad (1.2.5)$$

It is more convenient to calculate these kinematic tensors by the recursion formulae

$$\begin{aligned}
 \mathbf{A}_1 &= \mathbf{L} + \mathbf{L}^T, \\
 &\dots\dots\dots, \\
 \mathbf{A}_i &= \dot{\mathbf{A}}_{i-1} + \mathbf{A}_{i-1}\mathbf{L} + \mathbf{L}^T\mathbf{A}_{i-1}, \quad (1.2.6)
 \end{aligned}$$

where  $\mathbf{L} = \nabla\mathbf{v}$  is the special velocity gradient. When  $m = 0$ , both (1.2.1) and (1.2.2) are reduced to the second-order fluid model:

$$\mathbf{T} + p\mathbf{I} = \mu\mathbf{A}_1 + \alpha_1\mathbf{A}_2 + \alpha_2\mathbf{A}_1^2. \quad (1.2.7)$$

When  $\alpha_1 = \alpha_2 = 0$ , both (1.2.1) and (1.2.2) become the power-law fluid model:

$$\mathbf{T} + p\mathbf{I} = \mu\|\mathbf{A}_1\|. \quad (1.2.8)$$

Moreover, it can be shown from (1.1.2) and (1.1.3) that (1.2.8) is consistent with (1.1.2), i.e. Glen's flow law, if

$$B = 2(6)^{m/2}\mu, \quad n = 1/(1 + m). \quad (1.2.9)$$

Hence models (I) and (II) can be taken as modifications of Glen's flow law and the second-order fluid model.

The well-known Rivlin-Ericksen constitutive relation may be considered as the theoretical background of models (I) and (II). A fluid of the differential type and

complexity  $n$  is defined by the constitutive relation:

$$\mathbf{T} = \mathbf{T}(\mathbf{A}_1, \mathbf{A}_2, \dots, \mathbf{A}_n), \quad (1.2.10)$$

where  $\mathbf{T}$  is an isotropic function of  $\mathbf{A}_i$ ,  $i=1, 2, \dots, n$ . By using

the principle of material frame-indifference and matrix theory, Rivlin and Ericksen (1955) have derived an explicit representation of (1.2.10):

$$\begin{aligned} \mathbf{T} = & \phi_1 \mathbf{I} + \phi_2 \mathbf{A}_1 + \phi_3 \mathbf{A}_2 + \phi_4 \mathbf{A}_1^{\otimes 2} + \phi_5 \mathbf{A}_2^{\otimes 2} + \phi_6 (\mathbf{A}_1 \mathbf{A}_2 + \mathbf{A}_2 \mathbf{A}_1) + \\ & \phi_7 (\mathbf{A}_1^{\otimes 2} \mathbf{A}_2 + \mathbf{A}_2 \mathbf{A}_1^{\otimes 2}) + \phi_8 (\mathbf{A}_2^{\otimes 2} \mathbf{A}_1 + \mathbf{A}_1 \mathbf{A}_2^{\otimes 2}) + \phi_9 \mathbf{A}_3 + \phi_{10} (\mathbf{A}_2 \mathbf{A}_3 + \mathbf{A}_3 \mathbf{A}_2), \end{aligned} \quad (1.2.11)$$

where  $\phi_1$  to  $\phi_{10}$  are functions of the invariants of  $\mathbf{A}_1, \mathbf{A}_2, \dots, \mathbf{A}_n$ . It is easy to see that models (I) and (II) are special instances of incompressible Rivlin-Ericksen fluids of complexity 2.

In principle, the Rivlin-Ericksen model (1.2.10) might be used to describe any motion of the fluids, since there is no restriction on the magnitudes of  $\mathbf{A}_1, \mathbf{A}_2, \dots, \mathbf{A}_n$ . On the other hand, models (I) and (II) may possibly be suitable only for the description of slow motions of fluids because they could be regarded as approximations of (1.2.11) by omitting higher order terms which are small in slow motions. Nevertheless, considering the fact that the Newtonian fluid

model which is also a specification of (1.2.11) can be used to describe fast motions of some fluids, one may apply models (I) and (II) as exact models for any motion of some fluids. For simplicity, we shall call the classes of fluids characterized by models (I) and (II) as fluids (I) and (II).

In chapter 2, we shall deal with the dynamic and thermodynamic constitutive restrictions on models (I) and (II), basing on the requirements that the boundedness of stresses, smoothness of velocity and compatibility with thermodynamics, in the case of slow motion. We shall show that cannister flows of fluids (I) and (II) are asymptotically stable when (I) and (II) are compatible with thermodynamic restrictions and if  $A_1$  remains in a neighbourhood of 0. But I find that cannister flows and triaxial homogeneous motion of fluids (I) and (II) are not asymptotically stable if  $\alpha_1 < 0$ , i.e., if  $\alpha_1$  assumes a sign that violates thermodynamics.

In chapters 3 to 5, we shall use fluids (I) and (II) to fit the creep data of polycrystalline ice measured from pressuremeter and triaxial tests. It will be seen that the fits are very satisfactory for both the primary and secondary creep of the two kinds of tests. In particular, the positive value of the material parameter  $\alpha_1$ , obtained from the fits, gives a strong and important support to the conclusion of thermodynamic restrictions on the two models. Thus polycrystalline ice may be considered as the first

material which is in the class of Rivlin-Ericksen fluid model with positive  $\alpha_1$ .

## CHAPTER 2 Constitutive restrictions on the two models

### Section 2.1 Introduction

Controversy about the characteristics of the second-order (or second grade) fluid model, especially about the sign of  $\alpha_1$  has lasted about 20 years. Coleman & Markovitz (1964) asserted that the sign of  $\alpha_1$  should be negative according to experiments on polymers if they were assumed to be second-order fluids. Truesdell (1965) supported a negative  $\alpha_1$ ; he drew on arguments which regarded second-order fluids as fluids of convected elasticity. But Coleman, Duffin & Mizel (1965) and Coleman & Mizel (1966) showed the unboundedness of nontrivial solution in shearing flows of second order fluids with  $\alpha_1 < 0$ . Several years ago, Joseph (1981) concluded by using Lyapounov theory about stability that the rest state of an  $n$ -th grade ( $n > 1$ ) fluid is unstable if the ratio of the coefficients of the  $n$ -1th and the  $n$ -th Rivlin-Ericksen kinematic tensors (1.2.5) is negative (in particular, for  $n = 2$ ,  $\mu \geq 0$  and  $\alpha_1 < 0$ ). When applying thermodynamics to finding the constitutive restrictions on the second and third grade fluids, Dunn & Fosdick (1974), and Fosdick & Rajagopal (1980) concluded that  $\alpha_1$  must be non-negative if those fluids are compatible with thermodynamics. Besides, Dunn & Fosdick (1974) showed that the Cauchy stress of fluids with convected elasticity

must only be spherical and hence there is no basis for Truesdell's results for second order fluids with  $\alpha_1 < 0$ . Dunn & Fosdick (1974) also denied the possibility that the polymers studied by Coleman & Markovitz (1964) and others belong to the class of second order fluids.

In this chapter we shall show in Sec. 2.2 that the exponent  $m$  of fluids (I) and (II) must obey  $m > -1$  to satisfy the requirement of smoothness of stress, through an example of shearing flow between two fixed infinite parallel planes. We shall also prove that a unique weak solution exists for the problem of steady shearing flow between two fixed infinite parallel planes.

In Sec. 2.3, we shall investigate the thermodynamic restrictions on fluids (I) and (II) for slow motion of the fluids. With an attitude different from Dunn & Fosdick (1974) and Fosdick & Rajagopal (1980), we shall not allow the kinematic tensors in the response functions to assume arbitrary values because we require the models to be valid only for slow motion of the fluids. Our analysis will also be based on the Clausius-Duhem inequality and on the assumption that the Helmholtz free energy be convex with respect to  $A_1$  in a neighbourhood of  $A_1 = 0$  and be a minimum at the rest state. It will be found that a necessary condition for compatibility with thermodynamics is  $\alpha_1 \geq 0$ .

In Sec. 2.4 we shall show that for cannister flows of fluids which satisfy the thermodynamic restrictions,

stability of the rest state implies its asymptotic stability. In Sec. 2.5 we shall study some consequences that the inequality  $\alpha_1 < 0$  would entail in cannister flows and triaxial homogeneous motions of fluids which violate the thermodynamic restriction  $\alpha_1 \geq 0$ .

Section 2.2 Effect of the exponent  $m$  on the regularity  
of solution of steady isothermal  
channel-flow

In this section, an existence and uniqueness theorem for steady isothermal channel-flow of fluids (I) and (II) will be proved. Moreover, it will be shown that smoothness of the solution depends on the value of the exponent  $m$ .

Consider an (possibly unsteady) isothermal shearing flow between two fixed, infinite and parallel planes which are at a distance  $2h$  from each other. Choose a Cartesian coordinate system  $(x, y, z)$  such that the two infinite planes are at  $x = -h$  and  $x = h$ , respectively. Consider flows in which the velocity has the form:

$$\mathbf{v} = (0, v(x, t), 0). \quad (2.2.1)$$

In what follows, it is assumed that during the flow the fluid in question adheres to the walls of the channel, i.e.,  $v(\pm h, t) = 0$ .

Let  $\mathbf{e}_1$ ,  $\mathbf{e}_2$  and  $\mathbf{e}_3$  be the unit base vectors of the chosen Cartesian coordinate system, and let

$$K \equiv \partial v / \partial x \quad (2.2.2)$$

be the shear rate. It can be easily shown that in a channel

flow,

$$\dot{\kappa} = \partial \kappa / \partial t,$$

$$\mathbf{L} = \kappa \mathbf{e}_x \otimes \mathbf{e}_1,$$

$$\mathbf{A}_1 = \kappa (\mathbf{e}_1 \otimes \mathbf{e}_x + \mathbf{e}_x \otimes \mathbf{e}_1),$$

$$\mathbf{A}_x = 2\kappa^2 \mathbf{e}_1 \otimes \mathbf{e}_1 + \dot{\kappa} (\mathbf{e}_1 \otimes \mathbf{e}_x + \mathbf{e}_x \otimes \mathbf{e}_1), \quad (2.2.3)$$

$$\mathbf{A}_1^x = \kappa^2 (\mathbf{e}_1 \otimes \mathbf{e}_1 + \mathbf{e}_x \otimes \mathbf{e}_x),$$

$$\Pi = |\kappa|^m,$$

where  $|\kappa|$  is the absolute value of  $\kappa$  and  $\otimes$  denotes the tensor product of vectors. It is obvious from (2.2.3) that the condition of incompressibility  $\text{tr} \mathbf{A}_1 = 0$  is automatically satisfied in the shear flows. By substituting (2.2.2) and (2.2.3) into (1.2.1) and (1.2.2), the stress tensor may be specified as:

$$\begin{aligned} \text{(I)} \quad \mathbf{T} = & -p\mathbf{I} + (\mu |\kappa|^m \kappa + \alpha_1 \kappa_t) (\mathbf{e}_1 \otimes \mathbf{e}_x + \mathbf{e}_x \otimes \mathbf{e}_1) \\ & + (2\alpha_1 + \alpha_2) \kappa^2 \mathbf{e}_1 \otimes \mathbf{e}_1 + \alpha_2 \kappa^2 \mathbf{e}_x \otimes \mathbf{e}_x, \end{aligned} \quad (2.2.4)$$

$$\begin{aligned} \text{(II)} \quad \mathbf{T} = & -p\mathbf{I} + (\mu |\kappa|^m \kappa + \alpha_1 (|\kappa|^m \kappa)_t / (1+m)) (\mathbf{e}_1 \otimes \mathbf{e}_x + \mathbf{e}_x \otimes \mathbf{e}_1) \\ & + |\kappa|^m [(2\alpha_1 + \alpha_2) \kappa^2 \mathbf{e}_1 \otimes \mathbf{e}_1 + \alpha_2 \kappa^2 \mathbf{e}_x \otimes \mathbf{e}_x], \end{aligned}$$

where the subscript  $t$  denotes partial derivative w.r.t. the

time  $t$ .

Suppose at the instant  $t$  the velocity field satisfies:

$$v(\cdot, t) \in C^1([-h, h]); \quad \partial v(\cdot, t)/\partial x \in C^0((-h, h)).$$

Then by Rolle's theorem there exists a point  $\xi$  in  $(-h, h)$  such that

$$K(\xi, t) = 0. \quad (2.2.5)$$

A glance at (2.2.4) reveals that the extra stress  $T+pI$  will be undefined at  $\xi$  if  $m \leq -1$ . Henceforth, it will be assumed that  $m > -1$ .

Let us now restrict our attention to steady isothermal flows for which the body force is null. By substituting (2.2.4) into the balance equation of linear momentum, we obtain the following equations of motion:

$$\begin{aligned} \text{(I)} \quad & -\partial p/\partial x + (2\alpha_1 + \alpha_2)\partial K^2/\partial x = 0, \\ & -\partial p/\partial y + \mu\partial(|K|^m K)/\partial x = 0, \\ & -\partial p/\partial z = 0; \end{aligned} \quad (2.2.6)$$

$$\begin{aligned} \text{(II)} \quad & -\partial p/\partial x + (2\alpha_1 + \alpha_2)\partial(|K|^{2+m})/\partial x = 0, \\ & -\partial p/\partial y + \mu\partial(|K|^m K)/\partial x = 0, \\ & -\partial p/\partial z = 0. \end{aligned} \quad (2.2.7)$$

It can be easily deduced from (2.2.6) and (2.2.7) that for fluids (I) and (II),

$$\partial p / \partial y = C, \quad (2.2.8)$$

where  $C$  is a constant measuring the pressure gradient in the direction of flow. Without loss of generality, let  $C \leq 0$ . It follows from (2.2.6)\* and (2.2.7)\*, respectively, that for fluids (I) and (II) the velocity field  $v$  should satisfy the following boundary value problem:

$$\begin{aligned} d[|\partial v / \partial x|^m \partial v / \partial x] / dx &= C / \mu, \\ v(\pm h) &= 0, \end{aligned} \quad (2.2.9)$$

where  $C \leq 0$  and  $\mu \geq 0$ . Let us proceed to prove an existence and uniqueness theorem for (2.2.9).

Define  $I \equiv (-h, h)$ . Let  $L^2(I)$  denote the space of square (Lebesgue) integrable functions defined on  $I$ . Let  $H^k(I) \in L^2(I)$  be the Sobolev space of functions whose  $k$  weak derivatives are also in  $L^2(I)$ .  $H^k(I)$  is a Hilbert space under the inner product

$$\langle u, w \rangle \equiv \int_{-h}^h \left( \sum_{i=0}^k u^{(i)} w^{(i)} \right) dx,$$

where  $u^{(i)}$  and  $w^{(i)}$  denote the  $i$ -th weak derivative of  $u$  and

w, respectively. Since the elements of  $H^1(I)$  are in fact absolutely continuous, the subspace

$$H_0^1 \equiv \{ u \in H^1(I) \mid u(\pm h) = 0 \}$$

is well defined. By a weak solution of the boundary value problem (2.2.9), I mean a function in  $H^2(I) \cap H_0^1(I)$  which satisfies

$$\int_{-h}^h |dv/dx|^m (dv/dx)(d\phi/dx) dx = -C \int_{-h}^h \phi dx / \mu \quad \text{for all } \phi \in H_0^1(I). \quad (2.2.10)$$

The preceding equation makes sense because  $dv/dx$  is absolutely continuous on  $[-h, h]$  and  $d\phi/dx$  is in  $L^2(I)$ .

In the proof of existence and uniqueness of weak solution  $v$  for (2.2.9), the following simple mathematical lemma will be applied.

LEMMA 2.2.1 For any real numbers  $a$  and  $b$ , and for any  $m > 1$ ,

$$(|a|^m - |b|^m)(a - b) \geq 0.$$

Equality holds if and only if  $a = b$ .

Proof: This lemma follows easily from the inequality

$$(1 - |r|^m)(1 - r) \geq 0 \quad \text{for } |r| \leq 1.$$

THEOREM 2.2.2 Let  $m > -1$ . There is a unique weak solution of (2.2.9), which satisfies (2.2.10).

Proof: At first construct a solution of (2.2.10). Consider the boundary-value problem

$$d(w')^{m+1}/dx = C/\mu, \quad w'(0) = w(h) = 0.$$

Its solution is

$$w(x) = \frac{m+2}{m+1} (-C/\mu)^{1/(m+1)} h^{(m+2)/(m+1)} (1 - (x/h)^{(m+2)/(m+1)}), \quad (2.2.11)$$

where  $0 \leq x \leq h$ . Now, define a function  $v$  on  $[-h, h]$  as follows:  $v(x) = w(x)$ , if  $0 \leq x \leq h$ ;  $v(x) = w(-x)$ , if  $-h \leq x \leq 0$ . Explicitly,

$$v(x) = \frac{m+2}{m+1} (-C/\mu)^{1/(m+1)} h^{(m+2)/(m+1)} (1 - (|x|/h)^{(m+2)/(m+1)}). \quad (2.2.12)$$

The function  $v$  is even, and its derivative is

$$v'(x) = -(-C/\mu)^{1/(m+1)} |x|^{-m/(m+1)} x. \quad (2.2.13)$$

It is clear that both  $v$  and  $v'$  are in  $L^2(I)$  and  $v$  satisfies (2.2.9) and (2.2.10).

Suppose  $v_1$  and  $v_2$  are two solutions of (2.2.10). Then

$$\int_{-h}^h (|v_1'|^m v_1' - |v_2'|^m v_2') \phi' dx = 0, \text{ for all } \phi \text{ in } H_0^1(I). \quad (2.2.14)$$

Let  $\phi = v_1 - v_2$ . It follows from (2.2.14) that

$$\int_{-h}^h (|v_1'|^m v_1' - |v_2'|^m v_2') (v_1' - v_2') dx = 0. \quad (2.2.15)$$

Lemma 2.2.1 implies that  $v_1' = v_2'$  almost everywhere on  $[-h, h]$ . It follows from the boundary conditions and continuity of the function that  $v_1 = v_2$ .

Remark: It is clear from (2.2.12) and (2.2.13) that the solution  $v$  is of class  $C^1(I)$  for any  $m > -1$ . For  $0 \leq m > -1$ ,  $v$  is of class  $C^n$ , where  $n$  is the largest integer such that  $n \leq 1/(m+1)$ . Thence  $v$  is at least of class  $C^2$  if  $0 \leq m > -1$ . For  $m > 0$ , however,  $v$  will not be of class  $C^2$  because  $v'' \rightarrow +\infty$  as  $x \rightarrow 0$ . In other words for  $m > 0$ , the boundary-value problem (2.2.9) does not admit a classical solution (by which I mean a solution of class  $C^2$ ).

### Section 2.3 Thermodynamic restrictions

Before the detailed discussion, let us introduce some notions and preliminaries which will be used throughout the remaining sections of this chapter.

$\mathbb{R}$ : the set of all real numbers;

$\mathbb{V}$ : the translation space of the three dimensional Euclidean space;

$\text{Lin}$ : the set of all linear transformations from  $\mathbb{V}$  to  $\mathbb{V}$ ;

$\text{Sym} \equiv \{ T \in \text{Lin} \mid T^T = T \}$ ;

$\text{Lin}_0 \equiv \{ T \in \text{Lin} \mid \text{tr}T = 0 \}$ ;

$\text{Sym}_0 \equiv \text{Sym} \cap \text{Lin}_0$ ;

$A \cdot B \equiv \text{tr}(AB^T)$ ,  $A, B \in \text{Lin}$ ;

$|A|^2 \equiv A \cdot A$ ,  $A \in \text{Lin}$ ;

$B$ : a continuous body;

$\Omega_0$ : the reference configuration of  $B$ ;

$\Omega$ : the current configuration of  $B$  at time  $t$ ;

$X$ : the position of a general material point in  $\Omega_0$ ;

$x$ : the position of  $X$  in  $\Omega$  at time  $t$ .

The balance law of linear momentum, the balance law of energy and the Clausius-Duhem inequality are given in the global form as follows:

$$d\left(\int_{\Omega} \rho v dV\right)/dt = \int_{\partial\Omega} T n da + \int_{\Omega} \rho b dV,$$

$$d[\int_{\Omega} \rho (e + |\mathbf{v}|^2/2) dV]/dt = \int_{\partial\Omega} (\mathbf{T}\mathbf{n} \cdot \mathbf{v} - \mathbf{q} \cdot \mathbf{n}) da + \int_{\Omega} \rho (\mathbf{b} \cdot \mathbf{v} + \gamma) dV,$$

$$d(\int_{\Omega} \rho \eta dV)/dt \geq - \int_{\Omega} (\mathbf{q}/\Theta) \cdot \mathbf{n} da + \int_{\Omega} \rho (\gamma/\Theta) dV; \quad (2.3.1)$$

here  $dV$  and  $da$  are the volume and surface measure, respectively;  $\mathbf{n}$  is the outward unit normal field on  $\partial\Omega$ ;  $\rho$  is the mass density;  $\mathbf{v} \equiv \partial\mathbf{x}/\partial t$  is the velocity field associated with the motion  $\mathbf{x} = \mathbf{x}(\mathbf{X}, t)$ ; a superposed dot "." denotes the material time derivative;  $\mathbf{A}_1$  is the first Rivlin-Ericksen tensor (cf.(1.2.5));  $\Theta$  is the absolute temperature;  $\mathbf{T}$  is the Cauchy stress tensor,  $\mathbf{q}$  is the heat flux vector, and  $e$ ,  $\eta$ ,  $\gamma$  and  $\mathbf{b}$  are the internal energy, entropy, radiant heating and body force per unit mass, respectively. When all the fields in question are sufficiently smooth, (2.3.1) can be recasted in local form:

$$\operatorname{div}\mathbf{T} + \rho\mathbf{b} = \rho\dot{\mathbf{v}},$$

$$\rho\dot{e} = \mathbf{T} \cdot \mathbf{A}_1/2 - \operatorname{div}\mathbf{q} + \rho\gamma,$$

$$\rho(\dot{e} - \Theta\dot{\eta}) \leq \mathbf{T} \cdot \mathbf{A}_1/2 - (\mathbf{q} \cdot \operatorname{grad}\Theta)/\Theta. \quad (2.3.2)$$

Henceforth (2.3.1) and (2.3.2) will be regarded as equivalent.

The Helmholtz free energy is defined as

$$\psi = e - \Theta\eta, \quad (2.3.3)$$

in terms of which (2.3.2) may be represented as

$$\rho (\dot{\psi} + \eta \dot{\theta}) - \mathbf{T} \cdot \mathbf{A}_1 / 2 + (\mathbf{q} \cdot \text{grad} \theta) / \theta \leq 0 \quad (2.3.4)$$

which is usually called the dissipation inequality.

An eight tuple of functions  $(\mathbf{x}, \theta, \mathfrak{s}, \eta, \mathbf{T}, \mathbf{q}, \mathbf{b}, \gamma)$  defined on  $\Omega_0 \times [t_1, t_2]$  is said to be a thermodynamic process if it satisfies (2.3.1) or (2.3.2);  $t_1 - t_2$  is called the duration of the process.

For the class of fluids (I) and (II) (cf. (1.2.1) and (1.2.2)), the response functions of the free energy and heat flux can be generally assumed in the form

$$(I, II) \quad \psi = \psi(\theta, \mathbf{g}, \mathbf{A}_1, \mathbf{A}_2), \quad (2.3.5)$$

$$(I, II) \quad \mathbf{q} = \mathbf{q}(\theta, \mathbf{g}, \mathbf{A}_1, \mathbf{A}_2),$$

where  $\mathbf{g} \equiv \text{grad} \theta$ . Of course, the response functions of models (I) and (II) are usually different. Henceforth, we shall use the following assumptions:

Assumption 2.1 The constitutive relations of (I) and (II) are defined for

$$\mathbf{A}_1 \in N_1(0), \quad \dot{\mathbf{A}}_1 \in N_2(0), \quad (2.3.6)$$

where  $N_1(0), N_2(0) \subset \text{Sym}_0$  are small neighbourhoods of the

point  $\mathbf{0} \in \text{Sym}$ ;

Assumption 2.2 In motion of fluids of (I) and (II),

$$\dot{\theta} \in \mathbb{R}, \quad \dot{\mathbf{g}} \in V, \quad \dot{\mathbf{A}}_2 \in \text{Sym} \quad (2.3.7)$$

may be arbitrary;

Assumption 2.3 The free energy has the property

$$(I, II) \quad \psi(\theta, \mathbf{g}, \mathbf{A}_1, \mathbf{A}_2) - \psi(\theta, \mathbf{g}, \mathbf{0}, \mathbf{0}) \geq 0, \quad (2.3.8)$$

for any  $\theta > 0$ ,  $\mathbf{g} \in V$ ,  $\mathbf{A}_1 \in N_1(\mathbf{0})$  and  $\mathbf{A}_2 \in N_2(\mathbf{0})$ .

Assum. 2.1 is suggested to meet the requirement of slow motion. Assum. 2.2 is based on the fact that the response functions of stress, free energy and heat flux are independent from the quantities in (2.3.7). Assum. 2.3 says that the free energy is a minimum at the rest state.

Now, it turns out from (2.3.4) and (2.3.5) that

$$\rho (\psi_{\theta} \dot{\theta} + \psi_{\mathbf{g}} \cdot \dot{\mathbf{g}} + \psi_{\mathbf{A}_1} \cdot \dot{\mathbf{A}}_1 + \psi_{\mathbf{A}_2} \cdot \dot{\mathbf{A}}_2 + \eta \dot{\theta}) - \mathbf{T} \cdot \mathbf{A}_1 / 2 + \mathbf{q} \cdot \mathbf{g} / \theta \leq 0. \quad (2.3.9)$$

We conclude from Assum. 2.2 and linearity of  $\dot{\theta}$ ,  $\dot{\mathbf{g}}$  and  $\dot{\mathbf{A}}_1$  in (2.3.9) that (2.3.9) can be valid only if

$$(I, II) \quad \psi_{\theta} + \eta = 0, \quad \psi_{\mathbf{g}} = \mathbf{0}, \quad \psi_{\mathbf{A}_2} = \mathbf{0}$$

or

$$(I, II) \quad \eta = -\psi_{\Theta}, \quad \psi = \psi(\Theta, \mathbf{A}_1) \quad (2.3.10)$$

To find the thermodynamic restriction on the material parameter  $\alpha_1$  of fluids (I) and (II), we shall concentrate on the unsteady shear flows (2.2.1) with uniform temperature, i.e.,  $\mathbf{g} = \mathbf{0}$ . In that case,

$$(I, II) \quad \psi(\Theta, \mathbf{A}_1) = \bar{\psi}(\Theta, \kappa), \quad (2.3.11)$$

where  $\kappa$  is the shear rate. For convenience, we shall suppress the superposed bar " - " and argument  $\Theta$  in what follows. Then it follows from (2.3.10) that

$$\dot{\psi} = \psi_{\Theta} \dot{\Theta} + \psi_{\mathbf{A}_1} \cdot \dot{\mathbf{A}}_1 = \psi_{\Theta} \dot{\Theta} + \psi_{\kappa} \dot{\kappa} \quad (2.3.12)$$

from which and (2.2.3), the dissipation inequality (2.3.9) may be written as:

$$(I) \quad \rho \psi_{\kappa} \dot{\kappa} - \alpha_1 \kappa \dot{\kappa} - \mu |\kappa|^{2+m} \leq 0, \quad (2.3.13)$$

$$(II) \quad \rho \psi_{\kappa} \dot{\kappa} - \alpha_1 |\kappa|^m \kappa \dot{\kappa} - \mu |\kappa|^{2+m} \leq 0.$$

It is obvious from (2.3.11) that in the given case, (2.3.8) is simplified to

$$\psi(\kappa) - \psi(0) \geq 0, \quad \text{for } \kappa \in N_1(0) \quad (2.3.14)$$

where  $N(0) \in R$  is a small neighbourhood of the point  $0 \in R$ . Suppose the free energy is a convex function of  $K$  on  $N_1(0)$ , namely,

$$(I, II) \quad (\partial\Psi/\partial K)K \geq \Psi(K) - \Psi(0), \text{ for } K \in N_1(0). \quad (2.3.15)$$

Then it is clear from (2.3.14) and (2.3.15) that for  $K \in N(0)$

$$(I) \quad (\partial\Psi/\partial K)K/K^2 \geq 0, \quad (2.3.16)$$

$$(II) \quad (\partial\Psi/\partial K)K/|K|^{2+m} \geq 0, \quad \text{for } m > -1$$

When the initial velocity in unsteady shear flows and pressure gradient are arbitrary, one may find a state in which

$$K = 0, \text{ but } DK/Dt \neq 0, \quad (2.3.17)$$

where, of course, the velocity is assumed to be continuous.

Now, we take the limit as  $K \rightarrow 0^+$  in (2.3.13) so that we obtain

$$(I) \quad \lim_{K \rightarrow 0^+} (\Psi_K/K - \alpha_1)K \leq 0,$$

(2.3.18)

$$(II) \quad \lim_{K \rightarrow 0^+} \rho (\psi_K / |K|^{1+m} - \alpha_1) K \leq 0.$$

Since the sign of  $K \in \mathbb{N}_k(0)$  is arbitrary (i.e.,  $K$  may be positive or negative), (2.3.8) holds if and only if

$$(I) \quad \alpha_1 = \lim_{K \rightarrow 0^+} \rho \psi_K / K, \tag{2.3.19}$$

$$(II) \quad \alpha_1 = \lim_{K \rightarrow 0^+} \rho \psi_K / |K|^{1+m} \quad \text{for } m > -1$$

from which and (2.3.16), we find that

$$(I, II) \quad \alpha_1 \geq 0. \tag{2.3.20}$$

When steady flows of fluids (I) and (II) take place in a uniform temperature field, namely,

$$\dot{\mathbf{A}}_1 = \mathbf{0}, \quad \mathbf{g} = \mathbf{0}, \tag{2.3.21}$$

we immediately obtain from (2.3.9) and (2.3.10) that

$$(I) \quad \phi(\mathbf{A}_1) \equiv [\mu \mathbb{I} |\mathbf{A}_1|^2 + (\alpha_1 + \alpha_2) \text{tr} \mathbf{A}_1^3] / 2 \geq 0, \tag{2.3.22}$$

$$(II) \quad \phi(\mathbf{A}_1) \equiv \mathbb{I} [\mu |\mathbf{A}_1|^2 + (\alpha_1 + \alpha_2) \text{tr} \mathbf{A}_1^3] / 2 \geq 0,$$

where  $\mathbb{I}$  is given in (1.2.4). Particularly, choosing the

shear flows (2.2.1) in which  $|A_1|^2 = 2K^2 \neq 0$ ,  $\text{tr}(A_1^3) = 0$  as the special case of the flows (2.3.21), we obtain from (2.3.22) that

$$(I, II) \quad \mu \geq 0. \quad (2.3.23)$$

By using the well known Hamilton-Cayley theorem in matrix theory and the Cardano's formula for the real roots of the equation  $x^3 + ax + b = 0$ ,  $a, b, x \in \mathbb{R}$  (Zaguskin, 1961, p150), we can easily prove that the inequality

$$|\text{tr}(A_1^3)| \leq |A_1|^3 / \sqrt{6} \quad (2.3.24)$$

should hold for any  $A_1 \in \text{Sym}_0$  whose all eigenvalues are real. (2.3.24) was also shown by Fosdick & Rajagopal (1979).

For further discussion, consider a cylindrical fluid body. Let  $l(t)$  be the length of the cylindrical body at time  $t$  and let the body be confined by a uniform pressure  $-p \circ I$ . Suppose the cylindrical body undergoes a homogeneous and irrotational motion under a superimposed axial load  $\sigma$ . Then the following relations should be valid:

$$\begin{aligned} x &= F(t)x(0), \\ F &= (\alpha - 1/\sqrt{\alpha})e \otimes e + I/\sqrt{\alpha}, \\ A_1 &= a(I - 3e \otimes e), \\ dA_1/dt &= da/dt(I - 3e \otimes e), \end{aligned} \quad (2.3.25)$$

$$\mathbf{A}_t = a^2 (\mathbf{I} + 3e \otimes e) + da/dt (\mathbf{I} - 3e \otimes e),$$

where  $\mathbf{e}$  is the unit vector parallel to the axis of the cylindrical body,  $\otimes$  is the tensor product of vectors,  $\alpha \equiv \ell(t)/\ell(0)$ , and  $a \equiv -d\ell(t)/dt/\ell(t)$ . Consequently, for both fluids (I) and (II), the extra part of the Cauchy stress is also homogeneous and hence the balance equation of linear momentum (2.3.2)<sub>1</sub> becomes

$$\rho \mathbf{b} = \text{grad}(p) + \rho \dot{\mathbf{v}}, \quad (2.3.26)$$

where

$$\dot{\mathbf{v}} = \frac{d}{dt} \mathbf{F} \mathbf{F}^{-1} \mathbf{x}. \quad (2.3.27)$$

Now suppose the body force is derivable from a potential  $\Gamma$ , namely,  $\mathbf{b} = -\text{grad}\Gamma$ . Then by choosing

$$p(\mathbf{x}, t) - p^*(t) = -\rho \mathbf{x} \cdot \mathbf{F} \mathbf{F}^{-1} \mathbf{x} - \rho \Gamma(\mathbf{x}), \quad (2.3.28)$$

where  $p^*$  is a function of time  $t$ , we see that (2.3.25) can be exactly satisfied. In other words, the motion (2.3.25) is dynamically possible (Passman, 1982). For convenience, I shall henceforth refer to the homogeneous motion (2.3.25) as triaxial homogeneous motion.

For the triaxial homogeneous motion, we can easily

obtain from (2.3.25) the equation

$$|\text{tr} \mathbf{A}_1^3| = |\mathbf{A}_1|^3 / \sqrt{6}. \quad (2.3.29)$$

which appeared in the work of Fosdick and Rajagopal (1980, Lemma 2). Dunn (1982, footnote) gave a special case of (2.3.25) in the form  $\mathbf{A}_1 = (3e \otimes e - I)$ . By (2.3.22) and (2.3.29), we obtain another constitutive restriction: for  $\mathbf{A}_1 \in N_1(0)$ ,

$$(I) \quad -(\sqrt{6})\mu_{III}/|\mathbf{A}_1| \leq \alpha_1 + \alpha_2 \leq (\sqrt{6})\mu_{III}/|\mathbf{A}_1|, \quad (2.3.30)$$

$$(II) \quad -(\sqrt{6})\mu/|\mathbf{A}_1| \leq \alpha_1 + \alpha_2 \leq (\sqrt{6})\mu/|\mathbf{A}_1|.$$

Finally, by summarizing the results, we can state the thermodynamical restrictions on fluids (I) and (II) as follows:

**THEOREM 2.3.1.** Suppose the constitutive relations of fluids (I) and (II) are defined when  $\mathbf{A}_1 \in N_1(0)$  and  $D\mathbf{A}_1/Dt \in N_2(0)$ . If the free energy  $\psi$  is convex in the variable  $\mathbf{A}_1$ , the necessary and sufficient conditions that the response functions of  $\mathbf{T}$ ,  $\psi$  and  $\mathbf{q}$  of fluids (I) and (II) are compatible with the Clausius-Duhem inequality are that

(a) the free energy  $\psi$  and the entropy  $\eta$  satisfy

$$(I, II) \quad \psi = \psi(\theta, \mathbf{A}_1), \quad (2.3.31)$$

$$(I, II) \quad \partial\psi/\partial\theta + \eta = 0;$$

(b) the viscosity  $\mu$  meets

$$(I, II) \quad \mu \geq 0; \quad (2.3.32)$$

(c) the normal stress coefficients  $\alpha_1$  and  $\alpha_2$  obey

$$(I, II) \quad \alpha_1 \geq 0,$$

$$(I) \quad -2^{-m/2}(\sqrt{6})^\mu/|\mathbf{A}_1|^{1-m} \leq \alpha_1 + \alpha_2 \leq 2^{-m/2}(\sqrt{6})^\mu/|\mathbf{A}_1|^{1-m}, \quad (2.3.33)$$

$$(II) \quad -(\sqrt{6})^\mu/|\mathbf{A}_1| \leq \alpha_1 + \alpha_2 \leq (\sqrt{6})^\mu/|\mathbf{A}_1|;$$

(d) the dissipation inequality has the form

$$(I, II) \quad \rho\psi_{\mathbf{A}_1} \cdot \dot{\mathbf{A}}_1 - \mathbf{T} \cdot \mathbf{A}_1/2 + \mathbf{q} \cdot \mathbf{g}/\theta \leq 0, \quad (2.3.34)$$

where the material parameters may be functions of material point and temperature.

Remark: If arbitrary  $\mathbf{A}_1$ ,  $D\mathbf{A}_1/Dt \in \text{Sym}_\phi$  are included in constitutive domains of fluids (I) and (II) (i.e., fast motion of fluids (I) and (II) may then take place), by following arguments similar to those used by Dunn and

Fosdick (1974), we can immediately obtain the following stronger constitutive restrictions:

$$(I, II) \quad \alpha_1 \geq 0, \quad \alpha_1 + \alpha_2 = 0;$$

$$(I, II) \quad \mathbf{q} \cdot \mathbf{g} / \Theta \leq \phi(\mathbf{A}_1);$$

$$(I) \quad \Psi(\Theta, \mathbf{A}_1) = \Psi(\Theta, \mathbf{0}) + \alpha_1 |\mathbf{A}_1|^2 / (4^\rho);$$

$$(II) \quad \Psi(\Theta, \mathbf{A}_1) = \Psi(\Theta, \mathbf{0}) + \alpha_1 |\mathbf{A}_1|^{2+m} / [2^{1+m/2} (2+m)^\rho],$$

where  $\phi(\mathbf{A}_1)$  is defined by (2.3.22).

By taking  $\mathbf{A}_1 = \mathbf{0}$  in (2.3.33)<sub>2</sub>, we get

COROLLARY 2.3.1. Under the same assumptions in Theorem 2.3.1, (2.3.33)<sub>2</sub> holds when  $m > 1$  if and only if

$$(I) \quad \alpha_1 + \alpha_2 = 0. \quad (2.3.35)$$

Suppose the response function of the heat flux  $\mathbf{q}$  satisfies the principle of frame-indifference. Then it is not difficult to show that

$$(I, II) \quad \mathbf{q}(\cdot, \mathbf{0}, \cdot, \cdot) = \mathbf{0}, \quad (2.3.36)$$

Now, let  $\Theta_0 > 0$ ,  $\Theta$ ,  $\mathbf{A}_1$ ,  $\mathbf{A}_2$  be fixed, and  $\delta \equiv |\Theta - \Theta_0| + |\mathbf{A}_1| + |\mathbf{A}_2| + |\mathbf{g}|$ . Then by using (2.3.36), we have

$$(I, II) \quad \mathbf{q}(\Theta, \mathbf{g}, \mathbf{A}_1, \mathbf{A}_2) = -\mathbf{K}\mathbf{g} + o(\delta), \quad \text{as } \delta \rightarrow 0 \quad (2.3.37)$$

according to Taylor's expansion, where

$$(I, II) \quad \mathbf{K} \equiv -\partial \mathbf{q}(\Theta_\phi, \mathbf{g}, \mathbf{A}_1, \mathbf{A}_2) / \partial \mathbf{g} \quad \text{at } \mathbf{g} = \mathbf{0}. \quad (2.3.38)$$

(2.3.37) asserts that in slow motion, the response function of the heat flux can be approximated by Fourier's law

$$(I, II) \quad \mathbf{q} = -\mathbf{K}\mathbf{g} \quad (2.3.39)$$

if the temperature difference and the temperature gradient are small. Let fluids (I) and (II) be at the rest state. Then it turns out from (2.3.34) and (2.3.38) that

$$(I, II) \quad (-\mathbf{K}\mathbf{g}) \cdot \mathbf{g} \leq 0$$

which leads to

COROLLARY 2.3.2. Under the same assumptions of Theorem 2.3.1, if  $|\Theta - \Theta_\phi| + |\mathbf{A}_1| + |\mathbf{A}_2| + |\mathbf{g}|$  is small, the response function of the heat flux can be approximated by Fourier's law, and the conductivity tensor  $\mathbf{K}$  must be positive semi-definite at a rest state.

Section 2.4 Cannister flows for models compatible with  
thermodynamics: stability implies asymptotic  
stability

In this section we shall study cannister flows of fluids characterized by models (I) and (II) that satisfy the thermodynamic restrictions. For motions whose  $A_1$  remains in  $N_1(0)$  for all time  $t$ , we shall prove that  $v \rightarrow 0$  as  $t \rightarrow \infty$ . In other words we shall show that for cannister flows stability implies asymptotic stability of the rest state.

Suppose a fluid occupies the entire volume of a rigid closed container  $\Omega$ . After the container is shaken at time  $t \leq 0$ , and then suddenly fixed for  $t > 0$ , the fluid satisfies the adherence condition  $v = 0$  on  $\partial\Omega$ . The flows inside  $\Omega$  for  $t > 0$  are called cannister flows and are introduced by Dunn and Fosdick (1974) for the analysis of mechanical stability of second order fluids. It can be easily shown that an incompressible fluid undergoing cannister flows must be consistent with the condition of mechanical isolation (Gurtin, 1972) when the body force  $b$  has a potential:

$$\int_{\partial\Omega} Tn \cdot v da + \int_{\Omega} \rho b \cdot v dV = 0. \quad (2.4.1)$$

In what follows, the body force of any fluid is always assumed to be derivable from a potential function. Thus in cannister flows of an incompressible fluid, by (2.4.1) the

balance equation of mechanical energy (Gurtin, 1981)

$$d(\int_{\Omega} \rho |\mathbf{v}|^2 dV/2)/dt + \int_{\Omega} \mathbf{T} \cdot \mathbf{A}_1 dV/2 = \int_{\partial\Omega} \mathbf{Tn} \cdot \mathbf{v} da + \int_{\Omega} \rho \mathbf{b} \cdot \mathbf{v} dV$$

may be simplified to

$$d(\int_{\Omega} \rho |\mathbf{v}|^2 dV/2)/dt + \int_{\Omega} \mathbf{T} \cdot \mathbf{A}_1 dV = 0. \quad (2.4.2)$$

Equation (2.4.2) is usually used as a point of departure for the analysis of mechanical stability of cannister flows.

For simplicity, let us consider the case in which the fluids (I) and (II) are homogeneous and the temperature is uniform. Then the material parameters  $\mu$ ,  $\alpha_1$ ,  $\alpha_2$  and  $m$  of fluids (I) and (II) are constants. Substituting (1.2.1) and (1.2.2) into (2.4.2), we obtain

$$(I) \quad d(\int_{\Omega} \rho |\mathbf{v}|^2 dV)/dt + \int_{\Omega} \alpha_1 \mathbf{A}_1 \cdot \dot{\mathbf{A}}_1 dV + 2 \int_{\Omega} \phi(\mathbf{A}_1) dV = 0, \quad (2.4.3)$$

$$(II) \quad d(\int_{\Omega} \rho |\mathbf{v}|^2 dV)/dt + \int_{\Omega} \alpha_1 \mathbb{H} \mathbf{A}_1 \cdot \dot{\mathbf{A}}_1 + 2 \int_{\Omega} \phi(\mathbf{A}_1) dV = 0,$$

where  $\phi$  is defined by (2.3.22). Furthermore, we define a function  $E$  by

$$(I) \quad E(t) = \int_{\Omega} \rho |\mathbf{v}|^2 dV + \alpha_1 \int_{\Omega} |\mathbf{A}_1|^2 dV/2, \quad (2.4.4)$$

$$(II) \quad E(t) = \int_{\Omega} \rho |\mathbf{v}|^2 dV + \alpha_1 \int_{\Omega} |\mathbf{A}_1|^{2+m} dV / [(2+m)2^{m/2}],$$

which measures the kinetic energy and stretching energy in the fluid body.

Since

$$D|A_1|^{2+m}/Dt = (2+m)|A_1|^m A_1 \cdot \dot{A}_1, \quad (2.4.5)$$

by (2.4.4) and (2.4.5), (2.4.3) can be represented as

$$(I, II) \quad dE/dt = -2 \int_{\Omega} \phi dV. \quad (2.4.6)$$

Then by using

$$\phi(A_1) \geq 0, \quad \text{for any } A_1 \in N_1(0),$$

(cf. Theorem 2.3.1), we obtain

LEMMA 2.4.1. If fluids (I) and (II) are compatible with the thermodynamic restrictions, the energy function  $E$  should obey

$$(I, II) \quad E(t) \geq 0, \quad dE(t)/dt \leq 0, \quad \text{for } t \geq 0 \quad (2.4.7)$$

in cannister flows whose  $A_1$  remain in  $N_1(0)$  for all  $t \geq 0$ .

The lemma shows us that the non-negative function  $E$  must have a upper bound in the class of motions in question. Since  $\rho > 0$  and  $\alpha_1 \geq 0$ , it follows (2.4.4) that

$$(I) \quad \int_{\Omega} |A_1|^2 dV \leq 2E(t)/\alpha_1,$$

$$(II) \quad \int_{\Omega} |A_1|^{2+m} dV \leq 2^{m/2} (2+m)E(t)/\alpha_1.$$

For the class of motions in question (i.e.,  $A_1 \in N_1(0)$ ), there exists a positive real number  $k_1$  such that

$$|A_1(x, t)| < k_1 \quad \text{for } x \in \Omega, t > 0, \quad (2.4.8)$$

from which when  $-1 < m \leq 0$ ,

$$|A_1|^m \geq k_1^m,$$

or

$$\int_{\Omega} |A_1|^2 dV \leq k_1^{-m} \int_{\Omega} |A_1|^{2+m} dV. \quad (2.4.9)$$

On the other hand, it follows from Hölder's inequality (Hewitt & Stromberg, 1965) that when  $m > 0$ , there must exist a positive number  $k_2$  increasing with the measure of the domain  $\Omega$  such that

$$\int_{\Omega} |A_1|^2 dV \leq k_2 \int_{\Omega} |A_1|^{2+m} dV. \quad (2.4.10)$$

Let

$$s = \text{Max}(k_1^{-m}, k_2). \quad (2.4.11)$$

In cannister flows, the Poincaré inequality (Rektorys, 1975) may be simplified to

$$\int_{\Omega} |\mathbf{v}|^2 dV \leq C \int_{\Omega} |\text{grad} \mathbf{v}|^2 dV, \quad (2.4.12)$$

where  $C$  is a positive number which increases with the diameter of the domain  $\Omega$ . Besides, it can be easily shown that in cannister flows of any incompressible fluid,

$$\int_{\Omega} |\text{grad} \mathbf{v}|^2 dV = \int_{\Omega} |\mathbf{A}_1|^2 dV/2 \quad (2.4.13)$$

Next, we shall show that there is a positive real number  $\lambda$  such that  $dE/dt + \lambda E \leq 0$  for  $t \geq 0$ . The foregoing inequality will play an important role in the analysis of asymptotical stability of cannister flows. Let  $\lambda$  be a positive number which will be defined shortly. It turns out from (2.4.4), (2.4.6), (2.4.11), (2.4.12) and (2.4.13) that by  $\alpha_1 + \alpha_2 = 0$  as  $m > 1$  for model (I),

$$\begin{aligned} \text{(I)} \quad dE/dt + \lambda E &= -2 \int_{\Omega} [2^{-m/2} \mu |\mathbf{A}_1|^{2+m} + (\alpha_1 + \alpha_2) \text{tr} \mathbf{A}_1^3] dV \\ &+ \lambda \int_{\Omega} \rho |\mathbf{v}|^2 dV + \lambda \alpha_1 \int_{\Omega} |\mathbf{A}_1|^2 dV/2 \leq -2 \int_{\Omega} [2^{-m/2} \mu |\mathbf{A}_1|^{2+m} - |\alpha_1 \\ &+ \alpha_2| |\mathbf{A}_1|^3 / \sqrt{6}] dV + \lambda C \rho s \int_{\Omega} |\mathbf{A}_1|^{2+m} dV/2 + \lambda \alpha_1 s \int_{\Omega} |\mathbf{A}_1|^{2+m} dV/2 \\ &\leq \int_{\Omega} [\lambda s (C \rho + \alpha_1) / 2 - 2(2^{-m/2} \mu - |\alpha_1 + \alpha_2| k_1^{1-m} / \sqrt{6})] |\mathbf{A}_1|^{2+m} dV \end{aligned}$$

and similarly for model (II)

$$\text{(II)} \quad dE/dt + \lambda E \leq \int [\lambda (C \rho s / 2 + 2^{-m/2} \alpha_1 / (2 + m))$$

$$-2^{1-m/2}(\mu - |\alpha_1 + \alpha_2|k_1/\sqrt{6})|A_1|^{2+m}dV. \quad (2.4.14)$$

Now, define the number  $\lambda$  by

$$(I) \quad \lambda = 4[2^{-m/2}\mu - |\alpha_1 + \alpha_2|k_1^{1-m}/\sqrt{6}]/s/(C^\rho + \alpha_1) \text{ as } 0 < m \leq 1, \\ \lambda = 2^{2-m/2}\mu/s/(C^\rho + \alpha_1) \text{ as } m > 1, \quad (2.4.15)$$

$$(II) \quad \lambda = 2[\mu - |\alpha_1 + \alpha_2|k_1/\sqrt{6}]/[2^{m/2-1}C^\rho s + \alpha_1/(2+m)],$$

from which with (2.4.14), we find that for  $t \geq 0$ ,

$$(I, II) \quad dE(t)/dt + \lambda E \leq 0$$

or

$$(I, II) \quad E(t) \leq E(0)\text{Exp}(-\lambda t), \quad (2.4.16)$$

where the positivity of  $\lambda$  is guaranteed by  $\phi(A_1) \geq 0$ .

Hence from (2.4.4) and (2.4.16), we have established the following

**THEOREM 2.4.1.** If fluids (I) and (II) are compatible with thermodynamic restrictions, for cannister flows whose  $A_1$  remains in  $N_1(0)$  for all  $t \geq 0$ , the flows will decay exponentially with  $t$  in the sense that

$$(I, II) \quad \int_{\Omega} |\mathbf{v}|^2 dV \leq E(0)e^{-\lambda t/\rho},$$

$$(I) \quad \int_{\Omega} |\mathbf{A}_1|^2 dV \leq 2E(0)e^{-\lambda t/\alpha_1},$$

$$(II) \quad \int_{\Omega} |\mathbf{A}_1|^{2+m} dV \leq 2^{m/2} (2 + m)E(0)e^{-\lambda t/\alpha_1}.$$

### Section 2.5 What happens if $\alpha_1 < 0$ ? Some consequences

It has been shown in the last section that cannister flows of fluids (I) and (II) are asymptotically stable when the fluids satisfy the thermodynamic restrictions

$$(I, II) \quad \mu \geq 0, \quad \alpha_1 \geq 0, \quad \phi(\mathbf{A}_1) \geq 0,$$

and if  $\mathbf{A}_1$  remains in  $N_1(0)$ . But what will happen to models which violate the thermodynamic restrictions? We shall see in this section that for flows of fluids (I) and (II) in sufficiently small cannisters, if  $\alpha_1 < 0$ , the flows will never stop after any initial disturbance so long as  $\mu \geq 0$  and  $\phi(\mathbf{A}_1) \geq 0$ .

To explain it, let

$$(I, II) \quad \alpha_1 < 0, \quad \mu \geq 0, \quad \phi(\mathbf{A}_1) \geq 0. \quad (2.5.1)$$

We still start from the balance equation of mechanical energy (2.4.2). For convenience, set  $\alpha_1 = -|\alpha_1|$ . Thus (2.4.3) can be represented as

$$(I) \quad d[\int_{\Omega} \rho |\mathbf{v}|^2 dV - |\alpha_1| \int_{\Omega} |\mathbf{A}_1|^2 dV/2]/dt + 2 \int_{\Omega} \phi dV = 0, \quad (2.5.2)$$

$$(II) \quad d\{\int_{\Omega} \rho |\mathbf{v}|^2 dV - |\alpha_1| \int_{\Omega} |\mathbf{A}_1|^{2+m} dV/[2^{m/2}(2+m)]\}/dt$$

$$+ 2 \int_{\Omega} \phi \, dV = 0$$

from (2.4.5). Let

$$(I) \quad N(t) = |\alpha_1| \int_{\Omega} |\mathbf{A}_1|^2 \, dV / 2 - \int_{\Omega} \rho |\mathbf{v}|^2 \, dV, \quad (2.5.3)$$

$$(II) \quad N(t) = |\alpha_1| \int_{\Omega} |\mathbf{A}_1|^{2+m} \, dV / [2^{m/2} (2 + m)] - \int_{\Omega} \rho |\mathbf{v}|^2 \, dV,$$

which obviously have the property

$$dN(t)/dt \geq 0 \quad \text{for } t \geq 0 \quad (2.5.4)$$

from (2.5.1) and (2.5.2). It follows from (2.4.12) and (2.4.13) that the function  $N$  satisfies

$$(I) \quad N(t) \geq (|\alpha_1| - C^{\rho}) \int_{\Omega} |\mathbf{A}_1|^2 \, dV / 2, \quad (2.5.5)$$

$$(II) \quad N(t) \geq |\alpha_1| \int_{\Omega} |\mathbf{A}_1|^{2+m} \, dV / [2^{m/2} (2 + m)] - C^{\rho} \int_{\Omega} |\mathbf{A}_1|^2 \, dV / 2$$

for  $t \geq 0$ , where  $C$  is the Poincaré number, a monotonic increasing function of the diameter of the cannister. Let  $b > 0$  be such that

$$|\mathbf{A}_0| = |\mathbf{A}_1(\mathbf{x}, 0)| < b, \quad \mathbf{x} \in \Omega.$$

Then by the same argument as that used in Sec. 2.4, we can find a positive number  $S$  for which

$$\int_{\Omega} |\mathbf{A}_\phi|^2 dV \leq S \int_{\Omega} |\mathbf{A}_\phi|^{2+m} dV \quad (2.5.6)$$

holds for  $m > -1$ . Now we choose a small cannister (but still finite) such that

$$(I) \quad C < |\alpha_1|/\rho, \quad (2.5.7)$$

$$(II) \quad C < 2|\alpha_1|/[2^{m/2}(2+m)\rho S],$$

which with (2.5.5) and (2.5.6) leads to

$$(I, II) \quad N(0) > 0. \quad (2.5.8)$$

But since  $N(t)$  is a non-decreasing function of time  $t$  from (2.5.4), it obviously satisfies

$$(I, II) \quad N(t) \geq N(0) > 0 \quad \text{for } t \geq 0. \quad (2.5.9)$$

According to (2.5.3) in which the second term on the right-hand side is always non-negative, we find that for  $t \geq 0$ ,

$$(I) \quad \int_{\Omega} |\mathbf{A}_1|^2 dV \geq 2N(t)/|\alpha_1| > 0, \quad (2.5.10)$$

$$(II) \quad \int_{\Omega} |\mathbf{A}_1|^{2+m} dV \geq 2^{m/2}(2+m)N(t)/|\alpha_1| > 0.$$

(2.5.1), (2.5.7) and (2.5.10) indicate that if  $\alpha_1$  is

negative and the size of cannister is small enough, cannister flows of fluids (I) and (II) will never stop so long as  $\mu \geq 0$  and  $\phi(\mathbf{A}_1) \geq 0$ .

For second order (or grade) fluids, Fosdick and Rajagopal (1979) concluded that if the material moduli satisfy

$$\mu \geq 0, \quad \alpha_1 < 0,$$

and if the viscosity  $\mu$  is sufficiently large and the size of the cannister is sufficiently small, then for any given positive constant  $M$ , it is necessary that

$$\int_{\Omega} |\mathbf{A}_1|^3 dV > M$$

at some time. In fact no matter what values of  $\mu$  and  $\alpha_1 + \alpha_2$  are, triaxial homogeneous motion (2.3.25) will be unstable, and the length of fluids (I) and (II) will elongate or shrink without limit under any initial disturbance, as long as

$$(I, II) \quad \alpha_1 < 0, \quad \mu \geq 0, \quad \phi \geq 0. \quad (2.5.11)$$

For triaxial homogeneous motion (2.3.25), it is shown in Sec. 4.1 that when there is no axial load  $\sigma$ , the motion equation of fluids (I) and (II) should be

$$(I) \quad \alpha_1 \dot{a} + 3^{m/2} \mu |a|^m a - (\alpha_1 + \alpha_2) a^2 = 0, \quad (2.5.12)$$

$$(II) \quad \alpha_1 \dot{a} + \mu a - (\alpha_1 + \alpha_2) a^2 = 0$$

for  $t > 0$ , with the initial condition  $a(0) = a_\phi$ , where  $a_\phi$  is a non-zero constant. It should be emphasized that the motion (2.3.25) and equation of motion (2.5.12) are exact when (2.3.28) is satisfied, and they may be approximately valid for those experiments for which inertia and body forces can be ignored (Passman, 1982). The analysis in this section will be based on the assumption that (2.3.28) is valid. It follows from (2.3.25) and (2.3.22) that

$$(I) \quad \dot{\phi} = 3a[3^{m/2} \mu |a|^m a - (\alpha_1 + \alpha_2) a^2],$$

$$(II) \quad \dot{\phi} = 3^{m/2+1} |a|^m a [\mu a - (\alpha_1 + \alpha_2) a^2]$$

from which and (2.5.12), we find that if  $\alpha_1 < 0$ ,

$$(I) \quad -3|\alpha_1| a \dot{a} + \dot{\phi} = 0, \quad (2.5.13)$$

$$(II) \quad -3^{m/2+1} |\alpha_1| |a|^m a \dot{a} + \dot{\phi} = 0$$

for  $t > 0$ . But  $\dot{\phi}$  is non-negative; cf. (2.3.22). Then after integration of (2.5.13) w.r.t. time  $t$ , we find that for  $t \geq 0$ ,

$$(I) \quad |\alpha_1| (a^2 - a_\phi^2) \geq 0,$$

$$(II) \quad |\alpha_1| (a^{2+m} - a_0^{2+m}) \geq 0$$

or

$$(I) \quad a^2 \geq a_0^2 > 0, \tag{2.5.14}$$

$$(II) \quad a^{2+m} \geq a_0^{2+m} > 0.$$

It turns out from a  $\equiv -d\ell/dt/\ell$  and (2.5.14) that for any time  $t$

$$(I, II) \quad |\dot{\ell}(t)| \geq \text{constant} > 0 \tag{2.5.15}$$

which illustrates that the length of the fluids will elongate or shrink without limit after a initial disturbance so long as  $\alpha_1 < 0$ ,  $\mu \geq 0$  and  $\phi \geq 0$ .

Indeed, it can be easily calculated from (2.5.12) that for fluids (II),

$$a(t) = [\mu a_0 / (\alpha_1 + \alpha_2)] / \{ [\mu / (\alpha_1 + \alpha_2) - a_0] e^{\mu t / \alpha_1} + a_0 \}, \tag{2.5.16}$$

for  $t \geq 0$ . In other words, if  $\mu \geq 0$  and  $\alpha_1 \geq 0$ , then  $a(t)$  will approach zero as  $t \rightarrow \infty$  and hence the motion is asymptotically stable. But if  $\mu \geq 0$  and  $\alpha_1 < 0$ , then  $a(t) \rightarrow \mu / (\alpha_1 + \alpha_2)$  as  $t \rightarrow \infty$ .

Chapter 3      Evaluation of material parameters by  
                 fitting data of pressuremeter tests

Section 3.1    Initial-boundary value problem pertaining  
                 to pressuremeter tests

In pressuremeter tests, a testing probe which is essentially a cylindrical rubber membrane is inserted into a cylindrical cavity of the tested substance and is then inflated to expand the cavity, the deformation of which is recorded in the meantime; cf. the monograph by Baguelin & others(1978). Specifically, by performing the pressuremeter test on ice which undergoes creeping, one may measure the cavity radius of the ice versus time. Usually the pressuremeter test is performed either in-situ or in the labloratoty. In both situations, the size of the tested substance is much larger than that of the probe itself.

In pressuremeter tests, the length of the cavity is finite and the ratio of length to radius of the cavity usually is large thanr 10. When analysing the initial-boundary value problem pertaining to the pressuremeter test, we let the origin of the cylindrical coordinate system  $(r, \theta, z)$  and the  $z$ -axis locate at the middle point of and along the central line of the cavity, respectively. Let  $\mathbf{v} = (u, v, w)$  denote the velocity field within the tested substance, where  $u, v$  and  $w$  are the physical components of  $\mathbf{v}$  under the

cylindrical coordinate system. In particular, when the tested substance is polycrystalline ice, we introduce the following assumptions:

3.1 The sample is a homogeneous, isotropic and incompressible continuum.

3.2 Its temperature is uniform and remains constant with time.

3.3 The body and inertia forces appearing in the balance equation of motion are negligible.

3.4 The primary and secondary creep of the sample can be described by models (I) and (II), defined by (1.2.1) and (1.2.2).

3.5 During the test the deformation of the sample is axisymmetric and the velocity component  $w \approx 0$  for a thin slab  $N(z = 0)$  which contains the cross-section at  $z=0$ .

Assum. 3.5 is based on the fact that only the radius at the middle point ( $z = 0$ ) of the ice cavity is measured and deformation even at the free surface of the ice, which is perpendicular to the axis  $z$ , is too small to be measured during the test period. In other words, it is assumed that the middle segment of the ice sample undergoes a plane deformation. The following analysis will be restricted to the domain  $N(z = 0)$ .

By Assum. 3.5, the velocity field is simplified to

$$\mathbf{v}(r,t) = (u(r,t), 0, 0) \quad (3.1.1)$$

from which, the first Rivlin-Ericksen tensor (1.2.4)<sub>1</sub> should be

$$[\mathbf{A}_1(r,t)] = \text{diag}[2\partial u(r,t)/\partial r, 2u(r,t)/r, 0], \quad (3.1.2)$$

where  $[\cdot]$  denotes the matrix form of a second order tensor and  $\text{diag}[\cdot, \cdot, \cdot]$  the diagonal form of a matrix. Since the ice is assumed to be incompressible, we have

$$\text{tr}\mathbf{A}_1 = 0 \quad \text{or} \quad \partial u/\partial r + u/r = 0, \quad (3.1.3)$$

which leads to

$$u(r,t) = c(t)/r, \quad (3.1.4)$$

where  $c$  is a function of time  $t$ . Then (3.1.2) and (3.1.4) yield

$$\begin{aligned} [\mathbf{A}_1] &= \text{diag}[-2c/r^2, 2c/r^2, 0], \\ [\mathbf{A}_1^2] &= \text{diag}[4c^2/r^4, 4c^2/r^4, 0]; \\ \mathbb{I} &= (2c/r^2)^m \end{aligned} \quad (3.1.5)$$

follows from (1.2.4)<sub>2</sub>; similarly the second Rivlin-Ericksen tensor  $\mathbf{A}_2$  is given by

$$[\mathbf{A}_z] = \text{diag}[-2\dot{c}/r^2 + 8c^2/r^4, 2\dot{c}/r^2, 0]. \quad (3.1.6)$$

Substituting (3.1.5) and (3.1.6) into (1.2.1) and (1.2.1), we obtain the stress distribution in the ice:

$$(I) \quad T_{rr} = -p - \mu(2c/r^2)^{1+m} + 4\alpha_2 c^2/r^4 + \alpha_1(-2\dot{c}/r^2 + 8c^2/r^4),$$

$$T_{\theta\theta} = -p + \mu(2c/r^2)^{1+m} + 4\alpha_2 c^2/r^4 + \alpha_1(2\dot{c}/r^2), \quad (3.1.7)$$

$$(II) \quad T_{rr} = -p + (2c/r^2)^m[-\mu(2c/r^2) + 4\alpha_2 c^2/r^4 + \alpha_1(-2\dot{c}/r^2 + 8c^2/r^4)],$$

$$T_{\theta\theta} = -p + (2c/r^2)^m[\mu(2c/r^2) + 4\alpha_2 c^2/r^4 + \alpha_1(2\dot{c}/r^2)]; \quad (3.1.8)$$

all other stress components vanish.

Since Assum. 3.3 specifies the balance equation of motion

$$\text{div}\mathbf{T} + \rho\mathbf{b} = \rho\dot{\mathbf{v}}$$

to

$$\partial T_{rr}/\partial r + (T_{rr} - T_{\theta\theta})/r = 0, \quad (3.1.9)$$

by substituting (3.1.7) and (3.1.8) into (3.1.9), we obtain

$$(I) \quad \partial T_{rr}/\partial r - 2\mu(2c/r^2)^{1+m}/r + \alpha_1(-4\dot{c}/r^2 + 8c^2/r^4)/r = 0, \quad (3.1.10)$$

$$(II) \quad \partial T_{rr}/\partial r - (2c/r^2)^m[-2\mu(2c/r^2) + \alpha_1(-4\dot{c}/r^2 + 8c^2/r^4)]/r = 0$$

with the boundary conditions:

$$T_{rr}(r_0, t) = -P(t), \quad T_{rr}(\infty, t) = -P_0(t), \quad (3.1.11)$$

where  $r_0$  is the cavity radius which is a function of time  $t$  during the creep process,  $-P(t)$  and  $-P_0(t)$  are the radial stresses on the cavity and at infinity, respectively. A straightforward integration of (3.1.10) from  $r_0$  to  $\infty$  yields:

$$(I) \quad -P(t) + P_0(t) + \frac{\mu}{1+m}(2c/r_0^2)^{1+m} + \alpha_1(2\dot{c}/r_0^2) - 2c^2/r_0^4 = 0, \quad (3.1.12)$$

$$(II) \quad -P(t) + P_0(t) + \frac{\mu}{1+m}(2c/r_0^2)^{1+m} + \frac{2\alpha_1}{1+m}(2c/r_0^2)^m(\dot{c}/r_0^2) - \alpha_1(2c/r^2)^{2+m}/(2+m) = 0.$$

Let  $\dot{r}$  denote the rate of  $r$ , namely  $u$ . We have

$$c(t) = \dot{r}(r, t)r(t) \quad (3.1.13)$$

from (3.1.4), and especially at the wall of the cavity,

$$c(t) = \dot{r}_0(r_0, t)r_0(t). \quad (3.1.14)$$

Then (3.1.12) and (3.1.14) yield the cavity creep equation of the ice:

$$(I) \quad \alpha_1 \ddot{r}_0/r_0 + \frac{\mu}{2(1+m)}(2\dot{r}_0/r_0)^{1+m} - [P(t) - P_0(t)]/2 = 0, \quad (3.1.15)$$

$$(II) \quad \alpha_1 \ddot{r}_0/r_0 + \mu \dot{r}_0/r_0 - \frac{m}{2+m}\alpha_1 [\dot{r}_0/r_0]^2 - \frac{1+m}{2}[P(t)$$

$$- P_0(t) \left[ \frac{2\dot{r}_0}{r_0} \right]^{-m} = 0.$$

In practice  $r_0(t_0)$  and  $\dot{r}_0(t_0)$  are usually determined from experimental data for some initial time  $t_0$ .

I should like to add a few comments:

(a) The term containing the material parameter  $\alpha_2$  has been cancelled in the derivation. Thus  $\alpha_2$  cannot be directly evaluated by fitting the data of pressuremeter tests.

(b) (3.1.15) can be used to fit the data of tests which have variable cavity pressure. Of course, it may be much easier to use a constant cavity pressure in pressuremeter test.

(c) (3.1.15) cannot be solved analytically because of their strong non-linearity. But fortunately, numerical methods such as the Runge-Kutta method can be used by the aid of the computer (Lambert, 1972). In what follows, we shall call the solution of (3.1.15) the predicted radius.

To end this section, define

$$\dot{\epsilon}(r,t) = \dot{r}(r,t)/r(t) \quad (3.1.16)$$

which is often called the creep rate in the engineering literature. Then by (3.1.5)<sub>1</sub> and (3.1.16),

$$[A_1] = \text{diag} [ -2\dot{\epsilon}(r,t), 2\dot{\epsilon}(r,t), 0 ]$$

which implies that  $A_1$ , a kinematic tensor measuring stretching in continuum mechanics, indeed delivers creep

rates in three directions in the present problem. Henceforth, we shall often use the cavity creep rate

$$\beta_0 = \dot{r}_0/r_0 \quad (3.1.17)$$

which can be determined from (3.1.15) as long as the values of the material parameters, the cavity pressure and initial conditions are given.

### Section 3.2 Effect of the material parameters on the predicted creep rate

For convenience of analysis, we shall use  $\mathbf{u} = (u_1, u_2, u_3)$  to denote  $(\mu, \alpha_1, m)$ . There are two reasons to find an explicit expression of  $\partial r_0 / \partial \mathbf{u}$  and of  $\partial \dot{\beta}_0 / \partial \mathbf{u}$ , where  $r_0$  is the predicted cavity radius,  $\dot{\beta}_0$  the predicted creep rate defined by (3.1.17), and both are dependent on (3.1.15). One of the reasons is that by those partial derivatives, we can see how the material parameters influence the predicted creep and which parameter will dominate more importantly the predicted creep and creep rate. Another reason is that those partial derivatives are useful to evaluating the material parameters by least squares estimation if the analytic expressions of the gradient of objective function and of predicted solution w.r.t.  $\mathbf{u}$  are needed (see (A.2.7) and (A.2.8) in Appendix A.2).

It is obvious from (3.1.15) that both the predicted radius  $r_0$  and the creep rate  $\dot{\beta}_0$  depend on the material parameters  $\mathbf{u}$  and time  $t$ , namely,

$$r_0 = r_0(\mathbf{u}, t) \tag{3.2.1}$$

$$\dot{\beta}_0 = \dot{\beta}_0(\mathbf{u}, t)$$

from which and from (3.1.17),

$$\begin{aligned}\partial \beta_{\phi} / \partial \mathbf{u} &= (\partial \dot{r}_{\phi} / \partial \mathbf{u}) / r_{\phi} - (\dot{r}_{\phi} / r_{\phi}^2) (\partial r_{\phi} / \partial \mathbf{u}) \\ &= d(\partial r_{\phi} / \partial \mathbf{u}) / dt / r_{\phi} - (\beta_{\phi} / r_{\phi}) (\partial r_{\phi} / \partial \mathbf{u}),\end{aligned}\quad (3.2.2)$$

since  $\mathbf{u}$  and  $t$  are independent of each other. (3.2.2) can be represented as

$$d(\partial r_{\phi} / \partial \mathbf{u}) / dt - \beta_{\phi} (\partial r_{\phi} / \partial \mathbf{u}) = r_{\phi} \partial \beta_{\phi} / \partial \mathbf{u} \quad (3.2.3)$$

with the initial condition:

$$\partial r_{\phi} / \partial \mathbf{u} = 0 \quad \text{at } t = t_{\phi} \quad (3.2.4)$$

which is based on the fact that the initial predicted radius is given by the experimental data and hence is independent of  $\mathbf{u}$ . An integration of (3.2.3) from  $t_{\phi}$  to  $t$  yields

$$\partial r_{\phi} / \partial \mathbf{u} = \text{Exp} \left[ \int_{t_{\phi}}^t \beta_{\phi} d\tau \right] \left[ \int_{t_{\phi}}^t r_{\phi} \frac{\partial \beta_{\phi}}{\partial \mathbf{u}} \text{Exp} \left( - \int_{t_{\phi}}^{\tau} \beta_{\phi} ds \right) d\tau \right], \quad (3.2.5)$$

where  $r_{\phi}$  and  $\beta_{\phi}$  will be numerically solved from (3.1.15), but  $\partial \beta_{\phi} / \partial \mathbf{u}$  is still an undetermined function. By the chain rule of differentiation we have

$$d(\partial \beta_{\phi} / \partial \mathbf{u}) / dt = \dot{\partial \beta_{\phi} / \partial \mathbf{u}} = \delta \dot{\beta}_{\phi} / \delta \mathbf{u} + (\partial \dot{\beta}_{\phi} / \partial \beta_{\phi}) (\partial \beta_{\phi} / \partial \mathbf{u}), \quad (3.2.6)$$

which leads to an ordinary differential equation in  $\partial \beta_{\phi} / \partial \mathbf{u}$ :

$$d(\partial\dot{\beta}_\phi/\partial\mathbf{u})dt - (\partial\dot{\beta}_\phi/\partial\beta_\phi)(\partial\beta_\phi/\partial\mathbf{u}) = \delta\dot{\beta}_\phi/\delta\mathbf{u}, \quad (3.2.7)$$

where  $\delta(\cdot)/\delta\mathbf{u}$  is the gradient of  $(\cdot)$  w.r.t.  $\mathbf{u}$  at the fixed point  $\beta_\phi$ . The initial condition of (3.2.7) should be

$$\partial\beta_\phi/\partial\mathbf{u} = 0 \quad \text{at } t = t_\phi, \quad (3.2.8)$$

because the initial creep rate is given and is independent of  $\mathbf{u}$ . The solution of (3.2.7) can be expressed as:

$$\partial\dot{\beta}_\phi/\partial\mathbf{u} = \text{Exp}\left(\int_{t_\phi}^t (\partial\dot{\beta}_\phi/\partial\beta_\phi)d\tau\right) \left[ \int_{t_\phi}^t \delta\dot{\beta}_\phi/\delta\mathbf{u} \text{Exp}\left(-\int_{t_\phi}^\tau (\partial\dot{\beta}_\phi/\partial\beta_\phi)ds\right)d\tau \right], \quad (3.2.9)$$

where the initial condition (3.2.8) has been satisfied.

For the given models (I) and (II), the material parameter vector  $\mathbf{u}$  has three components. But it can be clearly observed from the above formulation that (3.2.5) and (3.2.8) may be specialized or generalized to the case in which the constitutive relation of a material has  $n$  material parameters,  $n = 1, 2, \dots$ , when the problem in question is one dimensional with  $r_\phi$  and  $\beta_\phi$  as the general creep and creep rate. Of course

$$\partial\dot{\beta}_\phi/\partial\mathbf{u} \text{ and } \partial\dot{\beta}_\phi/\partial\beta_\phi$$

in (3.2.9) should be solved for the assigned material from the equations which pertain to the given initial-boundary

value problem.

For models (I), (II) and the initial-boundary value problem pertaining to pressuremeter tests, by taking the time derivative of (3.1.7), we have

$$\dot{\beta}_\phi = \ddot{r}_\phi / r_\phi - \dot{r}^2 / r_\phi^2$$

or

$$\ddot{r}_\phi / r_\phi = \dot{\beta}_\phi + \beta_\phi^2, \quad (3.2.10)$$

which with (3.1.15) leads to an alternative form of the creep equations:

$$(I) \quad \dot{\beta}_\phi = [P - P_\phi - \mu(2\beta_\phi)^{1+m} / (1+m)] / (2\alpha_1) - \beta_\phi^2 \quad (3.2.11)$$

$$(II) \quad \dot{\beta}_\phi = [(1+m)(P - P_\phi)(2\beta_\phi)^{-m} - 2\mu\beta_\phi] / (2\alpha_1) - 2\beta_\phi^2 / (2+m).$$

Then from the above equations, we obtain the explicit expressions:

$$(I) \quad \begin{aligned} \partial \dot{\beta}_\phi / \partial \beta_\phi &= -\mu(2\beta_\phi)^m / \alpha_1 - 2\beta_\phi, \\ \delta \dot{\beta}_\phi / \delta \mu &= -(2\beta_\phi)^{1+m} / [2(1+m)\alpha_1], \\ \delta \dot{\beta}_\phi / \delta \alpha_1 &= -[P - P_\phi - \mu(2\beta_\phi)^{1+m} / (1+m)] / 2\alpha_1^2 \\ &= -(\dot{\beta}_\phi + \beta_\phi^2) / \alpha_1 = -\ddot{r}_\phi / r_\phi / \alpha_1, \\ \delta \dot{\beta}_\phi / \delta m &= \mu(2\beta_\phi)^{1+m} [1/(1+m) - \text{Ln}(2\beta_\phi)] / [2(1+m)\alpha_1]; \end{aligned} \quad (3.2.12)$$

$$\begin{aligned}
\text{(II)} \quad \partial \dot{\beta}_\phi / \partial \beta_\phi &= [ -(1+m)m(P - P_\phi)(2\beta_\phi)^{-m-1} - \mu ] / \alpha_1 - 4\beta_\phi / (2+m), \\
\dot{\delta \beta}_\phi / \delta \mu &= -\beta_\phi / \alpha_1, \\
\dot{\delta \beta}_\phi / \delta \alpha_1 &= -[(1+m)(P - P_\phi)(2\beta_\phi)^{-m} - 2\mu\beta_\phi] / (2\alpha_1^2) \\
\dot{\delta \beta}_\phi / \delta m &= (P - P_\phi)(2\beta_\phi)^{-m} [1 - (1+m)\text{Ln}(2\beta_\phi)] / 2\alpha_1^2 + 2\beta_\phi / (2+m)
\end{aligned}
\tag{3.2.13}$$

For slow creep, it may be postulated that

$$\text{Ln}(2\beta_\phi) \leq 0, \quad \text{for } t \geq t_\phi. \tag{3.2.14}$$

In most engineering problems, the creep rate in question will indeed be slow. For instance, in the pressuremeter tests performed on polycrystalline ice at the University of Manitoba, the maximum creep rate  $\dot{\beta}_\phi$  was only about 0.001 1/min when the cavity pressure was 2 MPa. Another example is finished by the creep data of McTigue and others (1985) who performed triaxial tests on polycrystalline ice. The maximum creep rate was about 0.0018 1/day when the confining pressure was 50 MPa and the extra axial stress was .47 MPa. In what follows, we shall suppose that (3.2.14) be valid.

Since the material parameters should be compatible with the restrictions

$$1 + m > 0, \quad \mu \geq 0, \quad \alpha_1 \geq 0,$$

cf. (Sec.2.3), then for model (I), from (3.2.13), (3.2.14) and  $d^2 r_\phi / dt^2 \leq 0$  (as measured from the creep curves of the data), we obtain

$$\dot{\delta \beta}_\phi / \delta \mu \leq 0, \quad \dot{\delta \beta}_\phi / \delta \alpha_1 \geq 0, \quad \dot{\delta \beta}_\phi / \delta m \geq 0, \quad \text{for } t \geq t_\phi, \tag{3.2.15}$$

which yield

$$\partial \dot{\beta}_\phi / \partial \mu \leq 0, \quad \partial \dot{\beta}_\phi / \partial \alpha_1 \geq 0, \quad \partial \dot{\beta}_\phi / \partial m \geq 0, \quad \text{for } t \geq t_\phi, \quad (3.2.16)$$

from (3.2.12) and from the positivity of the exponential function. Using (3.2.16) and the fact that the cavity radius  $r_\phi$  is positive, we conclude that

$$\partial r_\phi / \partial \mu \leq 0, \quad \partial r_\phi / \partial \alpha_1 \geq 0, \quad \partial r_\phi / \partial m \geq 0, \quad \text{for } t \geq t_\phi \quad (3.2.17)$$

from (3.2.5).

(3.2.16) and (3.2.17) assert as expected that the creep  $r_\phi$  and creep rate  $\dot{\beta}_\phi$  of the ice in the pressuremeter test must decrease as the viscosity  $\mu$  of the ice increases. Secondly, they show that the creep and creep rate must increase with the increment of  $\alpha_\phi$  and  $m$ . This second conclusion is not obvious.

For further analysis, define

$$k = \inf_{t \geq t_\phi} [1/(1+m) - \ln(2\dot{\beta}_\phi(t))] \quad (3.2.18)$$

which is a positive constant from  $1+m \geq 0$  and Assum. (3.2.14). Since

$$0 \leq \delta \dot{\beta}_\phi / \delta \alpha_1 \leq \mu (2\dot{\beta}_\phi)^{1+m} / (1+m) / (2\alpha_1^2) \quad (3.2.19)$$

from (3.2.12), and  $P - P_\phi \geq 0$ , and

$$\delta \dot{\beta}_\phi / \delta m \geq \mu (2\dot{\beta}_\phi)^{1+m} k / (2\alpha_1) / (1+m) \quad (3.2.20)$$

from (3.2.18), then comparison of (3.2.12)<sub>2</sub>, (3.2.19) and (3.2.20) yields

$$\begin{aligned} \dot{\beta}_\phi / \delta\mu &\leq -\alpha_1 \dot{\beta}_\phi / \delta\alpha_1 / \mu \leq 0, \\ - (1/k\mu) \dot{\beta}_\phi / \delta m &\leq \dot{\beta}_\phi / \delta\mu \leq 0, \\ 0 &\leq \dot{\beta}_\phi / \delta\alpha_1 \leq (1/k\alpha_1) \dot{\beta}_\phi / \delta m. \end{aligned} \quad (3.2.21)$$

It can be shown by substitution of (3.2.21) into (3.2.9) that

$$\begin{aligned} |(\partial\beta_\phi/\partial\mu)/(\partial\beta_\phi/\partial\alpha_1)| &\geq \alpha_1/\mu, \\ |(\partial\beta_\phi/\partial\mu)/(\partial\beta_\phi/\partial m)| &\leq 1/(\mu k), \\ |(\partial\beta_\phi/\partial\alpha_1)/(\partial\beta_\phi/\partial m)| &\leq 1/(\alpha_1 k), \quad \text{for } t \geq t_0, \end{aligned} \quad (3.2.22)$$

and hence from (3.2.5),

$$\begin{aligned} |(\partial r_\phi/\partial\mu)/(\partial r_\phi/\partial\alpha_1)| &\geq \alpha_1/\mu, \\ |(\partial r_\phi/\partial\mu)/(\partial r_\phi/\partial m)| &\leq 1/(\mu k), \\ |(\partial r_\phi/\partial\alpha_1)/(\partial r_\phi/\partial m)| &\leq 1/(\alpha_1 k), \quad \text{for } t \geq t_0. \end{aligned} \quad (3.2.23)$$

The values of the ratios given in the right-hand side of (3.2.22) and (3.2.23) are certainly dependent on the unit of time, force and length as well as the maximum creep rate. But the ratios can be estimated as long as  $\mu$ ,  $\alpha_1$  and  $m$  are determined and the maximum  $\beta_\phi$  is given. When

$$|(\partial\beta_\phi/\partial u_i)/(\partial\beta_\phi/\partial u_j)| \gg 1, \quad |(\partial r_\phi/\partial u_i)/(\partial r_\phi/\partial u_j)| \gg 1$$

for  $i, j = 1, 2, 3$ ,  $i \neq j$ , it can be claimed that the parameter  $u_i$  must have a more important effect on the predicted creep

and creep rate than the parameter  $u_j$  does. A quantitative illustration will be given in Sec. 3.4.

Section 3.3 Evaluation of the material parameters  $\mu$   
and  $m$  by fitting data of secondary creep

The experimental data of pressuremeter tests on polycrystalline ice that I have in hand are provided by Kjartanson (1986). They are given in terms of the cavity radius  $r_0^*$  versus time  $t$  pressure  $P = 1000, 1250, 1500, 1750, 2000, 2250, 2500$  MPa in the single-stage tests and  $P = 1500, 1750, 2000, 2250, 2500$  MPa in one multistage test with each stage lasting one day. The ice temperature of all the tests was kept at  $-2^\circ\text{C}$ .

First of all the experimental creep rate  $\dot{r}_0^*$  is calculated by taking the least squares fitting of  $r_0^*$ . For this purpose, the cubic polynomial function  $f(t) = c_0 + c_1 t + c_2 t^2 + c_3 t^3$  is used to fit the data  $r_0^*$  group by group. Each group contains 14 points. It is more or less a matter of experience as far as the choice of the fitting function and the number of points in each group are concerned. After  $c_0$  to  $c_3$  are determined by fitting  $r_0^*$ , the rate of the radius, say  $g^*$ , will be directly calculated from the function  $g(t) = df/dt = c_1 + 2c_2 t + 3c_3 t^2$ . In order to ensure the accuracy of  $g^*$  in the fitting, the last two points in each group of  $g^*$  are deleted because their error may be larger. The first two points of the next group of  $f$  are forced to be equal to the last two points of the former group of  $f$ , which has 12 points after the deletion. The

related least squares fitting formulae are shown in Appendix A.1.

Two typical creep-rate curves of the pressuremeter tests are plotted in Fig. 1; they pertain to tests #3 and #6. Each curve, marked by the point C at which  $\dot{\epsilon}_{\phi}^*$  has the minimum value, can be divided into two parts: the first stands for the primary creep and the next for the secondary creep. It can be seen from Fig. 1 that tertiary creep, for which the creep curve of which should become warped up, has not appeared yet in the two tests. Other single-stage tests have creep curves similar to those of tests #3 and #6. For simplicity, define

$$B^* = \min_{t \geq t_0} (\dot{\epsilon}_{\phi}^* (t)) \quad (3.3.1)$$

for each test. The values of  $\dot{\epsilon}_{\phi}^*$  obtained from fitting of the experimental data are not smooth enough to be used for finding  $B^*$ . Hence, I have taken the average value of  $\dot{\epsilon}_{\phi}^*$  at several points after C as the approximate  $B^*$ . The values of  $B^*$  from the different tests are listed in Table 1, in which the second column is given by the author and those from the multistage tests are given by Kjartanson(1986). Thus we totally have 22 pairs of pressure  $p$  and the minimum creep rate  $B^*$ .

Let us return to (3.1.15). Since for each pressure we can find a point C at and after which  $d\dot{\epsilon}_{\phi}^*/dt \approx 0$ ,  $(\dot{\epsilon}_{\phi}^*)^2 \ll$

$\dot{\epsilon}_\phi^*$ , then for a given pressure and in the secondary creep, (3.2.11) are simplified as:

$$(I, II) \quad \mu (2B_\phi)^{1+m} / (1+m) - (P - P_\phi) = 0, \quad (3.3.2)$$

where  $B_\phi$  denotes the predicted secondary creep rate, and we have set  $d\dot{\epsilon}_\phi/dt = 0$ ,  $(\dot{\epsilon}_\phi)^2 \approx 0$  because we have postulated that the two models can describe secondary creep (Assum. 3.4). It should be noted that the secondary creep equation (3.3.2) of models (I) and (II) is precisely the same as the creep equation under the power-law fluid model which can satisfactorily describe the secondary creep of ice. Thus for pressuremeter test models (I) and (II) can at least describe the secondary creep of ice under different cavity pressures. This assertion will be corroborated in what follows.

Since the secondary creep equations (3.3.2) of models (I) and (II) coincide exactly, we may merge them into

$$B_\phi = [(1+m)(P - P_\phi)/\mu]^{1/(1+m)}/2. \quad (3.3.3)$$

To evaluate  $\mu$  and  $m$  by fitting the data, I define the objective function  $F_\phi$  by

$$F_\phi(\mu, m) = \sum_{i=1}^{22} [B^*(P_i) - B_\phi(\mu, m; P_i)]^2, \quad (3.3.4)$$

where  $B^*$  is given in Table 1 and  $B_\phi$  will be calculated from (3.3.3). we seek a pair of  $\mu$  and  $m$  such that the function  $F_\phi$

arrives at a relative minimum by employing the Levenberg-Marquardt algorithm (Appendix A.2). In all numerical analysis of this work, we will always set  $P_0 = 0$ .

The computer program named MUM for optimizing  $\mu$  and  $m$  by non-linear regression is given at the back of this dissertation. The detailed numerical results are listed in Table A from which it can be seen that after optimization,

$$\mu = 9114 \text{ KPa} \cdot \text{min}^{1+m}, \quad m = -.7111. \quad (3.3.5)$$

A comparison of  $B^*$  and  $B_0$  is shown in Fig. 2. Moreover (3.3.3) can be represented as:

$$\text{Ln}B_0 = [\text{Ln}((1 + m)/\mu) + \text{Ln}P]/(1 + m) - \text{Ln}2, \quad (3.3.6)$$

which gives a linear relation between  $\text{Ln}B_0$  and  $\text{Ln}P$ . Hence I have also plotted (3.3.6) with (3.3.5) in Fig. 3 for the comparison. In Figs. 2 and 3, a square "□" stands for an experimental data point; the solid line is from the prediction. It may be seen from Fig. 2 that (3.3.3) can really fit the data. I have also computed the standard statistical errors  $SE$ , the 95% confidence intervals and the 95% Bonferroni joint confidence intervals of estimated  $\mu$  and  $m$ , all of which are shown in Table A. Since the relative standard statistical errors  $SE(\mu)/\mu = 1367/9114 \approx 15\%$ ,  $SE(m)/m = 0.01194/.7111 \approx 1.7\%$  are acceptable for engineering problems, we shall take the estimated values in

(3.3.5) as the values of material parameters  $\mu$  and  $m$  for the given tested ice.

In the literature, the power law fluid model is usually presented in the version (Hooke, 1981):

$$\dot{\epsilon} = (\tau/B)^n, \quad (3.3.7)$$

where the notations are the same as those in Sec. 1.1. A simple analysis of (3.1.5), (3.1.7) or (3.1.8) shows that for the pressuremeter test problem,

$$\dot{\epsilon} = 6^{-1/2} (2\dot{r}_\phi / r_\phi), \quad (3.3.8)$$

$$\tau = (2/3)^{1/2} \mu (2\dot{r}_\phi / r_\phi)^{1+m} \quad (3.3.9)$$

in the secondary creep period, which can be combined as

$$\dot{\epsilon} = [\tau / (2(6)^{m/2} \mu)]^{1/(1+m)}. \quad (3.3.10)$$

Then (3.3.10) is consistent with (3.3.7) if and only if

$$B = 2(6)^{m/2} \mu, \quad n = 1/(1+m). \quad (3.3.11)$$

Then it follows from (3.3.11) and the results shown in Table A that  $n = 3.46$ ,  $SE(n) = .143$ , the 95% confidence interval of  $n$  is  $[3.19, 3.79]$ , the 95% Bonferroni joint confidence interval is  $[3.15, 3.85]$ , which are consistent with other estimated values of  $n$  for polycrystalline ice (Hooke, 1981). Since the temperature of the tested ice in the above analysis is  $-2^\circ\text{C}$ , which is near the melting point, the ice is rather soft.

It can be seen from Table A that the initial values of  $\mu$  and  $m$  are assigned for iteration. Indeed, the optimized values of  $\mu$  and  $m$  will drift a bit when different initial values are used. But they will still fall within small intervals. When the orders of magnitude of  $\mu$  and  $m$  are unknown before analysis, it is recommended that (3.3.6) be used to fit the data by linear regression, which does not require the assignment of initial values. Then the optimized values from linear regression can be taken as the initial values for the non-linear regression using (3.3.3). Along these lines, from the same data of the pressuremeter tests, I got

$$\mu = 9006 \text{ KPa} \cdot \text{min}^{1+m}, \quad m = -.7132 \quad (3.3.12)$$

by linear regression. The nonlinear regression analysis in which the values in (3.3.12) were used as the initial values showed that

$$\mu = 8956 \text{ KPa} \cdot \text{min}^{1+m}, \quad m = -.7128, \quad (3.3.13)$$

which are very close to the values in (3.3.5).

At the end of this section, I would like to emphasize that from the above discussion models (I) and (II) can satisfactorily fit the secondary creep data of polycrystalline ice under different cavity pressures in pressuremeter tests.

**Section 3.4** Evaluation of the material parameter  $\alpha_1$   
by fitting data of primary creep

In this section, we shall evaluate the material parameter  $\alpha_1$  by fitting the primary creep data of the given pressuremeter tests when  $\mu = 9114 \text{ KPa}\cdot\text{min}^{1+m}$  and  $m = -.7111$  are fixed.

As mentioned in Sec. 3.3, during secondary creep,  $d\beta_\phi/dt \approx 0$  and  $(\beta_\phi)^2 \approx 0$  so that  $d^2r_\phi/dt^2 \approx 0$  from (3.2.10). It implies that the term containing  $\alpha_1$  will not influence secondary creep and will only play its role during primary creep. The primary creep data may suffice for the determination.

When the values of  $\mu$  and  $m$  are fixed, the predicted radius  $r_\phi$  solved from (3.1.15) is a function of time  $t$  and the parameter  $\alpha_1$  for the given pressure  $P$ . Hence, we define the objective function

$$(I, II) \quad F_1(\alpha_1; t_0, t_N) = \sum_{i=0}^N [r_\phi^*(t_i) - r_\phi(\alpha_1; t_i)]^2; \quad (3.4.1)$$

here  $r_\phi^*$  is the measured cavity radius and  $r_\phi$  the predicted radius solved from (3.1.15),  $r_\phi^* - r_\phi$  is called the residual; for  $i=0, 1, 2, \dots, N$ , where  $N$  is a positive integer,  $t_i$  are the instants at which measurements were made in the test;  $t_0$  and  $t_N$  are the initial and terminative time of the

fitting period. We shall seek a value of  $\alpha_1$  such that the function  $F_1$  arrives at a minimum by using the Levenberg-Marquardt algorithm (Appendix A.2). Before doing it, we have to calculate  $r_\phi(\alpha_1, t)$ .

I took  $t_0 \approx 10$  min as the initial time for all the tests, although the data of each test were recorded from about 1 min. The reason is that at the beginning of each test deformation in both the rubber membrane of the pressuremeter and the tested ice would be mainly elastic, but what concerned us here is only the creep behaviour of the ice. Considering the fact that the creep rate of the ice specimen would decrease quickly from its initial value and the ice specimen would be in secondary creep after about 500 min for the given pressures, I set a value of  $N$  such that  $t_N \approx 200$  min. To examine whether my choice was feasible, I used several  $t_N$  which varied from 100 to 300 min, as the terminative time to fit the data of several tests. It was found (cf. Table 2) that the longer  $t_N$  was, the larger the value of  $\alpha_1$  became, but the variation of  $\alpha_1$  was small. The assigned values of  $t_N$  used in further analysis are shown in Table 3.

For a given pressure and a roughly assigned value of  $\alpha_1$ , we can obtain a numerical solution  $r_\phi(\alpha_1, t)$  of (3.1.15) by using the Runge-Kutta integration algorithm (see Appendix A.3). In my work I chose the integration step lengths  $h = 0.01j$ ,  $j = 1, 2, \dots, 300$  to save the CPU time occupying the

computer since my final aim was to evaluate  $\alpha_1$  by iteration in which (3.1.15) would be numerically solved repeatedly. For the chosen integration step lengths, the time nodes of the predicted solution  $r_\phi(\alpha_1, t)$  were given in a sequence  $\{t_j\}$  where

$$t_j = t_0 + 0.01j(j+1)/2. \quad j = 1, 2, \dots, \quad (3.4.2)$$

Then at  $t_1 \approx 10.01$  min,  $t_{150} \approx 123$  min and  $t_{250} \approx 343$  min, the integration step lengths are 0.01, 1.5 and 2.5 min, respectively, which are much smaller than the recorded time step lengths: 2, 10 and 10 min respectively in all the tests. Thus integration accuracy could be satisfied by the chosen  $h$ . Since the time nodes of  $r_\phi(\alpha_1, t)$  usually would not coincide with those of the experimental data, the Lagrange interpolation algorithm with variable distance were employed to get  $r_\phi(\alpha_1, t_i)$  in (3.4.1).

There remained the problem how to choose the initial value of  $\alpha_1$  to start the iteration and whether different choices of the initial  $\alpha_1$  would converge to the same value. Several initial values of  $\alpha_1$  were tried. It was found that for both models (I) and (II) initial values of  $\alpha_1$  which ranged over three orders of magnitude converged to effectively almost the same final value after iteration; cf. Table 4. Therefore, one is permitted to choose the initial value of  $\alpha_1$  rather roughly.

Eventually for each test, I took  $\alpha_1 = 10^9$  KPa.min<sup>2</sup> for model (I) and  $\alpha_1 = 10^6$  KPa.min<sup>2+m</sup> for model (II) as the initial value of  $\alpha_1$ ,  $t_0 \approx 10$  min,  $t_N \approx 200$  min as the initial and terminated time, and fixed  $\mu = 9114$  KPa.min<sup>1+m</sup>,  $m = -.7111$  to estimate  $\alpha_1$  of the two models by fitting the primary creep data of all the tests. The results are listed in Tables 5 and 6, where "objfun" is the value of the objective function defined by (3.4.1), and  $SE(\alpha_1)$  is the standard statistical error; the relative error in column 7 between the measured and the predicted cavity radius  $r_{\phi}^*$  and  $r_{\phi}$  is defined by

$$\text{Error} = [r_{\phi}^*(t) - r_{\phi}(t)]/[r_{\phi}^*(t) - r_{\phi}^*(t_0)], \quad (3.4.3)$$

where  $r_{\phi}^*(t_0)$  is the initial radius. A comparison of  $r_{\phi}^*$  and  $r_{\phi}$  is exhibited in Figs. 4 to 10 for model (I), where in each figure the symbol "□" stands for a data point, and the solid line denotes the predicted curve. Since the predicted radii of models (I) and (II) are very close to each other, I have omitted plotting the predicted curve  $r_{\phi}$  of model (II).

Based on the numerical analysis, I should like to add the following remarks:

(a) For the two models and for all the tests, the maximum relative error of the measured and predicted radii in long-term creep is about  $\pm 20\%$ , which is usually acceptable in civil engineering. Indeed the long-term relative error of

each test is only about or less than  $\pm 10\%$  except for test #5.

(b) From Figs. 4 to 10, all the predicted radii fit very well the test data of primary creep.

(c) The scatter of the optimized  $\alpha_1$  as determined from the data of each test is small. Especially for model (II), the variation of the value of  $\alpha_1$  determined from all the tests is very small.

(d) For the tested polycrystalline ice with temperature at  $-2^\circ\text{C}$ , the value of  $\alpha_1$  may be taken as:

$$(I) \quad \alpha_1 = 2.562 \times 10^8 \text{ KPa} \cdot \text{min}^2, \quad (3.4.4)$$

$$(II) \quad \alpha_1 = 1.255 \times 10^5 \text{ KPa} \cdot \text{min}^{1+m}, \quad (3.4.5)$$

which are the average of the evaluated  $\alpha_1$  from the given tests.

It can be concluded from the above observations that both model (I) and model (II) can adequately describe not only the secondary creep (cf. Sec. 3.3) but also the primary creep of polycrystalline ice.

Finally, I want to quantitatively compare the effect of the material parameters on the predicted creep and creep rate. By fitting the measured radius  $r_0^*$ , I get the approximate maximum creep rate  $\dot{\epsilon}_0 = .00089 \text{ 1/min}$ , which is estimated from test #2 with cavity pressure  $p = 2500 \text{ KPa}$ . Then from (3.2.18) and  $m = -.7111$ ,

$$k = 9.8. \quad (3.4.6)$$

Now for model (I), with  $k = 9.8$ ,  $\mu = 9114 \text{ KPa}\cdot\text{min}^{1+m}$ ,  $\alpha_1 = 2.562 \times 10^8 \text{ KPa}\cdot\text{min}^2$  and  $m = -.7111$  on hand, I find that for the ratios in (3.2.22) and (3.2.23),

$$\begin{aligned} \alpha_1 / \mu &= 2.8 \times 10^{-4} \text{ min}^{1-m}, \\ \mu k &\approx 10235 \text{ KPa}\cdot\text{min}^{1+m}, \\ \alpha_1 k &\approx .25 \times 10^{10} \text{ KPa}\cdot\text{min}^2, \end{aligned} \quad (3.4.7)$$

which with (3.2.22) and (3.2.23) show that for the given units, the importance of the effect of the material parameters on the predicted creep and creep rate of the ice in the pressuremeter problem is in the order of  $m$ ,  $\mu$  and  $\alpha_1$  for model (I). We can arrive at the same conclusion for model (II).

The complete program named ALPHAL to optimize  $\alpha_1$  for model (I) when  $\mu$  and  $m$  are fixed is given at the end of the dissertation; the subroutine ZXSSQ in the program is the finite difference analogue of the Levenberg-Marquardt method issued by IMSL. The program for model (II) is similar and is thence omitted.

### Section 3.5 Discussion

It is well known from the literature (Hooke, 1981) that the power-law fluid model can adequately represent the secondary creep of polycrystalline ice. For instance, velocity profile in shearing flows as predicted from this model is close to that measured from glaciers which undergoes shearing flows (Sec. 5.1). But the power-law fluid model has at least two shortcomings. A glance at (3.3.3), the creep equation which pertains to the power-law fluid model for pressuremeter tests, reveals that the predicted creep rate should remain constant with time under a constant cavity pressure. However, taking a look at the measured creep rates (Fig. 1), we observe that for a single-stage creep test with a constant cavity pressure the creep rate in fact decreases with time during primary creep. Consequently, the power-law fluid model cannot describe the primary creep of polycrystalline ice. And hence we cannot evaluate the material parameters of the model by fitting short-term data. The power-law fluid model also fails to exhibit normal stress effects in shearing flows (Sec. 5.1) and (McTigue and others, 1985).

Noticing the defects of the power-law fluid model, McTigue and others (1985) suggested to use the second-order fluid model (1.1.4) as the constitutive relation for polycrystalline ice undergoing creep when they initiated the

study of the possible significance of normal stress effects on the shearing flows of glaciers. By setting  $m = 0$  in (3.1.15), we have the creep equation:

$$\alpha_1 \ddot{r}_\phi / r_\phi + \mu \dot{r}_\phi / r_\phi - (P - P_\phi) / 2 = 0$$

or

$$\alpha_1 [\dot{\beta}_\phi + \beta_\phi^2] + \mu \beta_\phi - (P - P_\phi) / 2 = 0, \quad (3.5.1)$$

which is exactly the equation that pertains to the second order fluid model. It can be seen from (3.5.1) that the creep rate is no longer constant under a fixed pressure since the term containing the derivative of creep rate appears in the creep equation. In other words, the model may fit the primary creep. The second-order fluid model can certainly exhibit normal stress effects in shearing flows (Truesdell and Noll, 1965). Now, suppose the model can also fit the secondary creep. Then (3.4.8) is reduced to

$$\mu \beta_\phi(t) - (P - P_\phi) / 2 = 0 \quad (3.5.2)$$

in the secondary creep in which  $d\beta_\phi/dt = 0$ . (3.5.2) asserts that the relation between the creep rate and pressure is linear. However the experimental data definitely deny this relation (see Fig. 2). Thus the second-order fluid model fails to represent the secondary creep when the cavity pressure has different constant values. In addition, there

is an obvious discrepancy between the velocity profile predicted by the model and that measured from the shearing flows of glaciers (Sec. 5.1).

It is interesting from the above discussion that the merits of the second order fluid model seem to remedy the defects of the power law fluid model, and vice versa. Just for this reason, Man (1984) proposed the two special Rivlin-Ericksen fluid models (1.2.1) and (1.2.2) as tentative constitutive relations for polycrystalline ice undergoing primary and secondary creep; these two models have the same velocity profile as the power-law fluid model in steady shearing flows and show normal stress effects in such flows.

But when fluids (I) and (II) finish primary creep, they will always stay at secondary creep and never enter tertiary creep which indeed takes place in a complete creep process of a real material. Of course, it is hard to give a three-dimensional constitutive relation which can completely cover the three stages of creep.

The rest of this section will be focused on the comparison of models (I) and (II). Although the two models are cut from the same cloth, they will not have exactly the same performance in all events.

Recalling (3.1.15), one may feel inclined to choose model (I) since the creep equation of it is neater than that of model (II). But the creep equations of both models (I) and (II) are non-linear so that they have to be solved

numerically. With the computer as a tool, the fact that model (I) has a simpler creep equation is no longer significant. It remains to be seen which model will give the better fit to the experimental data.

Looking back at Tables 5 and 6, we observe that the scatter in the optimized values of the material parameter  $\alpha_1$  of model (II) is much smaller than that of model (I). Thus, model (II) seems to be more attractive than model (I) does. Secondly, Tables 5 and 6 show that the values of the objective function of model (II) is less than that of model (I) for every test. The reason, according to my numerically analysis, is that the predicted creep rate of model (II) arrives at a constant later and is closer to the experimental data than model (I) does. Consequently, model (II) can give a better fitting to the primary creep data. As for the secondary creep, the two models have the same performance.

When evaluating the material parameters by only fitting the primary creep data of polycrystalline ice, it is expected that model (II) will be more acceptable.

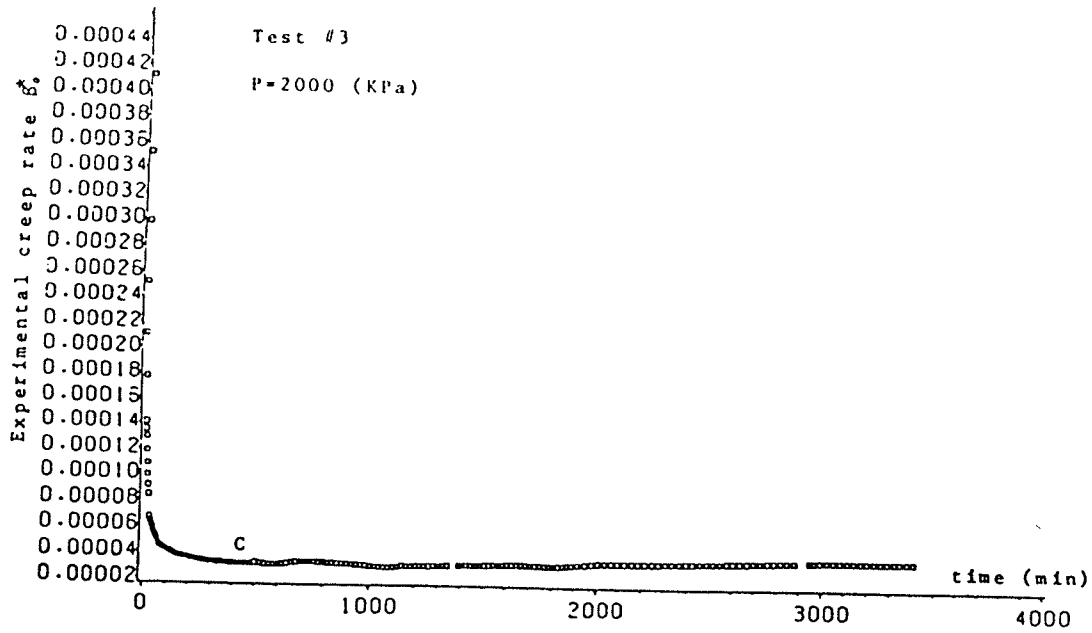


Fig. 1

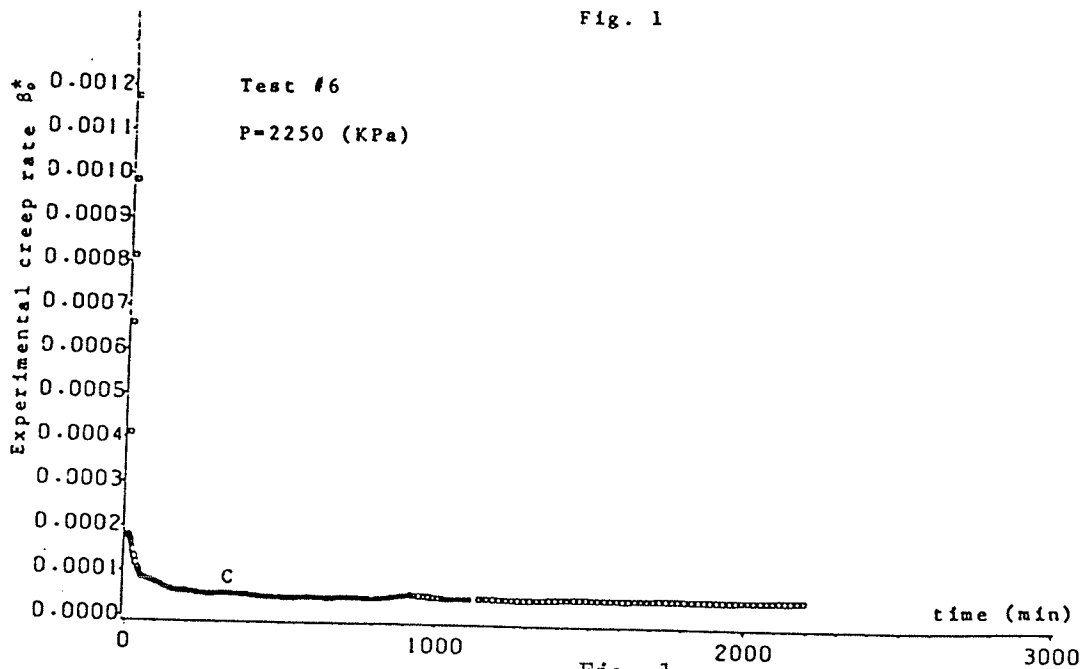


Fig. 1

Experimental creep rate versus time in  
pressuremeter tests #3 & #6

Table 1

-----  
 The minimum creep rate  $\beta^*$  of the pressuremeter tests.

Pressure P(KPA)	$\beta^* \cdot 10^4$ 1/min		
	(#10)	(#12)	(#13)
1000	.03692	-----	-----
1250	.07110	-----	-----
1500	.1052	.1340	.1050
1750	.2127	.2040	.1800
2000	.3147	.3420	.3100
2000	.3171	-----	-----
2250	.4582	.5400	.5450
2500	.8125	.8400	-----
			.7800

Table 2

-----  
 Optimize  $\alpha_1$  when  $\mu = 9114 \text{ KPa} \cdot \text{min}^{1+m}$  and  $m = -.7111$  are fixed by fitting the primary creep data of pressuremeter tests for several fitted time intervals.

Test	t <sub>0</sub> (min)	t <sub>N</sub> (min)	Model I	Model II
			$\alpha_1 \cdot 10^{-8}$	$\alpha_1 \cdot 10^{-5}$
#3	10	111	1.497	.8772
#3	10	170	1.594	.9187
#3	10	240	1.650	.9495
#3	10	315	1.658	.9393
#6	8	100	1.197	1.040
#6	8	160	1.384	1.154
#6	8	220	1.447	1.199
#6	8	290	1.505	1.207
#10	7	85	2.930	1.322
#10	7	135	3.141	1.431
#10	7	220	3.461	1.553
#10	7	280	3.759	1.693

-----  
 where the initial  $\alpha_1 \cdot 10^{-8} = 10. \text{ KPa} \cdot \text{min}^2$  (I)

$\alpha_1 \cdot 10^{-5} = 10. \text{ KPa} \cdot \text{min}^{2+m}$  (II)

Determination of mu and m from the secondary creep rates by nonlinear regression

Notation:

P---cavity pressure; b---rate of secondary creep; bb---predicted values of b;  
 residual---b(i)-bb(i); Dbjfun---sum of squared residuals;  
 $er1=100 \cdot [b(i)-bb(i)]/b(i)$ ;  $er2=100 \cdot [Ln(b(i))-Ln(bb(i))]/(-Ln(b(i)))$ .

Units:

P in KPa, b and bb in 1./min, mu in KPa.min<sup>m</sup>=[1 +m]; m is a real number

mu	m	Dbjfun: in iteration
9499.88609	- .709999740	.502099917E-09
9499.72266	- .709999740	.516631182E-09
9499.89809	- .709496798	.390131261E-09
9113.85328	- .711110294	.225588950E-09
9120.31250	- .711110055	.224595730E-09
9107.40625	- .711109817	.227070113E-09
9113.85837	- .710606156	.258575827E-09
9113.85847	- .711812999	.230008901E-09

Least square estimates: mu= 9113.85156 m= -0.71111 Dbjfun=.22559E-09 Convergence criterion: 2

XJAC, gradient of residuals w.r.t. mu and m at the least square estimates.	Residuals:
0.123234E-08	0.45425E-06
0.267000E-08	0.10130E-06
0.501818E-08	0.26591E-05
0.501818E-08	0.26781E-05
0.501818E-08	0.11761E-05
0.501818E-08	0.22387E-06
0.854898E-08	0.44659E-05
0.854898E-08	0.20659E-05
0.854898E-08	0.14659E-05
0.854898E-08	0.19594E-05
0.135807E-07	0.46659E-05
0.135807E-07	0.41968E-05
0.135807E-07	0.39569E-05
0.135807E-07	0.14668E-05
0.204009E-07	0.11689E-05
0.204009E-07	0.78005E-05
0.204009E-07	0.37948E-06
0.204009E-07	0.37948E-06
0.293964E-07	0.87947E-06
0.293964E-07	0.78129E-06
0.293964E-07	0.40313E-05
0.293964E-07	0.67813E-05

Matrix XJACT*XJACT	Inverse of XJACT*XJACT
0.558111E-14	0.165599E+18
0.638257E-09	0.144848E+13
	0.128484E+06

SE(mu): 1386.699 SE(m): 0.0119443  
 95% confidence interval of mu: [ 5262.9 , 11864.8] 95% confidence interval of m: [-.73603 , -.66619].  
 95% Bonferroni joint confidence interval of mu: [ 5802.2 , 12425.5], of m: [-.74005 , -.66217]

P:	b:	bb:	er1%:	Ln(P):	Ln(b):	Ln(bb):	er2%:
0.100E+04	0.3692E-05	0.3238E-05	0.1230E+02	0.6908E+01	-.1251E+02	-.1264E+02	0.1048E+01
0.1250E+04	0.7111E-05	0.7010E-05	0.1421E+01	0.7131E+01	-.1185E+02	-.1187E+02	0.1207E+00
0.1500E+04	0.1052E-04	0.1318E-04	-.2525E+02	0.7313E+01	-.1146E+02	-.1124E+02	-.1864E+01
0.1500E+04	0.1050E-04	0.1318E-04	-.2548E+02	0.7313E+01	-.1146E+02	-.1124E+02	-.1981E+01
0.1500E+04	0.1200E-04	0.1318E-04	-.8805E+01	0.7313E+01	-.1133E+02	-.1124E+02	-.8255E+00
0.1500E+04	0.1340E-04	0.1318E-04	0.1667E+01	0.7313E+01	-.1122E+02	-.1124E+02	0.1498E+00
0.1750E+04	0.1800E-04	0.2247E-04	-.2482E+02	0.7467E+01	-.1083E+02	-.1070E+02	-.2029E+01
0.1780E+04	0.2040E-04	0.2247E-04	-.1013E+02	0.7467E+01	-.1080E+02	-.1070E+02	-.8936E+00
0.1750E+04	0.2100E-04	0.2247E-04	-.6885E+01	0.7467E+01	-.1077E+02	-.1070E+02	-.6213E+01
0.1750E+04	0.2227E-04	0.2247E-04	-.8837E+00	0.7467E+01	-.1071E+02	-.1070E+02	-.6268E+00
0.2000E+04	0.3100E-04	0.3567E-04	-.1506E+02	0.7601E+01	-.1038E+02	-.1024E+02	-.1351E+01
0.2000E+04	0.3147E-04	0.3567E-04	-.1334E+02	0.7601E+01	-.1037E+02	-.1024E+02	-.1208E+01
0.2000E+04	0.3171E-04	0.3567E-04	-.1248E+02	0.7601E+01	-.1036E+02	-.1024E+02	-.1136E+01
0.2000E+04	0.3420E-04	0.3567E-04	-.4293E+01	0.7601E+01	-.1028E+02	-.1024E+02	-.4088E+00
0.2000E+04	0.3450E-04	0.3567E-04	-.3386E+01	0.7601E+01	-.1027E+02	-.1024E+02	-.3241E+00
0.2250E+04	0.4582E-04	0.5362E-04	-.1703E+02	0.7719E+01	-.9991E+01	-.9834E+01	-.1574E+01
0.2250E+04	0.5400E-04	0.5362E-04	0.6991E+00	0.7719E+01	-.9827E+01	-.9834E+01	0.7142E+01
0.2250E+04	0.5400E-04	0.5362E-04	0.6991E+00	0.7719E+01	-.9827E+01	-.9834E+01	0.7142E+01
0.2250E+04	0.5430E-04	0.5362E-04	0.1610E+01	0.7719E+01	-.9817E+01	-.9834E+01	0.1654E+00
0.2500E+04	0.7800E-04	0.7722E-04	0.9981E+00	0.7824E+01	-.9459E+01	-.9469E+01	0.1061E+00
0.2500E+04	0.8125E-04	0.7722E-04	0.4955E+01	0.7824E+01	-.9418E+01	-.9469E+01	0.5400E+00
0.2500E+04	0.8400E-04	0.7722E-04	0.8070E+01	0.7824E+01	-.9385E+01	-.9469E+01	0.8966E+00

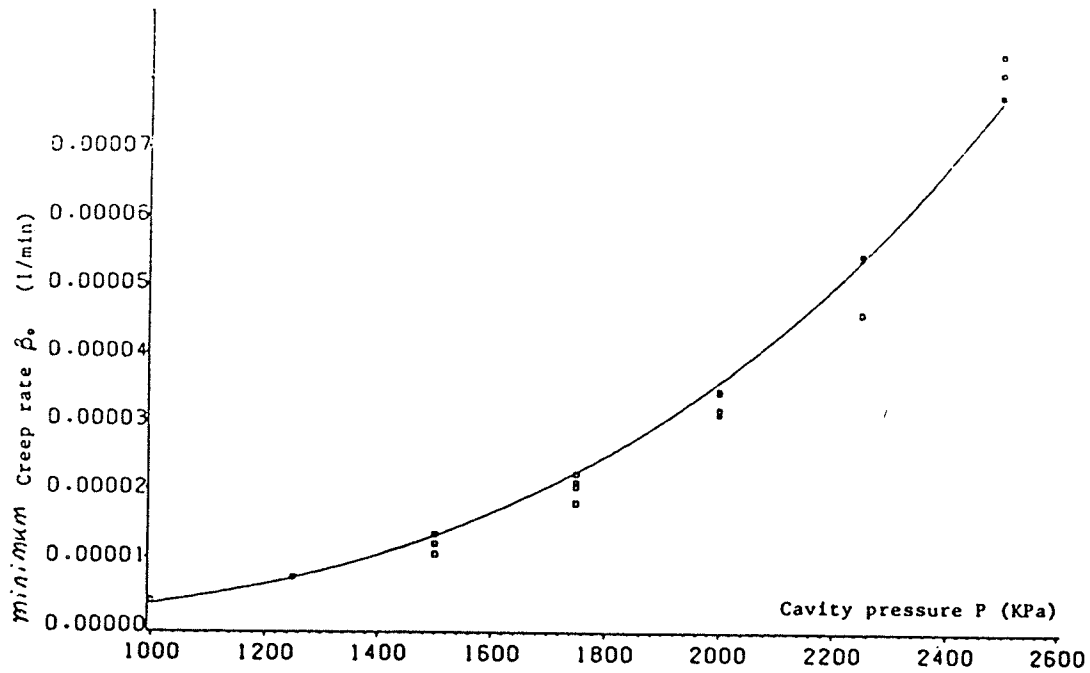


Fig. 2

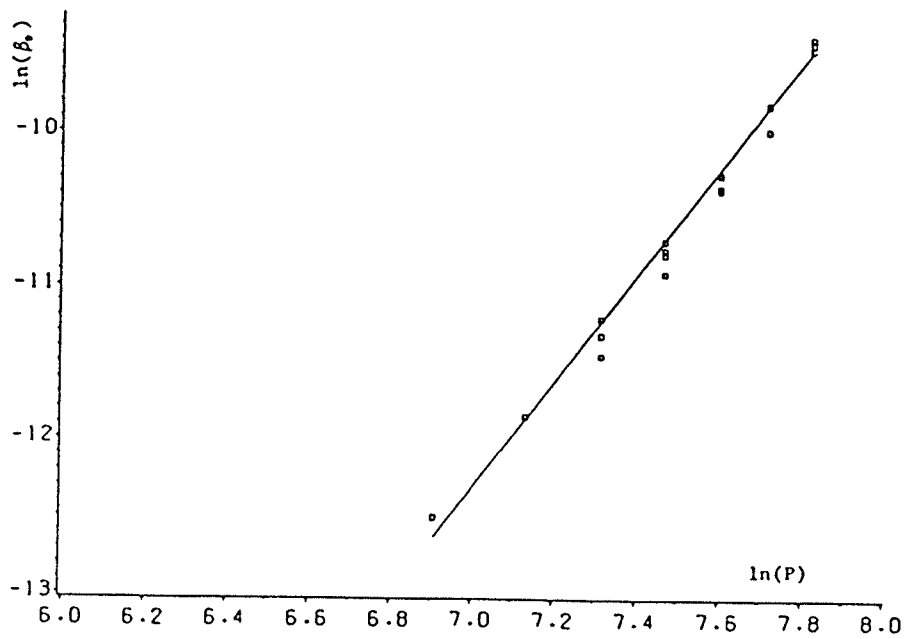


Fig. 3

Comparison of experimental & predicted secondary creep rates versus cavity pressure for pressuremeter tests

Table 3

-----  
 Cavity pressure  $p$ , fitted time interval  $[t_0, t_N]$  and  
 number of points for fitting.  
 -----

Test	P(KPa)	$[t_0, t_N]$ (min)	N
#2	2500	[5, 240]	25
#3	2000	[10, 240]	30
#4	2000	[8, 180]	30
#5	1500	[8, 260]	17
#6	2250	[8, 220]	30
#7	1750	[9, 200]	25
#10	1500	[7, 220]	50

-----  
 \*---The first stage pressure of multistage test #10.  
 -----

Table 4

Optimize  $\alpha_1$  when  $\mu = 9114 \text{ KPa} \cdot \text{min}^{1+m}$  and  $m = -.7111$  are fixed by  
 fitting the data of primary creep of pressuremeter tests for several  
 initial values of  $\alpha_1$ .

Test	initial		after iteration	
	(I) $\alpha_1 * 10^{-8}$	(II) $\alpha_1 * 10^{-5}$	$\alpha_1 * 10^{-8}$ Model I	$\alpha_1 * 10^{-5}$ Model II
#3	.1000		1.655	.9425
#3	1.000		1.651	.9403
#3	10.00		1.650	.9495
#3	100.0		1.337	.9079
#6	.1000		1.455	1.197
#6	1.000		1.464	1.198
#6	10.00		1.447	1.199
#6	100.0		1.340	1.068

Optimize  $\alpha_1$  by fitting the primary creep data of pressuremeter tests  
 when  $\mu=9114(\text{KPa}\cdot\text{min}^{1+m})$  and  $m=-.7111$  are fixed.

Table 5

Model (I)

Initial value of  $\alpha_1 \cdot 10^{-8} = 10. (\text{KPa}\cdot\text{min}^2)$

Test	P(KPa)	optimized $\alpha_1 \cdot 10^{-8}$	objfun $\cdot 10^5$	SE( $\alpha_1$ ) $\cdot 10^{-8}$	95%confidence interval $\cdot 10^{-8}$	Error%	at t (min)
#2	2500	.7223	14.2	.0254	[.6693 , .7754]	+10.7	2175
#3	2000	1.650	1.15	.0415	[1.565 , 1.735]	+.266	5095
#4	2000	1.491	1.93	.0295	[1.431 , 1.552]	-2.00	4530
#5	1500	5.951	.495	.4981	[4.895 , 7.007]	-19.4	6360
#6	2250	1.447	6.83	.0173	[1.412 , 1.483]	-10.2	2395
#7	1750	3.211	2.83	.1658	[3.045 , 3.376]	-9.21	1700
#10	1500	3.461	.903	.1113	[3.238 , 3.685]	+7.84	5810

Average  $\alpha_1 \cdot 10^{-8} = 2.562(\text{KPa}\cdot\text{min}^2)$

Table 6

Model (II)

Initial value of  $\alpha_1 \cdot 10^{-5} = 10. (\text{KPa}\cdot\text{min}^{2+m})$

Test	P(KPa)	optimized $\alpha_1 \cdot 10^{-5}$	objfun $\cdot 10^3$	SE( $\alpha_1$ ) $\cdot 10^{-5}$	95%confidence interval $\cdot 10^{-5}$	Error%	at t (min)
#2	2500	.8379	7.78	.0404	[.7533 , .9225]	+10.7	2175
#3	2000	.9495	.568	.0086	[.9320 , .9670]	+.332	5095
#4	2000	.9425	.646	.0108	[.9204 , .9646]	-1.95	4530
#5	1500	1.766	.485	.0782	[1.600 , 1.932]	-19.5	6360
#6	2250	1.199	2.58	.0110	[1.170 , 1.222]	-10.2	2395
#7	1750	1.686	2.07	.0501	[1.636 , 1.736]	-10.5	1700
#10	1500	1.553	.395	.0171	[1.518 , 1.587]	+8.35	5810

Average  $\alpha_1 \cdot 10^{-5} = 1.255(\text{KPa}\cdot\text{min}^{2+m})$

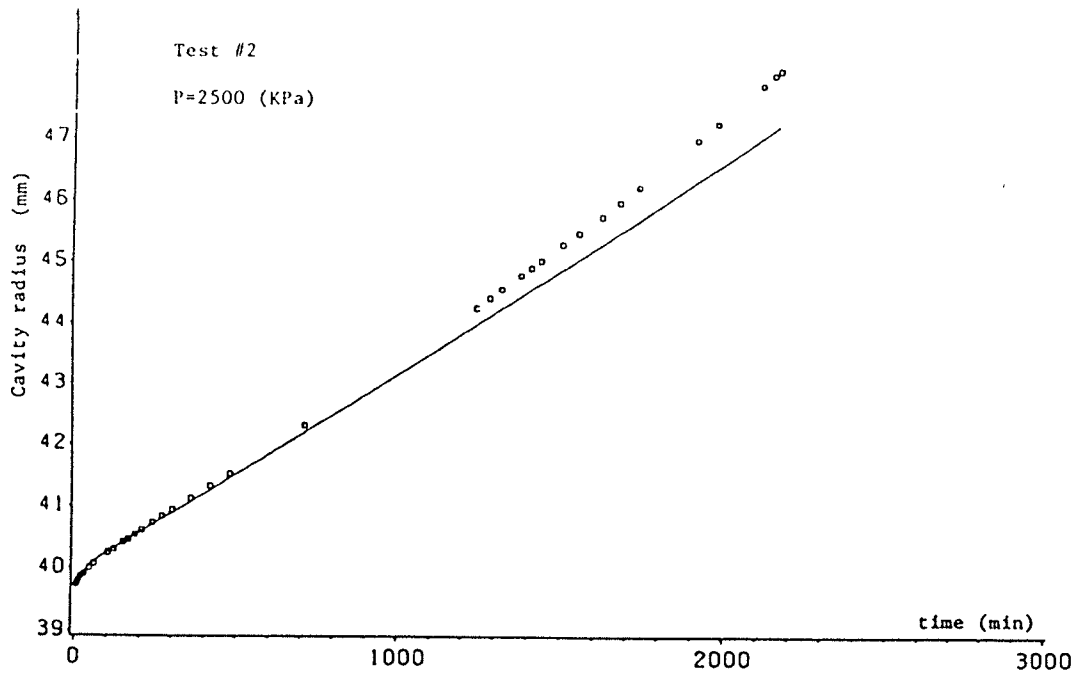


Fig. 4

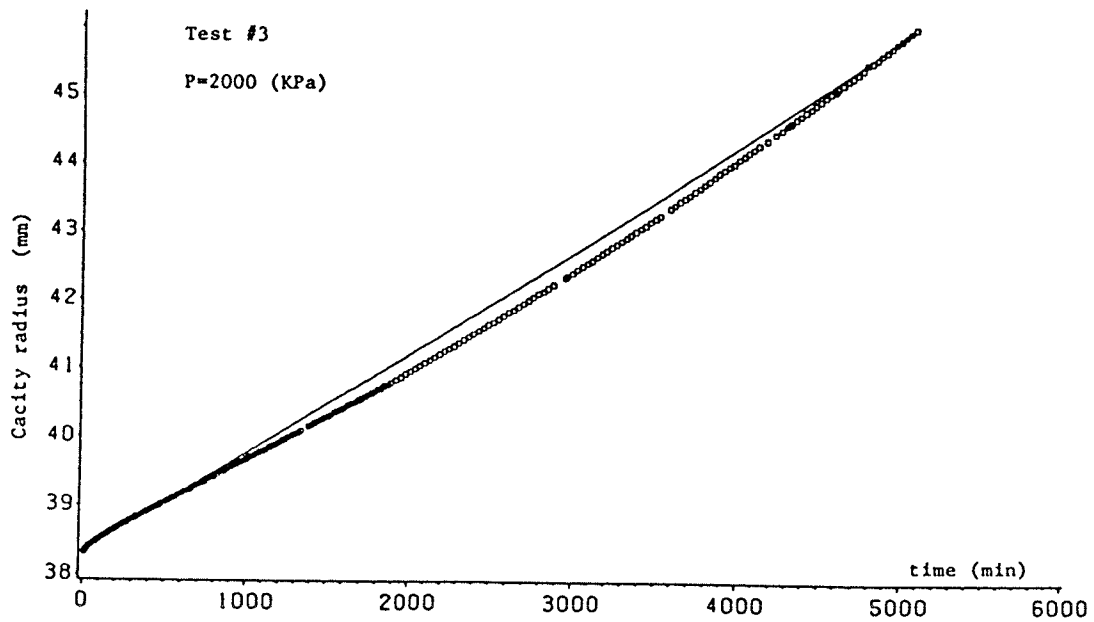


Fig. 5

Comparison of experimental & predicted creep by model (I)  
for pressuremeter tests #2 & #3

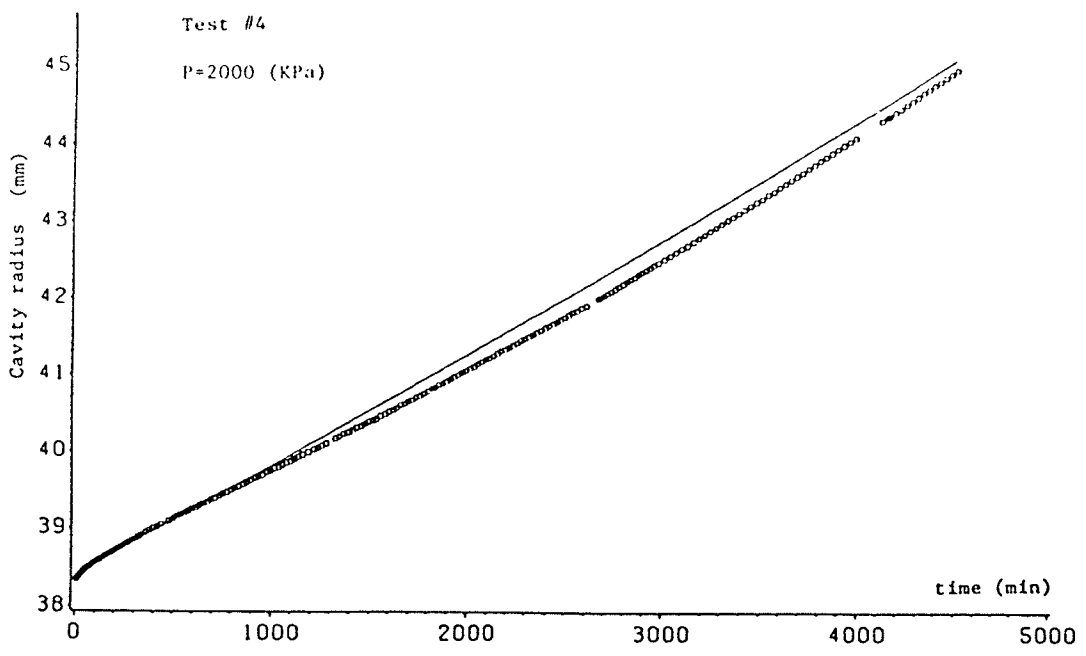


Fig. 6

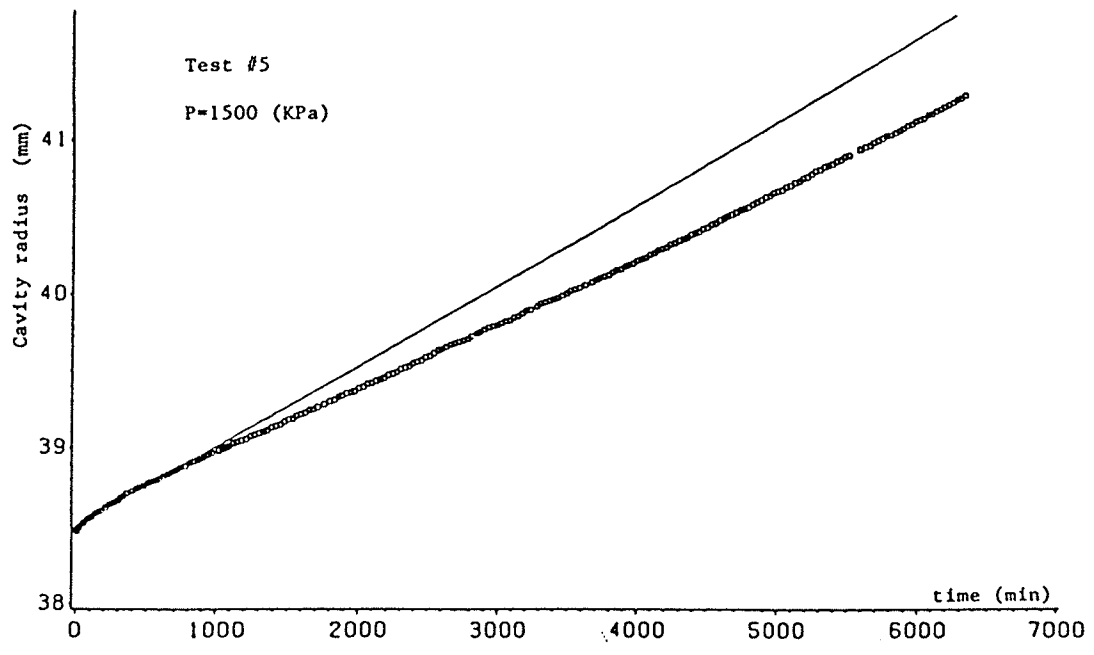


Fig. 7

Comparison of experimental & predicted creep by model (I) for pressuremeter tests #4 & #5

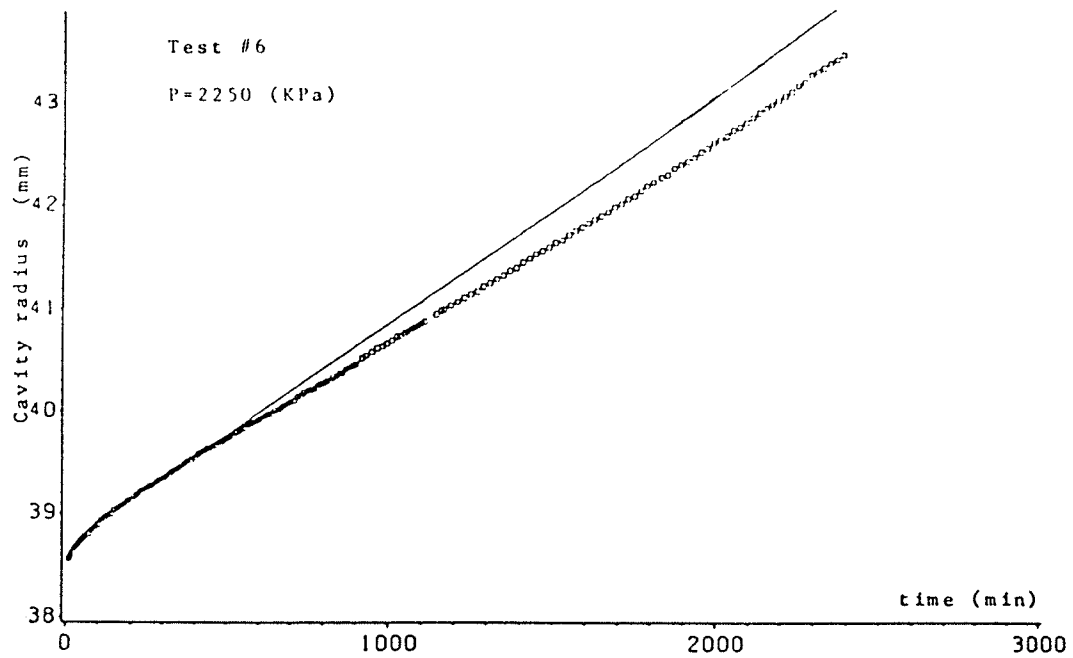


Fig. 8

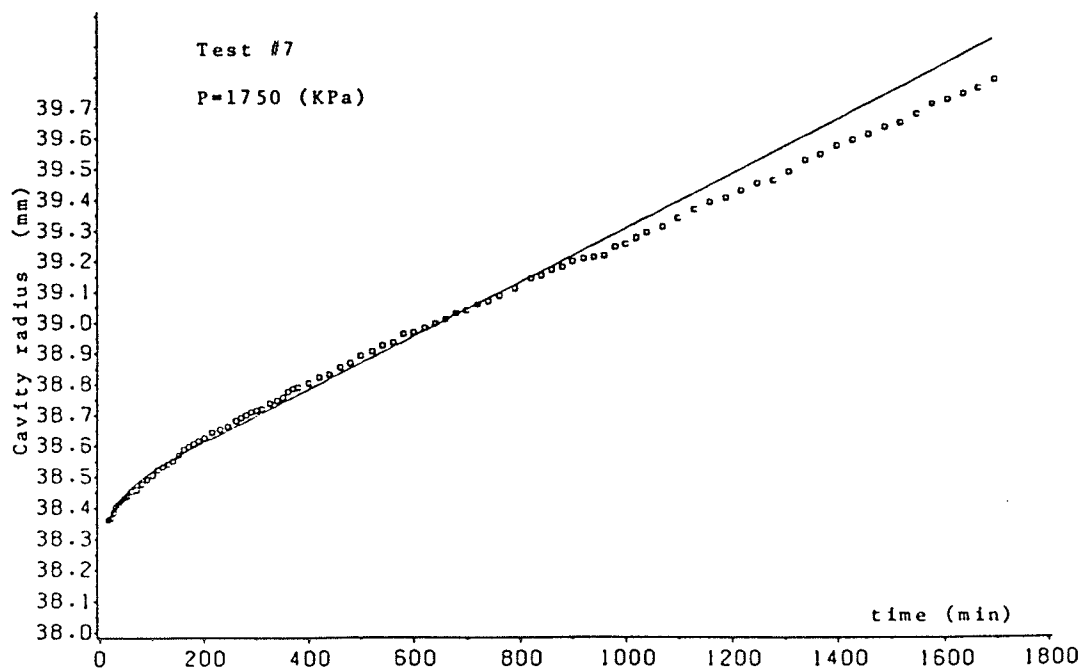


Fig. 9

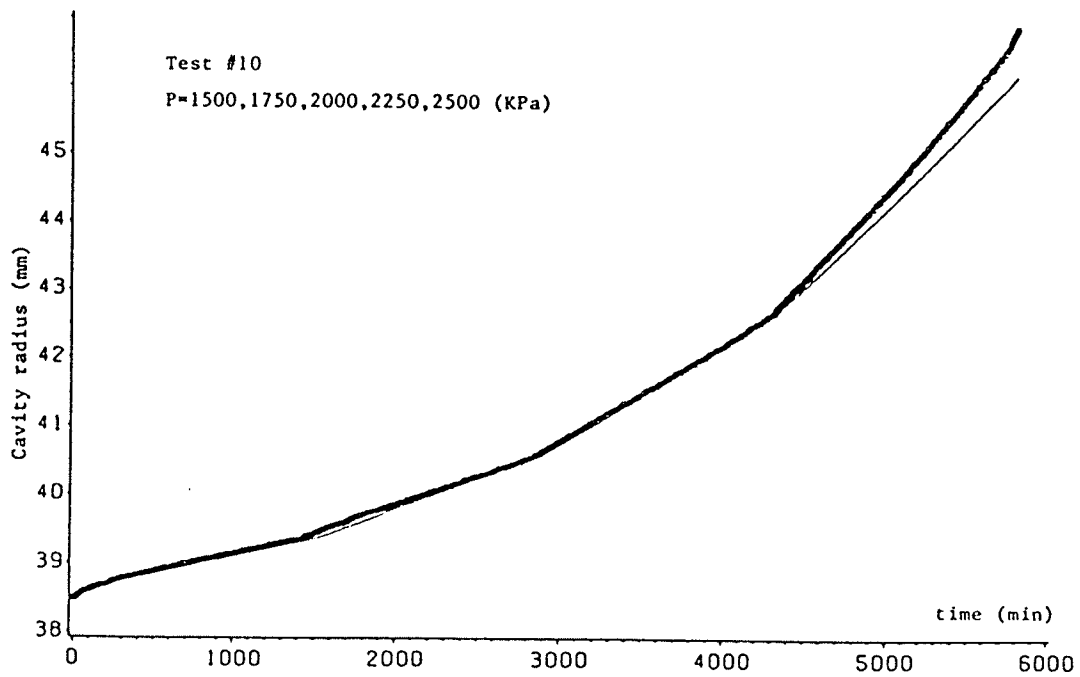


Fig. 10

Comparison of experimental & predicted creep by model (I)  
for multistage-pressure test #10

## Chapter 4 Evaluation of material parameters by fitting data of triaxial tests

### Section 4.1 Initial value problem pertaining to triaxial tests

It has been shown in Chapter 3 that the predicted creep from models (I) and (II) can fit very well the primary and secondary creep of polycrystalline ice in the pressuremeter tests. To examine the reliability of the two models as the constitutive relations of ice undergoing creep, we shall use them to fit the creep data from several triaxial tests of polycrystalline ice. It could be asserted that a good model which may be reliably used as a constitutive relation of a material should at least fit the experimental data of different tests for the material.

To reveal the possible significance of normal stress effects on the shear flow of glaciers, McTigue and others (1985) used the second order fluid model as the constitutive relation for polycrystalline ice. They evaluated the material parameters in the second order fluid model by fitting their experimental data of triaxial tests on ice. Their work was criticized by Man and Sun (1986), who used the same data of McTigue and others (1985) and adopted the assumptions 4.1 to 4.4 given by McTigue and others (1985) for the purpose of comparing models (I) and (II) with

theirs. In this Chapter I will supply the details about the data-fitting, which was only briefly described in the paper of Man and Sun (1986).

For each specimen of polycrystalline ice with the shape of a finite circular cylinder, McTigue and others(1985) introduced the assumptions:

4.1 The specimen is a homogeneous isotropic and incompressible continuum.

4.2 Its temperature is uniform and remains constant with time.

4.3 Body force and inertia force are negligible in the analysis.

4.4 The specimen undergoes a homogeneous deformation under the given surface traction during the entire test period.

Then as shown by McTigue and others, the deformation gradient, the first and second Rivlin-Ericksen tensors are:

$$[F] = \text{diag}[\alpha, \alpha^{-1/2}, \alpha^{-1/2}], \quad (4.1.1)$$

$$[A_1] = \text{diag}[-2a, a, a], \quad (4.1.2)$$

$$[A_2] = \text{diag}[-2da/dt + 4a^2, da/dt + a^2, da/dt + a^2], \quad (4.1.3)$$

where  $F$  satisfies the condition of incompressibility  $\det F = 1$ ,  $\alpha \equiv \ell(t)/L$  is the ratio of the current length  $\ell(t)$  at time  $t$  and the original length  $L$  of the specimen,  $a \equiv -d\alpha/dt/\alpha$  is the creep rate. I have put a negative sign in the

definition of the creep rate  $a$ , since  $d\alpha/dt \leq 0$  in compression tests and the quantity  $a^m$  will appear in what follows. Indeed, (1.2.4) and (4.1.2) gives us:

$$\Pi = 3^{m/2} a^m \quad (4.1.4)$$

By substituting (4.1.2), (4.1.3) and (4.1.4) into (1.2.1) and (1.2.2), we obtain for models (I) and (II), respectively, the extra stress:

$$\begin{aligned} \text{(I)} \quad [\mathbf{T} + p\mathbf{I}] = \text{diag} [ & -2\mu 3^{m/2} a^{1+m} + 2\alpha_1 (-\dot{a} + 2a^2) + 4\alpha_2 a^2, \\ & \mu 3^{m/2} a^{1+m} + \alpha_1 (\dot{a} + a^2) + \alpha_2 a^2, \\ & \mu 3^{m/2} a^{1+m} + \alpha_1 (\dot{a} + a^2) + \alpha_2 a^2 ], \end{aligned} \quad (4.1.5)$$

$$\begin{aligned} \text{(II)} \quad [\mathbf{T} + p\mathbf{I}] = 3^{m/2} a^m \text{diag} [ & -2\mu a + 2\alpha_1 (-\dot{a} + a^2) + 4\alpha_2 a^2, \\ & \mu a + \alpha_1 (\dot{a} + a^2) + \alpha_2 a^2, \\ & \mu a + \alpha_1 (\dot{a} + a^2) + \alpha_2 a^2 ]. \end{aligned} \quad (4.1.6)$$

McTigue and others(1985) pointed out that the extra stresses could be decomposed as follows:

$$[\mathbf{T} + p\mathbf{I}] = \text{diag} [\sigma + p_\phi, p_\phi, p_\phi], \quad (4.1.7)$$

where  $p_\phi$  is the confining pressure, and  $\sigma$  is the axial stress in excess of the confining pressure. For simplicity we call  $\sigma$  the extra axial stress in what follows. A comparison of (4.1.5), (4.1.6) and (4.1.7) leads to

$$\text{(I)} \quad \sigma + p_\phi = -2\mu 3^{m/2} a^{1+m} + 2\alpha_1 (-\dot{a} + 2a^2) + 4\alpha_2 a^2$$

$$p_{\phi} = \mu 3^{m/2} a^{1+m} + \alpha_1 (\dot{a} + a^2) + \alpha_2 a^2, \quad (4.1.8)$$

$$(II) \quad \sigma + p_{\phi} = 3^{m/2} a^m [-2\mu a + 2\alpha_1 (-\dot{a} + 2a^2) + 4\alpha_2 a^2]$$

$$p_{\phi} = 3^{m/2} a^m [\mu a + \alpha_1 (\dot{a} + a^2) + \alpha_2 a^2] \quad (4.1.9)$$

Hence by eliminating  $p_{\phi}$  in (4.1.8) and (4.1.9), the creep equations of models (I) and (II) for the triaxial tests of ice should be

$$(I) \quad \alpha_1 \dot{a} + 3^{m/2} \mu a^{1+m} - (\alpha_1 + \alpha_2) a^2 + \sigma/3 = 0, \quad (4.1.10)$$

$$(II) \quad \alpha_1 \dot{a} + \mu a - (\alpha_1 + \alpha_2) a^2 + \sigma a^{-m}/3^{1+m/2} = 0,$$

with the given  $a(t_{\phi})$  as the initial condition.

It is well known that the power-law fluid model can adequately represent the secondary creep of ice in triaxial tests through the creep equation

$$\mu a^{1+m} + \sigma/3^{1+m/2} = 0. \quad (4.1.11)$$

In secondary creep, since ice undergoes steady flow, i.e.  $da/dt \approx 0$ , models (I) and (II) will in effect lead to the same predictions as power-law fluid model if and only if

$$(I) \quad |\alpha_1 + \alpha_2| a^2 \ll 3^{m/2} \mu a^{1+m}, \quad (4.1.12)$$

$$(II) \quad |\alpha_1 + \alpha_2| a^2 \ll \mu a.$$

In other words, the term  $(\alpha_1 + \alpha_2) a^2$  in (4.1.10) should be

negligible. When substituting the first Rivlin-Ericksen tensor  $A_1$  expressed by (4.1.2) into (2.3.34), we precisely have

$$\begin{aligned} \text{(I)} \quad & |\alpha_1 + \alpha_2| a^2 \leq 3^{m/2} \mu a^{1+m}, \\ \text{(II)} \quad & |\alpha_1 + \alpha_2| a^2 \leq \mu a, \end{aligned} \tag{4.1.13}$$

which show that the condition (4.1.12) does not violate the thermodynamic restrictions.

On the other hand, the extra axial stress  $\sigma$  of the four tests of McTigue and others is the same, so one could not get enough information from the experiments which actually provided just one curve, to determine the four material parameters.

Therefore, we shall neglect the term  $(\alpha_1 + \alpha_2)a^2$  by setting

$$\text{(I,II)} \quad (\alpha_1 + \alpha_2)a^2 = 0 \tag{4.1.14}$$

in the following numerical analysis.

Since the experimental data are given in terms of  $\alpha$ , for the purpose of fitting we rewrite the creep equation (4.1.10) as:

$$\text{(I)} \quad \alpha_1 \left[ \frac{\ddot{\alpha}}{\alpha} - \left( \frac{\dot{\alpha}}{\alpha} \right)^2 \right] - 3^{m/2} \mu \left( -\frac{\dot{\alpha}}{\alpha} \right)^{1+m} - \sigma/3 = 0,$$

(4.1.15)

$$(II) \quad \alpha_1 [\ddot{\alpha}/\alpha - (\dot{\alpha}/\alpha)^2] - \mu (-\dot{\alpha}/\alpha) - \sigma (-\dot{\alpha}/\alpha)^{-m/3} 1+m/2 = 0$$

with the given  $\alpha(t_0)$ ,  $d\alpha(t_0)/dt$  as the initial conditions.

## Section 4.2 Evaluation of material parameters

The temperature, the confining pressure, the extra axial stress and the test period of the ice specimens in the four triaxial tests of McTigue and others (1985) are listed in Table 7. Their creep data with  $\epsilon$  versus time  $t$ , denoted by " $\square$ " are shown in Figs. 11 to 14, where  $\epsilon = [L(t) - L_0]/L_0$  is the strain of the specimen. It can be seen from Table 7 that all the tests were made at the same extra axial stress  $\sigma = -470$  KPa, at almost the same temperature from  $-9.5^\circ\text{C}$  to  $-9.8^\circ\text{C}$  but with different confining pressures. If ice is indeed an incompressible material as assumed, the creep curves in triaxial tests should be independent of the confining pressure. However the four curves of McTigue and others, for which  $\sigma$  is fixed, are not coincident at all (see Figs. 11 to 14 or McTigue and others (1985)). Since the temperature of the four tests are almost the same, the incoincidence of the four curves may be caused by compressibility, inhomogeneity, anisotropy and defects of the ice specimen as well as the inhomogeneity of the deformation. There is also the possibility that the confining pressure affects the initial response of the specimens. When the four curves of McTigue and others (1985) are plotted together in one figure, we find that they are essentially parallel and discrepancies among them are small if they are moved to the same initial point. Thus we

conclude that the apparent differences in creep behaviour of the four specimens are in fact differences in initial response. Since models (I) and (II) are only meant for describing the creep of ice, we can take Assums. 4.1 to 4.4 as approximately valid.

In Chapter 3, the parameters  $\mu$  and  $m$  of models (I) and (II) are evaluated by fitting the secondary creep rate of several pressuremeter tests with different cavity pressures, and then the value of the parameter  $\alpha_1$  is determined by fitting the primary creep of the tests when the values of  $\mu$  and  $m$  are fixed. By means of this treatment, a set of values of  $\mu$ ,  $\alpha_1$  and  $m$  were obtained which gave good fits to all the tests. However, we cannot evaluate the parameters  $\mu$ ,  $\alpha_1$  and  $m$  by fitting the data of the four triaxial tests in the same way since all the triaxial tests of McTigue and others (1985) have the same extra stress  $\sigma$  which determines the creep or creep rate according to (4.1.10) and (4.1.15). To deal with this problem, we define the objective function

$$(I, II) \quad F(\mu, \alpha_1, m) = \sum_{i=0}^{16} [\alpha^*(t_i) - \alpha(t_i; \mu, \alpha_1, m)]^2; \quad (4.2.1)$$

here  $\alpha^* = 1 + \delta$  is the given data;  $\alpha$  is the predicted solution of (4.1.15) by the use of the fifth-order Runge-Kutta-Nyström method with the integral step length  $h = 0.05$  day;  $t_{16} = 17$  day is taken as the terminal time of the fit because the creep of the ice specimens entered the tertiary

stage around that time. we seek a set of  $\mu$ ,  $\alpha_1$  and  $m$  such that the function  $F_{\#}$  assumes a relative minimum by using the Levenberg-Marquardt algorithm. At the beginning of the fitting, we met the problem of over-parametrization: there are many sets of the values of  $\mu$ ,  $\alpha_1$  and  $m$  ( $= -.671$  to  $-.70$ ) which can give "good" fits to the data of the tests. See Table 8, where "objfun" is the value of the objective function  $F_{\#}$  defined by (4.2.1), and "error" is defined by

$$\text{error} = [\alpha^*(t) - \alpha(t)]/\alpha^*(t_0). \quad (4.2.2)$$

An effective way to overcome the over-parametrization is to fix one parameter before fitting. Laboratory measurements on polycrystalline ice generally support values of  $n$  in the power-law fluid model (1.1.2) in the vicinity of 3 when the octahedral stress  $\tau$  is between 0.1 to 1 MPa (Hooke, 1981). It is also found out from experiments that the value of  $n$  seems to be independent of temperature, while the viscosity  $B$  is temperature dependent. For the given triaxial tests, the octahedral stress

$$\tau = -2^{1/2} 3^{-1} \sigma = 0.22 \text{ MPa}.$$

In addition, as is evident from Table 9, when the exponent  $m$  of models (I) and (II) ranges from  $-.65$  to  $-.71$ , the variation of the optimized  $\mu$  and  $\alpha_1$  are small (recall that  $m$

=  $1/n - 1$  from (1.2.8)). Consequently we fix  $m = -2/3$  or  $n = 3$  and evaluate  $\mu$  and  $\alpha_1$  by fitting the data.

Although having  $m = -2/3$  in hand, we still need an initial guess of  $\mu$  and  $\alpha_1$  before iteration in the optimization procedure can be started. we shall at first explore a rough value of  $\mu$ , which may be used as the initial  $\mu$  for iteration, through the secondary creep equation for the triaxial test:

$$\mu = -3^{-(1+m/2)} \alpha a^{-(1+m)} \quad (4.2.3)$$

which follows from (4.1.10) when we set  $da/dt = 0$  and  $(\alpha_1 + \alpha_2)a^2 = 0$ . For this purpose, we measured the slope of the creep curve for each test to obtain the approximate secondary creep rate  $a^*$ , which was found to be .00073, .00073, .001 and .00067 1/day at the 15th day so that the corresponding rough value of  $\mu$  was 2510, 2510, 2260 and 2583  $\text{KPa}\cdot\text{d}^{1/3}$  for tests #1, 2, 3 and 4, respectively. Next, from the creep curve of each test again, we estimated  $\alpha$ ,  $d\alpha/dt/\alpha$  and  $d^2\alpha/dt^2$  at day 2. While these estimates are admittedly very crude, they will be good enough for the present purpose. Then by using (4.1.15) with  $m = -2/3$  and  $\mu = 2466 \text{KPa}\cdot\text{d}^{1/3}$  which is the average of the rough values from the four tests, we obtained the crude values of  $\alpha_1$  as shown in Table 10. The average  $\alpha_1 = 2.\times 10^5 \text{KPa}\cdot\text{d}^2$  for model (I) and  $\alpha_1 = 4000 \text{KPa}\cdot\text{d}^{4/3}$  for model (II) were used as the initial

values for the optimization iteration.

After this preparation, we optimized the parameters  $\mu$  and  $\alpha_1$  by fitting the data of all the triaxial tests when  $m = -2/3$  was fixed. The numerical results are shown in Table 11, from which one can see that the scatter of the optimized values of  $\mu$  and  $\alpha_1$  for both models (I) and (II) are small and the fits are excellent because the relative error defined by (4.1.2) is under  $\pm 0.029\%$  at day 17 and is under  $\pm 0.33\%$  even at the end of each test. In what follows, we shall take the averages

$$(I) \quad \mu = 2414 \text{ KPa}\cdot\text{d}^{1/3}, \quad \alpha_1 = 1.617 \times 10^5 \text{ KPa}\cdot\text{d}^2, \quad (4.2.4)$$

$$(II) \quad \mu = 2434 \text{ KPa}\cdot\text{d}^{1/3}, \quad \alpha_1 = 3003 \text{ KPa}\cdot\text{d}^{4/3}, \quad (4.2.5)$$

and take  $m = -2/3$  as the values of the material parameters. To make the comparison transparent, the experimental and predicted strain rates of model (I) for all four tests are plotted in Figs. 11 to 14, respectively. In the figures each square "□" denotes an experimental data-point, and the solid line is the predicted curve. The predicted curves of model (II) are omitted since they are almost the same as those of model (I). It could also be seen from the figures that the predicted curve for each test fits the data very well both for the primary and for the secondary stage of creep. The

error after day 20 begins to increase since the ice specimens arrived at tertiary creep at about that time, whereas models (I) and (II) can only describe primary and secondary creep.

To examine the effect of the initial guess of  $\mu$  and  $\alpha_1$  on the optimization iteration, we also evaluated  $\mu$  and  $\alpha_1$  by using several sets of initial  $\mu$  and  $\alpha_1$  for the iteration. It is found from the computation that all these initial values converged to effectively the same final  $\mu$  and  $\alpha_1$  as the initial values  $\mu = 2466 \text{ KPa}\cdot\text{d}^{1/3}$ ,  $\alpha_1 = 2 \times 10^5 \text{ KPa}\cdot\text{d}^2$  for model (I), and  $\alpha_1 = 4000 \text{ KPa}\cdot\text{d}^{4/3}$  for model (II); cf. Table 12. It can be claimed, therefore, that models (I) and (II) are acceptable and the present computation algorithm is effective in fitting the primary and secondary creep data of the triaxial tests.

Before turning to the next section, we would like to discuss the effect of the material parameters on the predicted creep and creep rate of the ice in triaxial tests. For convenience, let  $\mathbf{u} = (u_1, u_2, u_3)$  denote  $(\mu, \alpha_1, m)$ . As in Sec. 3.2, it can be shown by a similar analysis that in the triaxial test problem, for  $t \geq t_0$ ,

$$\partial \alpha / \partial \mathbf{u} = - \text{Exp} \left( \int_{t_0}^t a d\tau \right) \left[ \int_{t_0}^t \alpha \frac{\partial a}{\partial \mathbf{u}} \text{Exp} \left( - \int_{t_0}^{\tau} a ds \right) d\tau \right], \quad (4.2.6)$$

$$\partial a / \partial \mathbf{u} = \text{Exp} \left( \int_{t_0}^t \partial \dot{a} / \partial a d\tau \right) \left[ \int_{t_0}^t (\delta \dot{a} / \delta \mathbf{u}) \text{Exp} \left( - \int_{t_0}^{\tau} \partial \dot{a} / \partial a ds \right) d\tau \right].$$

$$(4.2.7)$$

Let us concentrate on model (I), as for model (II) the analysis and conclusion will be similar. From (4.1.10) and (4.1.14), we have

$$\dot{a} = (-\sigma/3 - 3^{m/2}\mu a^{1+m})/\alpha_1, \quad (4.2.8)$$

from which

$$\begin{aligned} \partial \dot{a} / \partial a &= -3^{m/2}\mu(1+m)a^m/\alpha_1, \\ \delta \dot{a} / \delta \mu &= -3^{m/2}a^{1+m}/\alpha_1, \\ \delta \dot{a} / \delta \alpha_1 &= (\sigma/3 + 3^{m/2}\mu a^{1+m})/\alpha_1^2 = -\dot{a}/\alpha_1, \\ \delta a / \delta m &= -3^{m/2}\mu a^{1+m} \text{Ln}(3^{1/2}a)/\alpha_1. \end{aligned} \quad (4.2.9)$$

Since  $\mu > 0$ ,  $\alpha_1 > 0$ ,  $da/dt \leq 0$ , and  $a \ll 1$  or  $(\text{Ln}3)/2 + \text{Ln}(a) < 0$  from the previous computation and measurement of the data, then

$$\delta a / \delta \mu < 0, \quad \delta a / \delta \alpha_1 \geq 0, \quad \delta a / \delta m > 0 \quad (4.2.10)$$

from which and (4.2.6) and (4.2.7), we obtain

$$\partial a / \partial \mu < 0, \quad \partial a / \partial \alpha_1 \geq 0, \quad \partial a / \partial m > 0, \quad (4.2.11)$$

$$\partial \alpha / \partial \mu > 0, \quad \partial \alpha / \partial \alpha_1 \leq 0, \quad \partial \alpha / \partial m < 0 \quad (4.2.12)$$

due to the positivity of the exponential function.

To compare the effects of  $\mu$ ,  $\alpha_1$  and  $m$  on the creep and creep rate, we obtain from (4.2.9)<sub>2</sub> and (4.2.9)<sub>4</sub>

$$0 \leq \delta \dot{a} / \delta \alpha_1 < 3^{m/2} \mu a^{1+m} / \alpha_1^2 \quad (4.2.13)$$

for  $\sigma < 0$ , and

$$\delta \dot{a} / \delta m \geq - 3^{m/2} \mu a^{1+m} A / \alpha_1 > 0, \quad (4.2.14)$$

where the negative constant  $A$  is defined by

$$A = \sup_{t \geq t_0} \text{Ln}(3^{1/2} a). \quad (4.2.15)$$

A comparison of (4.2.9) and (4.2.13) with (4.2.15) then yields

$$\begin{aligned} (\delta \dot{a} / \delta \mu) / (\delta \dot{a} / \delta \alpha_1) &< -\alpha_1 / \mu < 0, \\ 0 &\geq (\delta \dot{a} / \delta \mu) / (\delta \dot{a} / \delta m) \geq 1 / (\mu A), \\ 0 &< (\delta \dot{a} / \delta \alpha_1) / (\delta \dot{a} / \delta m) \leq -1 / (\alpha_1 A), \end{aligned} \quad (4.2.16)$$

which with (4.2.4) and (4.2.5) lead to

$$\begin{aligned} |(\partial a / \partial \mu) / (\partial a / \partial \alpha_1)| &> \alpha_1 / \mu, \\ |(\partial a / \partial \mu) / (\partial a / \partial m)| &\leq |1 / (\mu A)|, \\ |(\partial a / \partial \alpha_1) / (\partial a / \partial m)| &\leq |1 / (\alpha_1 A)|, \text{ for } t \geq t_0, \end{aligned} \quad (4.2.17)$$

and hence

$$|(\partial \alpha / \partial \mu) / (\partial \alpha / \partial \alpha_1)| > \alpha_1 / \mu,$$

$$|(\partial\alpha/\partial\mu)/(\partial\alpha/\partial m)| \leq |1/(\mu A)|, \quad (4.2.18)$$

$$|(\partial\alpha/\partial\alpha_1)/(\partial\alpha/\partial m)| \leq |1/(\alpha_1 A)|, \text{ for } t \geq t_0.$$

By comparing (4.2.17) and (4.2.18) with (3.2.22) and (3.2.23), we see that for the same model, namely model (I), we have obtained the same estimates for the effect of the material parameters on the predicted creep and creep rate in the pressuremeter and the triaxial creep problems.

To have a quantitative comparison, by plugging the approximate maximum values of  $a = 0.0018$  1/day (which was measured from the triaxial test #4 at day 1) and the parameter values

$$A = - 5.221,$$

$$\alpha_1/\mu = 67 \text{ (day}^{5/3}\text{)},$$

$$|\mu A| = 1.27 \times 10^{-4} \text{ (KPa}\cdot\text{day}^{1/3}\text{)},$$

$$|\alpha_1 A| = 8.47 \times 10^5 \text{ (KPa}\cdot\text{day}^2\text{)},$$

in (4.2.17) and (4.2.18), we see that for model (I), under the given units, the parameter  $m$  and  $\alpha_1$  will give the largest and the smallest effect on the predicted creep and creep rate for the triaxial test problem.

Table 7

Temperature, confining pressure, extra axial stress and tested time interval of the triaxial tests.

test	temp. °C	confining pressure(MPa)	extra axial stress(KPa)	tested time (day)
#1	-9.5	0.	-470.	[1, 34]
#2	-9.8	0.	-470.	[1, 34]
#3	-9.5	-37.	-470.	[1, 23]
#4	-9.7	-50.	-470.	[1, 23]

Table 8

Optimize  $\mu$ ,  $\alpha_1$  and m by fitting the data  $l(t)/L$  of triaxial tests #1 and #4.

MODEL (I)

Test	initial	after iteration			objfun *10 <sup>6</sup>	error %	at (day)	error at %	at (day)
	m	$\mu$	$\alpha_1 * 10^{-5}$	m					
#1	-.65	2199	1.242	-.6871	.487	-.0004	17	-.25	34
#1	-.67	2206	1.263	-.6868	.488	-.0011	17	-.25	34
#1	-.69	2099	1.217	-.6940	.487	-.0014	17	-.24	34
#1	-.71	1958	1.163	-.7045	.489	-.0025	17	-.25	34
#4	-.65	2207	2.005	-.6707	.208	+.0038	17	-.11	23
#4	-.67	2091	1.764	-.6779	.216	+.0079	17	-.10	23
#4	-.69	1972	1.868	-.6882	.204	+.0022	17	-.12	23
#4	-.71	1941	1.733	-.6900	.214	+.0033	17	-.11	23

where initial  $\mu = 2000 \text{ KPa} \cdot \text{day}^{1/3}$  and  $\alpha_1 = 2 \cdot 10^5 \text{ KPa} \cdot \text{day}^2$ ,  
error:  $=(a-aa)/a$ , a and aa are experimental and predicted  $l(t)/L$ .

Table 9

Optimize  $\mu$  and  $\alpha_1$  by fitting the data  $l(t)/L$  of triaxial tests when m is fixed.

Model (I)

Model (II)

Test	fixed m	after iteration			objfun *10 <sup>6</sup>	after iteration		
		$\mu$	$\alpha_1 * 10^{-5}$	objfun *10 <sup>6</sup>		$\mu$	$\alpha_1$	objfun *10 <sup>6</sup>
#1	-.65	2818	1.397	.488	2844	2746	.538	
#1	-.68	2305	1.262	.487	2324	2025	.532	
#1	-.71	1886	1.141	.486	1896	1468	.530	
#4	-.65	2514	2.095	.203	2549	4901	.184	
#4	-.68	2077	1.907	.204	2102	3690	.183	
#4	-.71	1717	1.729	.205	1735	2782	.183	

In Tables 8~12,  $\mu$  has the same unit, so does  $\alpha_1$ .

Table 10

Estimate the initial  $\alpha_1$  by using the data of triaxial tests when  $\mu = 2466 (\text{KPa} \cdot \text{day}^{1/3})$  and  $m = -2/3$  are fixed.

Test	Model I			Model II
	$\alpha$	$\dot{\alpha} \cdot 10^2$ (day <sup>-1</sup> )	$\ddot{\alpha} \cdot 10^3$ (day <sup>-2</sup> )	$\alpha_1$
#1	.9953	-.1307	.2161	2424
#2	.9930	-.1387	.1784	3434
#3	.9918	-.1392	.1635	3776
#4	.9910	-.1636	.1428	6342
average:				3994

Table 11

Optimize  $\mu$  and  $\alpha_1$  by fitting the data  $l(t)/L$  of triaxial tests from day 1 to day 17 when  $m = -2/3$  is fixed.

Model (I)

Test	after iteration $\mu$	$\alpha_1 \cdot 10^5$	objfun $\cdot 10^6$	Error %	at t (day)	Error %	at t (day)
#1	2522	1.334	.488	-.0008	17	-.25	34
#2	2536	2.012	.230	-.0023	17	-.12	34
#3	2335	1.128	.255	-.0281	17	-.33	23
#4	2261	1.994	.203	+.0023	17	-.11	23

where the initial  $\mu = 2466 (\text{KPa} \cdot \text{day}^{1/3})$ ,  $\alpha_1 = 2 \cdot 10^5 (\text{KPa} \cdot \text{day}^2)$ , average  $\mu = 2414 (\text{KPa} \cdot \text{day}^{1/3})$  and  $\alpha_1 = 1.617 \cdot 10^5 (\text{KPa} \cdot \text{day}^2)$ .

Model (II)

Test	after iteration $\mu$	$\alpha_1$	objfun $\cdot 10^6$	Error %	at t (day)	Error %	at t (day)
#1	2532	2201	.528	-.0022	17	-.27	34
#2	2576	3676	.250	-.0054	17	-.17	34
#3	2340	1958	.293	-.0290	17	-.33	23
#4	2289	4176	.183	+.0001	17	-.13	23

where the initial  $\mu = 2466 (\text{KPa} \cdot \text{day}^{1/3})$ ,  $\alpha_1 = 4000 (\text{KPa} \cdot \text{day}^{4/3})$ , average  $\mu = 2434 (\text{KPa} \cdot \text{day}^{1/3})$  and  $\alpha_1 = 3003 (\text{KPa} \cdot \text{day}^{4/3})$ .

Table 12

Optimize the material parameters  $\mu$  and  $\alpha_1$  by fitting the data  $l(t)/L$  from day 1 to day 17 of triaxial tests when  $m=-2/3$  is fixed.

## Model (I)

Test	initial		after iteration		objfun *10 <sup>6</sup>	Error %	at t (day)	Error %	at t (day)
	$\mu$	$\alpha_1 * 10^{-5}$	$\mu$	$\alpha_1 * 10^{-5}$					
#1	2000	.05	2522	1.336	.487	-.0006	17	-0.25	34
#1	500.	1.0	2523	1.342	.488	-.0005	17	-0.25	34
#1	1000	1.0	2521	1.329	.487	-.0005	17	-0.25	34
#2	1000	1.0	2536	2.014	.230	-.0019	17	-0.12	34
#3	1000	1.0	2334	1.137	.255	-.0283	17	-0.33	23
#4	1000	1.0	2259	1.972	.203	+.0030	17	-0.11	23
#4	2000	.05	2259	1.975	.203	+.0030	17	-0.12	23
#4	2000	5.0	2260	1.983	.203	+.0030	17	-0.11	23

## Model (II)

Test	initial		after iteration		objfun *10 <sup>6</sup>	Error %	at t (day)	Error %	at t (day)
	$\mu$	$\alpha_1$	$\mu$	$\alpha_1$					
#1	500.	500.	2534	2223	.528	-.0030	17	-0.27	34
#1	1000	5000	2531	2214	.532	+.0005	17	-0.26	34
#1	1000	1000	2542	2317	.534	-.0041	17	-0.28	34
#2	1000	1000	2576	3677	.250	-.0052	17	-0.17	34
#3	1000	1000	2340	1958	.294	-.0286	17	-0.33	23
#4	1000	1000	2287	4146	.184	-.0224	17	-0.13	23
#4	500.	500.	2333	5011	.231	-.0052	17	-0.16	23
#4	2000	2000	2288	4148	.183	+.0006	17	-0.13	23

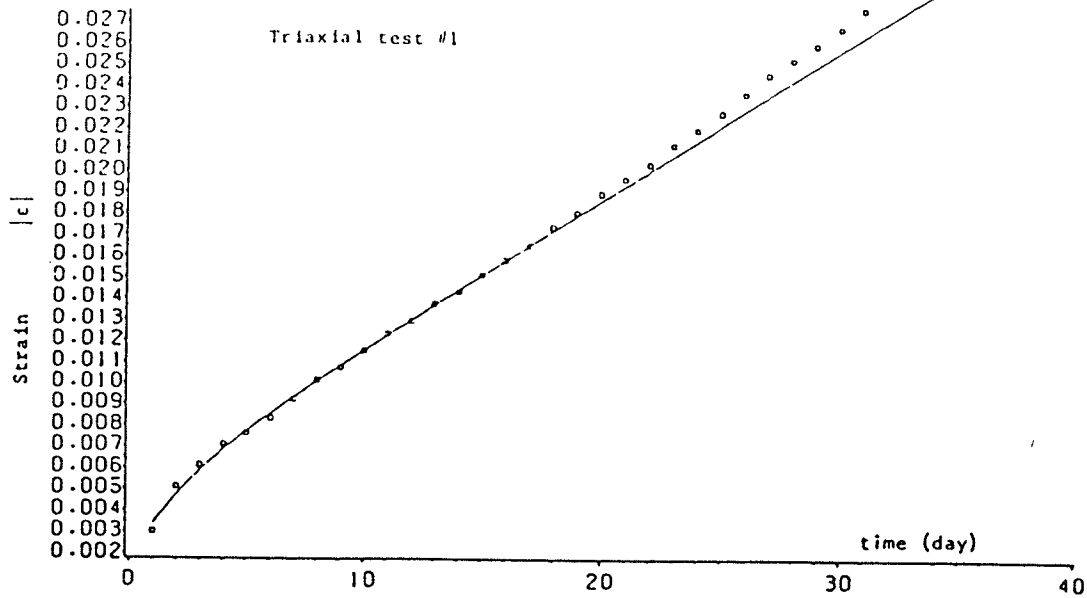


Fig. 11

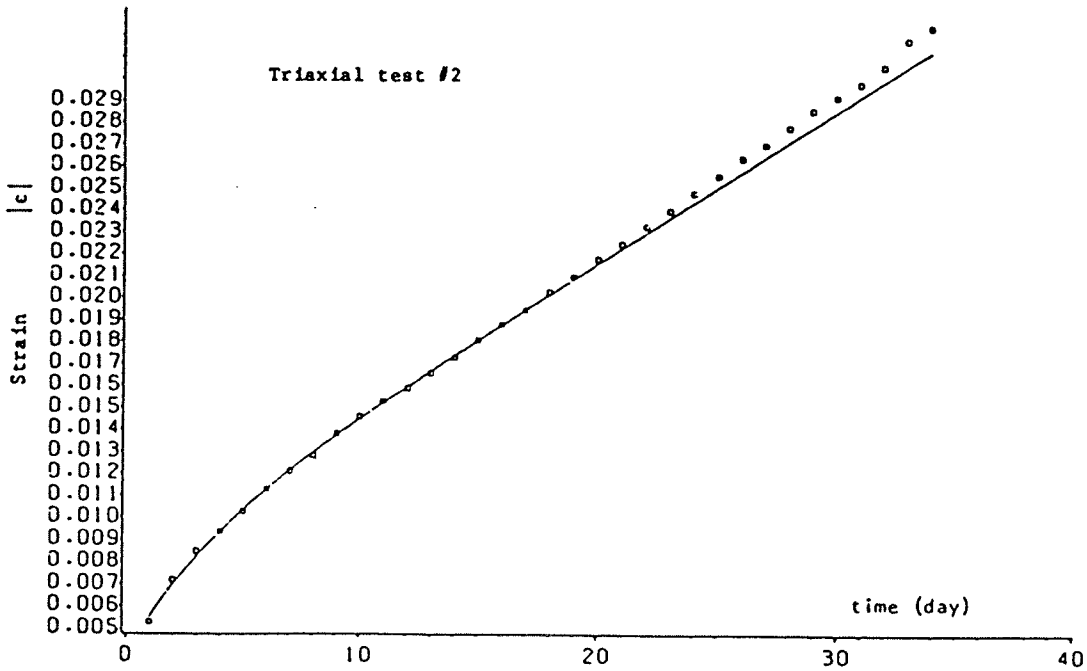


Fig. 12

Comparison of experimental & predicted strain by model (I) for triaxial tests #1 & #2

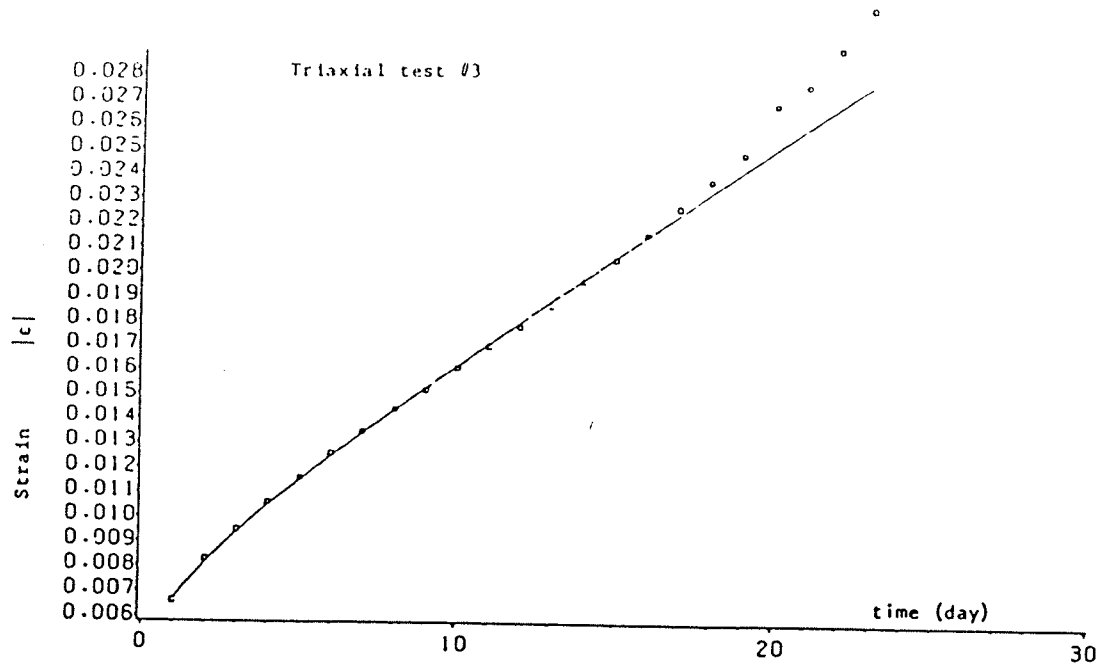


Fig. 13

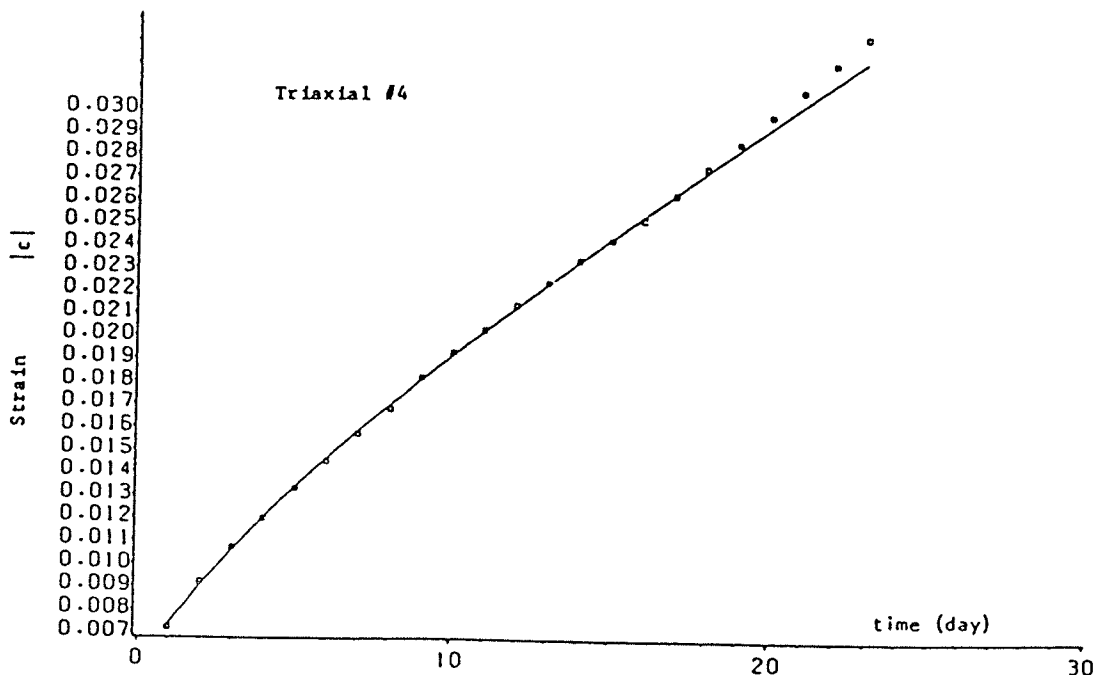


Fig. 14

Comparison of experimental & predicted strain by model (I) for triaxial tests #3 & #4

## Chapter 5 Evaluation of material parameters by fitting short-term creep data of pressuremeter tests

### Section 5.1 Introduction

In Chapters 3 and 4, I showed by example that models (I) and (II) could adequately describe both the primary and secondary creep of polycrystalline ice through fitting the long term data of some pressuremeter and triaxial tests which were performed in the laboratory. There I proposed an effective and feasible method of numerical analysis to evaluate the material parameters of both models. One of my main objectives is to analyze the mechanical properties of frozen material in foundations, such as ice, permafrost in cold regions. These frozen materials may hide under seabed, or on the mountains, or jostle between two soil layers. Should a sample of the frozen material be drawn out and delivered to the laboratory, their material properties would have changed upon arrival since ice and permafrost are not the usual elastic solids but are fluid-like materials which may undergo creep under load and even sustain melting, regelation, etc. For this reason, we would like to test the properties of the material in question in-situ. Among a variety of testing devices for the in-situ test, the pressuremeter is one of the most widely used (Baguelin and others, 1978; Ladanyi and Johnston, 1972).

For the foundation problem, we certainly wish to know the long term, in particular, the secondary creep properties of the frozen materials. It is found from experiments that the higher the cavity pressure applied by the pressuremeter, the earlier the secondary creep will take place for ice and frozen soils. There is the same observation in triaxial tests (Jacka, 1984). But we cannot shorten the test time without limit by increasing the cavity pressure because the material around the pressuremeter may be damaged when the pressure is too high. For instance, Kjartanson (1986) noticed from his experiment that some macrocracks appeared near the cavity of the ice when the pressure was 2.5 MPa. It is also observed from his pressuremeter tests that ice completely entered the secondary creep after the test started for 800 min or 15 hours, when the cavity pressure was less than 2.5 MPa. Consequently one has to wait at least 10 hours to measure the secondary creep properties for undamaged ice samples similar to those prepared by Kjartanson which were at  $-2^{\circ}\text{C}$ . Is it practical and necessary to perform a long term in-situ test about 10 hours in a cold region? The answer to the first question is straight: no, especially for tests under the Arctic ocean. In the following sections, we shall attempt to seek an answer to the second question.

Before we start, we would emphasize that it is meaningless to use the power-law fluid model to fit the

short term data obtained from creep tests on ice because that model cannot represent the primary creep of ice; cf. Sec. 3.5.

## Section 5.2 Evaluation of material parameters by fitting short-term data of a single-stage creep test

In this section we shall try to determine the material parameters in models (I) and (II) by fitting short-term data of a single-stage pressuremeter creep test and then use the models that result to predict the secondary creep pertaining to the pressuremeter test. The secondary creep data of the tests will only be used as comparison. In addition, let us temporarily forget the numerical results obtained in chapter 3.

For this purpose, we define the objective function

$$(I, II) F_3(\mu, \alpha_1, m; t_0, t_N) = \sum_{i=0}^N [r_0^*(t_i) - r_0(\mu, \alpha_1, m; t_i)]^2; \quad (5.2.1)$$

here  $r_0^*$  is the measured cavity radius,  $r_0$  the predicted radius from (3.1.15);  $t_0$  and  $t_N$  are respectively the initial and terminated times of the fitting period which are given in Table 3 for each test. These time intervals indeed fall in the primary creep period under the given pressures. we shall seek a set of  $\mu$ ,  $\alpha_1$  and  $m$  such that the function  $F_3$  arrives at a minimum by using the Levenberg-Marquardt optimization algorithm and then compare the predicted long term creep radii with those from those measured. The method to find the numerical solution of (3.1.15) has been

introduced in Sec. 3.4. The procedure of numerical analysis is given in Appendix A.3. It is obvious from (3.1.15) that here we have a nonlinear regression problem to determine the material parameters.

In nonlinear regression, it is necessary to assign the initial value of the parameters to start the iteration. But, when we are given the short-term data of a creep test, we don't even know the order of magnitude of the parameters except that  $m \approx -2/3$  or  $n \approx 3$  in the power-law fluid model (Hooke, 1981). Hence we have to search an initial value of  $\mu$  and  $\alpha_1$  from the short term data which are the only information gathered, while using  $m \approx -2/3$  as the rough value of  $m$ .

To this end, let us look back at (3.1.15). Both equations contain  $\mu$  and  $\alpha_1$  linearly. So what we shall do is to fix a certain value of  $m$  in the vicinity of  $-2/3$  and estimate the value of  $dr_\phi/dt$  and  $d^2r_\phi/dt^2$  at two instants, say  $t_1$  and  $t_2$ , in the short-term period of test, in order to get two simultaneous linear algebraic equations in  $\mu$  and  $\alpha_1$ . Thus a pair of rough estimates of  $\mu$  and  $\alpha_1$  can be found for each test when the cavity pressure is given. One may estimate  $dr_\phi/dt$  and  $d^2r_\phi/dt^2$  through fitting the measured cavity radii by using a polynomial, say  $f(t)$  from which  $dr_\phi/dt = f'$  and  $d^2r_\phi/dt^2 = f''$  could be directly calculated at the instants  $t_1$  and  $t_2$ . But in my work, I estimated  $d^2r_\phi/dt^2$  by using the difference quotient of  $dr_\phi/dt$ . One is

free to take one of the above methods because only rough estimates of  $\mu$  and  $\alpha_1$  are needed to start the iteration. For a given test the rough  $\mu$  and  $\alpha_1$  will be optimized with fixed  $m$  through (5.2.1). The question how to choose  $t_1$  and  $t_2$  may be raised. Will the rough  $\mu$  and  $\alpha_1$  estimated from different pairs of  $t_1$  and  $t_2$  lead to approximately the same end results after the optimization? The answer could be found in Table 13, where the fixed  $m = -.70$ . One can see from Table 13 that the end results are almost the same for rather different choices of  $t_1$  and  $t_2$ . Of course, the optimized  $\mu$  and  $\alpha_1$  will depend on the choice of  $m$ . To examine the effect of  $m$ , I took several values of fixed  $m$  and optimized the corresponding rough estimates of  $\mu$  and  $\alpha_1$  for model (II) and for tests #3, 5 and 6. The numerical results are shown in Table 15, from which one can see that when  $m$  changes from  $-.72$  to  $-.66$ , the optimized  $\mu$  and  $\alpha_1$  are at most tripled. Therefore up to this point, we can say that we can at least determine the order of magnitude of  $\mu$  and  $\alpha_1$  by using the short-term data of a single-stage creep test. For model (I), the discussion and conclusion are similar (Table 14).

For models (I) and (II), we have obtained the values of the parameters by fixing  $m$  in advance at a certain value in  $[-.72, -.66]$ . In other words, we have found the range of  $\mu$  and  $\alpha_1$  of the given ice. But we still do not know what is the value of  $m$  for the ice yet. To determine  $m$ , I allowed  $m$  to vary in the optimization procedure. In order to make the

discussion transparent, let us concentrate on one test and also on one model, e.g., test #3 and model (II). It can be read from Table 15 that the optimized  $\mu$  is 10307 and  $\alpha_1$  is 93670 when  $m$  is fixed at  $-.70$ . Here I have omitted the units of the parameters for convenience. I used  $\mu = 10307$ ,  $\alpha_1 = 93670$  and  $m = -.70$  as the initial value of  $\mu$ ,  $\alpha_1$  and  $m$  to fit the data by the Levenberg-Marquardt method. After the optimization, the three parameters stop at 10306, 93570 and  $-.70$ , respectively; cf. Table 17. The reason that the iteration did not run much is that the objective function  $F_3$  defined by (5.2.1) is already almost at a local minimum when  $\mu = 10307$ ,  $\alpha_1 = 93670$  and  $m = -.70$ . To overcome this "pre-optimized" problem, I took  $-.69$  and  $-.71$  as the initial values of  $m$  so that the initial values of the parameters would no longer render the objective function a local minimum. The motivation to change the initial  $m$  is based on the fact that the predicted  $r_0$  is most sensitive to  $m$  (Sec. 3.4). It is found from computation that after optimization  $m$  came back to  $-.70$  (Table 17). Indeed any initial value of  $m$  in  $[-.72, -.68]$  seem to converge to about  $-.70$  after iteration for test #3, model (II) (see Table 19). But here I encountered the over-parametrization problem: the initial  $m = -.66$  converged to  $-.68$  and could give the same "good" fit to the data like the other initial  $m$  (see Table 19). The over-parametrization problem can also be found in Tables 14 and 15 which show that when the fixed  $m$  varies from  $-.72$  to

-.66, the optimized values of the objective function of each model have almost the same value for each test, and so are the relative long term errors. Besides, the relative long term errors of tests #3 and 6 are about -11%, -33% for model (I), and -7.8%, -27% for model (II), respectively. The errors of test #6 for both models here are much higher than those in Tables 5 and 6. It should be pointed out that we cannot simply take the average of the optimized parameters  $\mu$ ,  $\alpha_1$  and  $m$  for either model (I) or model (II) because the units of  $\mu$  and  $\alpha_1$  contain the parameter  $m$  which varies from line to line in Tables 14 to 18.

In the next section, we shall discuss about the possibility of solving the over-parametrization problem and reducing the long term errors.

Section 5.3 Evaluation of material parameters by simultaneously fitting short-term data of two single-stage creep tests

As mentioned in the last section, the major problem that I met was over-parametrization when I was fitting short term data of a single pressuremeter test. The reason why over-parametrization appeared may be that a single creep curve is not enough to determine the three material parameters. we may follow either of two approaches in order to get enough information. One of them is to fit the data of a test in which the pressure varies within a short-term period. Another is to simultaneously fit the short term data of two tests with different pressures. As figured out in Sec. 3.2, it is not difficult to fit data with variable pressure by numerical analysis. But it is perhaps easier or more practical to undertake a multistage test in which each stage has a constant pressure. At present, I have only one set of data from multistage test #10 in which each stage lasted one day (see Fig. 10). With such data we cannot adopt the first approach. What I can do here for the first approach is only to give a suggestion. For polycrystalline ice, let each stage of the multistage test last about 80 min. Let the pressure of the first stage be 1500 KPa; increase the pressure by 500 KPa for each stage. Thus a test with three stages last only about 250 min, which is allowable for the

in-situ test.

When going by the second approach, namely, simultaneously fitting the data of two single-stage tests, we define the objective function

$$\begin{aligned}
 (I, II) \quad F_1(\mu, \alpha_1, m; P_1, P_2) &= \sum_1^n [r_{\phi}^*(t_i; P_1) - r_{\phi}(\mu, \alpha_1, m; t_i; P_1)]^2 \\
 &+ \sum_1^n [r_{\phi}^*(t_i; P_2) - r_{\phi}(\mu, \alpha_1, m; t_i; P_2)]^2; \quad (5.3.1)
 \end{aligned}$$

here  $r_{\phi}^*(\cdot; P_1)$  and  $r_{\phi}^*(\cdot; P_2)$  are the measured cavity radii under pressures  $P_1$  and  $P_2$ , respectively;  $r_{\phi}(\cdot, \cdot, \cdot; \cdot; P_1)$  and  $r_{\phi}(\cdot, \cdot, \cdot; \cdot; P_2)$  are the predicted radii from (3.1.15) under pressures  $P_1$  and  $P_2$ , respectively. We seek a set of  $\mu$ ,  $\alpha_1$  and  $m$  such that the function  $F_1$  arrives at a relative minimum by the Levenberg-Marquardt method. The procedure of numerical analysis is given in Appendix A.3. The results of computation are recorded in Tables 20 to 23.

I should like to add the following comments:

(a) From Tables 20 and 21, all initial  $m$  ranging from  $-.71$  to  $-.66$  seem to converge to about  $-.71$  by simultaneously fitting the short term data of the two tests #3 and 6 for both models.

(b) In contrast with fitting the data of a single test, shown in Tables 14 and 15, the objective function no longer has the same values after iteration when  $m$  is fixed at different values for both models; neither are the relative

long-term errors (see Tables 22 and 23).

(c) Comparing Tables 20 and 21 with Tables 18 and 19, we see that the relative long-term errors from the fit to test #6 for the two models are reduced. In particular, the reduction is impressive for model (II).

These findings reveal that the over-parametrization as well as the higher error problem in fitting the short-term data of a single-stage test could be improved by simultaneously fitting short-term data of two single-stage tests with different pressures. Whether or not it is practical to do two short-term in-situ pressuremeter tests at the same time remains a problem to be answered by the engineer or experimentalist.

Table 13

-----  
 Optimize  $\mu$  and  $\alpha_1$  by fitting the primary creep data of  
 pressuremeter tests when  $m=-0.70$  is fixed.  
 Model (II)  
 -----

Test	t1(min)	t2(min)	initial		after iteration	
			$\mu$	$\alpha_1 * 10^{-5}$	$\mu$	$\alpha_1 * 10^{-5}$
#3	5.	40.	9428	.3379	10293	.9250
#3	14.	60.	9882	.9408	10268	.9034
#3	5.	111.	10118	.4126	10307	.9367
#5	8.	59.	9421	.4567	10697	2.211
#5	20.	120.	10204	1.977	10583	2.004
#5	8.	160.	10173	.6130	10634	2.125
#6	4.	60.	9288	.4290	10041	1.054
#6	15.	90.	9650	.6896	10062	1.074
#6	4.	110.	9829	.5149	10061	1.072

In Tables 18~23,  $\mu$  has the same unit, so does  $\alpha_1$ .

Optimize  $\mu$  and  $\alpha_i$  by fitting the primary creep data of pressuremeter tests when  $m$  is fixed.

Table 14

Model (I)

Test	fixed m	t1 (min)	t2 (min)	initial		after iteration		objfun	Error at t
				$\mu$	$\alpha_i \cdot 10^{-8}$	$\mu$	$\alpha_i \cdot 10^{-8}$	$\cdot 10^3$	% (min)
#2	-.70	6.	165.	10232	.2557	9836	.4271	1.50	-8.7 2175
#3	-.66	5.	111.	16636	.3852	16894	1.500	.291	-11. 5095
#3	-.70	5.	111.	10076	.3285	10209	1.295	.293	-11. 5095
#4	-.70	8.	65.	9503	.2236	9967	1.056	.365	-23. 4530
#5	-.66	8.	160	17499	1.549	17529	5.334	.453	-38. 6360
#5	-.70	8.	160.	10186	1.334	10295	4.989	.444	-33. 6360
#6	-.66	4.	110.	15710	.3927	16087	1.252	1.63	-32. 2395
#6	-.70	4.	110.	9712	.3368	9912	.9929	1.66	-32. 2395
#7	-.70	7.	100.	9097	.5144	9457	1.644	.474	-53. 1700
#10	-.70	7.	150.	10285	2.717	9108	1.755	1.20	-56. 5810

Table 15

Model (II)

Test	fixed m	t1 (min)	t2 (min)	initial		after iteration		objfun	Error at t
				$\mu$	$\alpha_i \cdot 10^{-5}$	$\mu$	$\alpha_i \cdot 10^{-5}$	$\cdot 10^3$	% (min)
#3	-.66	5.	111.	16710	.7500	17034	1.710	.258	-7.8 5095
#3	-.68	5.	111.	13208	.5585	13267	1.256	.260	-7.8 5095
#3	-.70	5.	111.	10118	.4126	10307	.9367	.259	-7.2 5095
#3	-.72	5.	111.	7823	.3022	7950	.6736	.259	-7.7 5095
#5	-.66	8.	160.	17473	1.168	17931	3.590	.502	-38. 6360
#5	-.68	8.	160.	13359	.8495	13504	2.370	.530	-34. 6360
#5	-.70	8.	160.	10173	.6130	10634	2.125	.485	-20. 6360
#5	-.72	8.	160.	7712	.4384	8001	1.470	.487	-22. 6360
#6	-.66	4	110.	15912	.9207	16294	1.894	1.02	-27. 2395
#6	-.68	4.	110.	12531	.6921	12845	1.445	.997	-26. 2395
#6	-.70	4.	110.	9829	.5149	10061	1.072	.995	-26. 2395
#6	-.72	4.	110.	7676	.3802	7863	.8043	.996	-24. 2395
#2	-.70	6.	165.	10239	.3990	9904	.6187	.836	-6.0 2175
#4	-.70	8.	65.	9592	.2634	10127	.8843	.234	-17. 4530
#7	-.70	7.	100.	9157	.4279	9603	1.063	.556	-46. 1700
#10	-.70	7.	150.	12144	2.881	9448	1.145	.820	-36. 5810

Table 16

Optimize  $\mu$ ,  $\alpha_1$  and  $m$  of Model I by fitting the primary creep data of pressuremeter tests.

Test	$\mu$	initial $\alpha_1 * 10^{-8}$	$m$	objfun $* 10^2$	after $\mu$	iteration $\alpha_1 * 10^{-8}$	$m$	objfun $* 10^2$	Error at t % (min)
#2	9836	.4271	-.69	66.96	10629	.4378	-.6935	.1594	-8.7 2175
#2	9836	.4271	-.70	.1601	9835	.4269	-.7000	.1600	-8.7 2175
#2	9836	.4271	-.71	38.96	9308	.4191	-.7042	.1603	-8.7 2175
#3	10209	1.295	-.69	20.27	10626	1.322	-.6970	.0294	-11. 5095
#3	10209	1.295	-.70	.0293	10207	1.291	-.7000	.0292	-11. 5095
#3	10209	1.295	-.71	12.26	9777	1.292	-.7034	.0294	-11. 5095
#4	9967	1.056	-.69	13.23	10246	1.048	-.6977	.0364	-24. 4530
#4	9967	1.056	-.70	.0365	9967	1.056	-.7000	.0365	-23. 4530
#4	9967	1.056	-.71	8.342	9769	1.025	-.7014	.0366	-25. 4530
#5	10295	4.989	-.69	2.452	10909	5.045	-.6958	.0445	-33. 6360
#5	10295	4.989	-.70	.0479	10295	4.959	-.7000	.0478	-33. 6360
#5	10295	4.489	-.71	1.590	9902	5.984	-.7050	.0486	-20. 6360
#6	9912	.9929	-.69	49.37	10600	.9813	-.6943	.1691	-33. 2395
#6	9912	.9929	-.70	.1660	9912	.9926	-.7000	.1658	-32. 2395
#6	9912	.9929	-.71	31.33	9922	.9941	-.6999	.1664	-32. 2395
#7	9611	1.813	-.69	8.546	9186	1.611	-.7022	.0476	-53. 1700
#7	9611	1.813	-.70	.0664	9600	1.826	-.6999	.0551	-46. 1700
#7	9611	1.813	-.71	6.438	9587	1.639	-.6986	.0476	-53. 1700
#10	9108	1.755	-.69	10.79	9840	1.789	-.6942	.1202	-54. 5810
#10	9108	1.755	-.70	.1202	9106	1.753	-.7000	.1202	-57. 5810
#10	9108	1.755	-.71	6.679	8418	1.799	-.7064	.1219	-56. 5810

Table 17

Optimize  $\mu$ ,  $\alpha_1$  and  $m$  of Model II by fitting the primary creep data of pressuremeter tests.

Test	initial			objfun <sub>2</sub> *10 <sup>2</sup>	after iteration			objfun *10 <sup>2</sup>	Error at t	
	$\mu$	$\alpha_1 * 10^{-5}$	$m$		$\mu$	$\alpha_1 * 10^{-5}$	$m$		%	(min)
#2	9904	.6187	-.69	52.05	9980	.6308	-.6994	.0840	-5.8	2175
#2	9904	.6187	-.70	.0835	9905	.6197	-.7000	.0835	-6.0	2175
#2	9904	.6187	-.71	28.56	9288	.5690	-.7053	.0828	-6.2	2175
#3	10307	.9360	-.69	14.95	10503	.9692	-.6986	.0263	-7.0	5095
#3	10307	.9360	-.70	.0259	10306	.9357	-.7000	.0259	-7.2	5095
#3	10307	.9360	-.71	8.104	9889	.8855	-.7032	.0261	-7.3	5095
#4	10127	.8843	-.69	8.666	10128	.8180	-.6999	.0233	-17.	4530
#4	10127	.8843	-.70	.0233	10127	.8842	-.7000	.0233	-17.	4530
#4	10127	.8843	-.71	4.746	10179	.9177	-.7000	.0248	-15.	4530
#5	10634	2.215	-.69	1.372	11850	2.351	-.6917	.0487	-22.	6360
#5	10634	2.125	-.70	.0485	10615	2.195	-.7007	.0485	-17.	6360
#5	10634	2.215	-.71	.7488	10470	2.061	-.7011	.0487	-20.	6360
#6	10061	1.072	-.69	.3317	10512	1.142	-.6965	.0999	-25.	2395
#6	10061	1.072	-.70	.0994	10062	1.075	-.7000	.0992	-26.	2395
#6	10061	1.072	-.71	18.51	10466	1.116	-.6967	.0996	-26.	2395
#7	9775	1.169	-.69	5.300	9829	1.090	-.6982	.0554	-34.	1700
#7	9775	1.169	-.70	.0680	9660	1.093	-.6998	.0555	-44.	1700
#7	9775	1.169	-.71	3.640	9851	1.216	-.6993	.0604	-39.	1700
#10	9448	1.145	-.69	5.630	9882	1.211	-.6967	.0842	-35.	5810
#10	9448	1.145	-.70	.0828	9483	1.146	-.6997	.0820	-36.	5810
#10	9448	1.145	-.71	3.036	9314	1.160	-.7018	.0872	-32.	5810

Optimize  $\mu$ ,  $\alpha_1$  and m by fitting the primary creep data of single pressuremeter test.

Table 18 Model (I)

Test	Initial	after iteration		objfun *10 <sup>3</sup>	error %	
	m	$\mu * 10^{-4}$	$\alpha_1 * 10^{-8}$			m
#3	-.66	1.010	1.343	-.7011	.302	-9.83
#3	-.68	.9910	1.290	-.7024	.293	-10.7
#3	-.70	1.029	1.291	-.6994	.294	-11.1
#3	-.72	1.184	1.346	-.6885	.293	-11.0
#6	-.66	1.233	1.054	-.6820	1.65	-32.4
#6	-.68	1.073	.9876	-.6933	1.69	-33.3
#6	-.70	1.008	.9935	-.6985	1.70	-32.9
#6	-.72	1.046	.9798	-.6953	1.69	-33.6

where the initial  $\mu = 10^4$  (KPa.min<sup>1+m</sup>) and  $\alpha_1 = 10^8$  (KPa.min<sup>2+m</sup>).

Table 19 Model (II)

Test	initial	after iteration		objfun *10 <sup>3</sup>	error %	
	m	$\mu * 10^{-4}$	$\alpha_1 * 10^{-5}$			m
#3	-.66	1.333	1.266	-.6797	.260	-7.78
#3	-.68	1.014	.9116	-.7012	.259	-7.64
#3	-.70	1.000	.8924	-.7022	.259	-7.87
#3	-.72	1.048	.9442	-.6986	.258	-7.76
#6	-.66	1.424	1.645	-.6715	1.00	-25.6
#6	-.68	1.509	1.732	-.6665	1.00	-26.6
#6	-.70	1.013	1.014	-.6988	1.08	-29.2
#6	-.72	.9035	.9275	-.7086	.993	-26.1

where the initial  $\mu = 10^4$  (KPa.min<sup>1+m</sup>) and  $\alpha_1 = 10^5$  (KPa.min<sup>2+m</sup>); errors are calculated at t=5095(min) for #3, t=2395(min) for #6, so are in table 18.

Optimize  $\mu, \alpha_1$  and  $m$  by simultaneously fitting the short-term creep data of two pressuremeter tests.

Table 20

-----		Model (I)					-----	
#3 and #6								
Initial m	$\mu * 10^{-4}$	after iteration $\alpha_1 * 10^{-8}$	m	objfun $* 10^3$	error %	error %		
-.66	1.059	1.157	-.6961	1.98	-16.0	(#3)	-24.3	(#6)
-.68	1.096	1.602	-.6933	1.97	-16.9			
-.70	.9809	1.498	-.7020	2.11	-17.0			
-.72	.9009	1.463	-.7088	2.31	-16.1			

where the initial  $\mu = 10^4$  (KPa.min<sup>1+m</sup>) and  $\alpha_1 = 10^3$  (KPa.min<sup>2</sup>).

Table 21

-----		Model (II)					-----	
#3 and #6								
Initial m	$\mu * 10^{-4}$	after iteration $\alpha_1 * 10^{-5}$	m	objfun $* 10^2$	error %	error %		
-.66	1.134	2.061	-.6949	.338	+3.53	(#3)	-4.71	(#6)
-.68	1.146	1.972	-.6933	.359	-.060			
-.70	.9543	1.551	-.7076	.279	-.501			
-.72	1.215	1.801	-.7031	.299	+4.10			

where the initial  $\mu = 10^4$  (KPa.min<sup>1+m</sup>) and  $\alpha_1 = 10^5$  (KPa.min<sup>2+m</sup>), the fit time intervals of #3 and #6 are [10, 240](min) and [8, 220](min) respectively, the relative errors are calculated at t=5095(min) for #3 and t=2395(min) for #6.

Table 22

-----  
 Optimize  $\mu$  and  $\alpha_1$  when m is fixed by simultaneously fitting the primary creep data of two pressuremeter tests #3 and #6.

Model (I)  
 -----

Fixed m	after iteration $\mu * 10^{-4}$	iteration $\alpha_1 * 10^{-8}$	objfun $* 10^2$	error % (#3)	error % (#6)
-.66	1.668	2.003	.200	-15.	-19.
-.68	1.300	1.786	.185	-15.	-21.
-.70	1.006	1.521	.209	-17.	-26.
-.72	.7774	1.308	.280	-17.	-30.

where the initial  $\mu = 10^4$  (KPa.min<sup>1+m</sup>),  $\alpha_1 = 10^8$  (KPa.min<sup>2</sup>), the error is calculated at t=5095(min) for #3 and t=2395(min) for #6.

Table 23

-----  
 Optimize  $\mu$  and  $\alpha_1$  when m is fixed by simultaneously fitting the primary creep data of two pressuremeter tests #3 and #6.

Model (II)  
 -----

Fixed m	after iteration $\mu * 10^{-4}$	iteration $\alpha_1 * 10^{-5}$	objfun $* 10^2$	error % (#3)	error % (#6)
-.66	1.825	4.307	.528	+13.	+7.6
-.68	1.377	2.681	.419	+4.3	-2.2
-.70	1.059	1.481	.312	+2.4	-6.5
-.72	.8112	1.230	.217	+.15	-12.

where the initial  $\mu = 10^4$  (KPa.min<sup>1+m</sup>),  $\alpha_1 = 10^5$  (KPa.min<sup>2+m</sup>), the error is calculated at t=5095(min) for #3 and t=2395(min) for #6.

## Chapter 6 Applications of models (I) and (II)

### Section 6.1 Application to glacier flows

In this section, we shall study the velocity profile and normal stress difference in fluids modelled by the constitutive relations (1.2.1) and (1.2.2) when they undergo steady shearing flows, in order to indicate the merits of the two special Rivlin-Ericksen fluid models.

The motion of a glacier could be idealized as the steady shearing flow of a ice slab with uniform thickness  $h$  down a plane inclined to the horizontal by an angle  $\phi$  under gravitation (Nye, 1957). Choose a Cartesian coordinate system such that the inclined plane coincides with the  $x_1$ - $x_2$  plane; the base vectors  $e_1$  and  $e_2$  point along the line of greatest slope down the inclined plane and normally upward from the inclined plane, respectively. We seek a steady velocity field in the glacier with the form

$$\mathbf{v} = (v(x_2), 0, 0) \quad (6.1.1)$$

under the body force per unit mass

$$\mathbf{b} = g(\sin\phi e_1 - \cos\phi e_2) \quad (6.1.2)$$

and boundary conditions:

$$\mathbf{v}(0) = v_0 \mathbf{e}_1, \quad \mathbf{T}(h) \mathbf{e}_2 = -p_0 \mathbf{e}_2, \quad (6.1.3)$$

where  $g$  is the acceleration due to gravity,  $v_0$  a constant number,  $\mathbf{T}$  the Cauchy stress and  $p_0$  the atmospheric pressure acting on the glacier.

Suppose the glacier ice is modeled by (1.2.1) or (1.2.2). We assume that the glacier is assumed as homogeneous isotropic and incompressible continuum. Under those assumptions, the kinematic quantities should be

$$\begin{aligned} \mathbf{A}_1 &= v' (\mathbf{e}_1 \otimes \mathbf{e}_2 + \mathbf{e}_2 \otimes \mathbf{e}_1), \\ \mathbf{A}_2 &= 2(v')^2 \mathbf{e}_2 \otimes \mathbf{e}_2, \\ \mathbf{A}_1^2 &= (v')^2 (\mathbf{e}_1 \otimes \mathbf{e}_1 + \mathbf{e}_2 \otimes \mathbf{e}_2), \\ \mathbb{I} &= (v')^m \end{aligned} \quad (6.1.4)$$

from (1.2.5) and (1.2.4), where  $v' \equiv dv/dx_2$ ,  $\otimes$  is the tensor product of vectors. By substituting (6.1.4) into (1.2.1) and (1.2.2), we obtain the Cauchy stress in the glacier:

$$\begin{aligned} \text{(I)} \quad \mathbf{T} &= -p\mathbf{I} + [\alpha_2 (v')^{2+m}] \mathbf{e}_1 \otimes \mathbf{e}_1 + \mu v' (\mathbf{e}_1 \otimes \mathbf{e}_2 + \mathbf{e}_2 \otimes \mathbf{e}_1) \\ &\quad + (2\alpha_1 + \alpha_2) (v')^2 \mathbf{e}_2 \otimes \mathbf{e}_2, \end{aligned} \quad (6.1.5)$$

$$\begin{aligned} \text{(II)} \quad \mathbf{T} &= -p\mathbf{I} + (v')^m [\alpha_2 (v')^2 \mathbf{e}_1 \otimes \mathbf{e}_1 + \mu v' (\mathbf{e}_1 \otimes \mathbf{e}_2 + \mathbf{e}_2 \otimes \mathbf{e}_1) \\ &\quad + (2\alpha_1 + \alpha_2) (v')^2 \mathbf{e}_2 \otimes \mathbf{e}_2 ]. \end{aligned}$$

Then using the balance equation of linear momentum and taking

a simple analysis of the corresponding boundary value problem, we obtain

$$(I, II) \quad v(xz) - v\phi = [(\rho g \sin\phi)/\mu]^{1/(1+m)} \left(\frac{1+m}{2+m}\right) h^{(2+m)/(1+m)} \\ [1 - (1 - xz/h)^{(2+m)/(1+m)}]. \quad (6.1.6)$$

A glance at (6.1.6) reveals that the velocity of models (I) and (II) in the present glacier problem is precisely the same as that of the power law fluid model since the parameters  $\alpha_1$  and  $\alpha_2$  do not appear in (6.1.6). For further discussion, we set  $m = -2/3$  which is usually acceptable for ice in a glacier (Hooke, 1981). Then (6.1.6) is reduced to

$$(I, II) \quad v(xz) - v\phi = [(\rho g \sin\phi)/\mu]^{3/4} h^{3/4} [1 - (1 - xz/h)^{3/4}]/4. \quad (6.1.7)$$

We can also find from (6.1.6) that in this problem the velocity associated with the second order fluid model ( $m = 0$  in (6.1.6)) should be

$$v(xz) - v\phi = [(\rho g \sin\phi)/\mu] h^2 [1 - (1 - xz/h)^2]/2. \quad (6.1.8)$$

Before talking about which model has the velocity profile more compatible with empirical data obtained from real glaciers, let us look at some empirical data. By

measuring four boreholes distributed along a flowplane on Barnes Ice Cap, Baffin Island, Canada (Fig. 15), Hooke and Hanson(1985) gathered the velocity profile at the four boreholes in the glacier (Fig. 16). The four curves have the common character that the velocity profile is almost vertical in the great upper portion of each borehole. The glacier measured by Hooke and Hanson(1985) is certainly not identical to the idealized one in the above analysis. But the information provided by Fig. 16 suffices for qualitative analysis.

For the purpose of comparison, (6.1.7) and (6.1.8) are plotted in Fig. 17 with a given  $v_0$ ,  $\rho$ ,  $g$ ,  $\phi$ ,  $\mu$  and  $h$ . It is obvious by comparison that the curve with  $m = -2/3$  is closer to the real velocity profile than that with  $m = 0$  (which pertains to the second-order fluid model). In other words, models (I) and (II) as well as the power-law fluid model, rather than the second-order fluid model or the Newtonian fluid model, can adequately describe the velocity profile of a glacier.

Some phenomena in shearing flows of fluids, for instance, climbing in Couette flow, swelling in Poiseuille flow, depression or heaving of free surface in open channel flow, can be explained by normal stress differences; cf. Coleman and others (1966) and Schowalter (1978). Noticing that the power-law fluid model does not exhibit any normal stress effect shearing flows, McTigue and others (1985)

applied the second-order fluid model to study the possible effects of normal stress differences in glacier flows. But as pointed out before, the second-order fluid model cannot satisfactorily predict the velocity profile. Cf. Man and Sun (1986) for further comments on the work of McTigue and others. Indeed, by using the two special Rivlin-Ericksen fluid models (I) and (II), Man and Sun (1986) pointed out that the effect of normal stress differences on glacier flows may be far less pronounced than that envisaged by McTigue and others (1985).

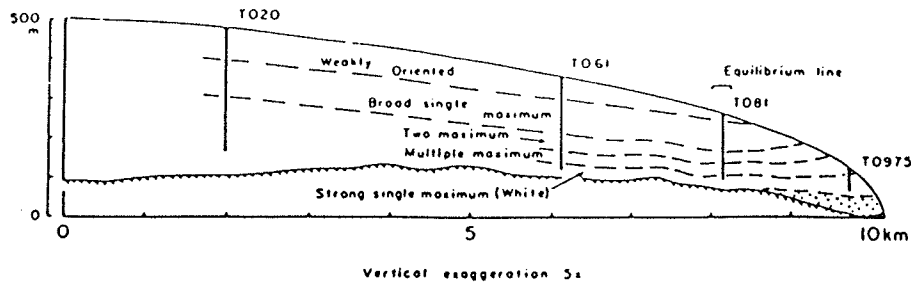


Fig. 15

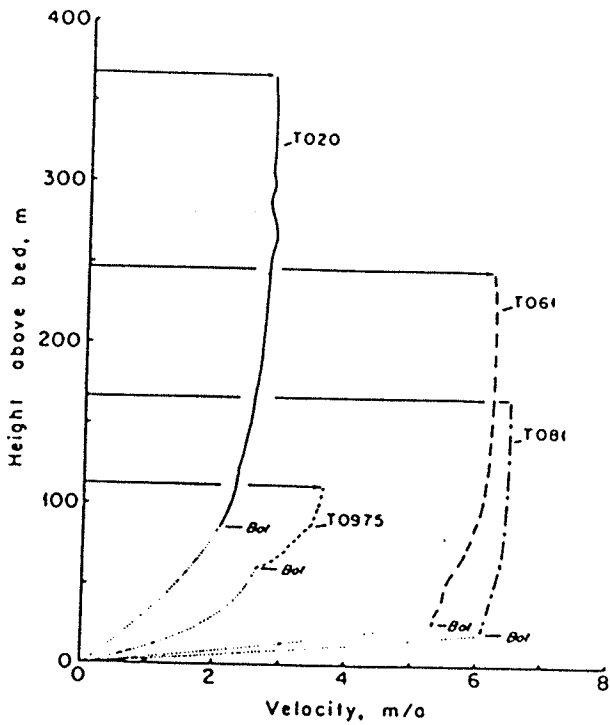


Fig. 16  
From Hooke and Hanson (1985)

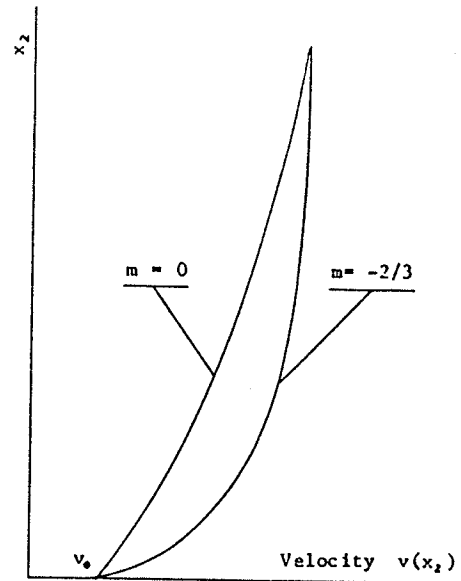


Fig. 17  
Quantitative comparison of  
velocity profiles for  $m = 0$   
&  $m = -2/3$

## Section 6.2 Heat and mass transfer in a pipe

In this section, we shall apply the special Rivlin-Ericksen fluid models (I) and (II) given by (1.2.1) and (1.2.2) to analyze the heat and mass transfer problem of fluid in a fixed pipe by following the same method provided by Szeri and Rajagopal (1985). Suppose a pipe of circular cross-section and radius  $R$  has infinite length. The wall temperature of the pipe is fixed as a constant, say  $\Theta_0$ . Let the fluid with constitutive relations (I) or (II) undergo a steady flow under the constant pressure drop  $k$  in the flow direction  $e_z$ , i.e.,

$$\partial T_{zz} / \partial z = k; \quad (6.2.1)$$

here  $(r, \phi, z)$  denotes cylindrical coordinates, where the  $z$ -axis coincides with the axis of the pipe. Let

$$(e_r, e_\phi, e_z)$$

denote the unit base vectors. We seek a velocity field  $\mathbf{v}$  and temperature distribution  $\Theta$  with the forms:

$$\mathbf{v} = (0, 0, w(r)), \quad (6.2.2)$$

$$\Theta = \Theta(r). \quad (6.2.3)$$

For the given problem, the first and second Rivlin-

Ericksen tensors are given by the formulae

$$\begin{aligned} \mathbf{A}_1 &= w' (\mathbf{e}_r \otimes \mathbf{e}_z + \mathbf{e}_z \otimes \mathbf{e}_r), \\ \mathbf{A}_2 &= 2(w')^2 \mathbf{e}_r \otimes \mathbf{e}_r, \end{aligned} \tag{6.2.4}$$

from which we deduce

$$\begin{aligned} \mathbf{A}_1^2 &= (w')^2 (\mathbf{e}_r \otimes \mathbf{e}_r + \mathbf{e}_z \otimes \mathbf{e}_z), \\ \Pi &= [(w')^2]^{m/2} = (-w')^m, \end{aligned} \tag{6.2.5}$$

where

$$w' \equiv dw/dz \leq 0, \quad \text{for } 0 \leq r \leq R, \tag{6.2.6}$$

and  $\otimes$  indicates the tensor product of vectors. Then by substituting (6.2.4) and (6.2.5) into (1.2.1) and (1.2.2), we obtain the Cauchy stress:

$$\begin{aligned} \text{(I)} \quad \mathbf{T} &= -p\mathbf{I} + (2\alpha_1 + \alpha_2)(-w')^2 \mathbf{e}_r \otimes \mathbf{e}_r - \mu(-w')^{m+1} (\mathbf{e}_r \otimes \mathbf{e}_z \\ &\quad + \mathbf{e}_z \otimes \mathbf{e}_r) + \alpha_2 (-w')^2 \mathbf{e}_z \otimes \mathbf{e}_z, \end{aligned} \tag{6.2.7}$$

$$\begin{aligned} \text{(II)} \quad \mathbf{T} &= -p\mathbf{I} + (-w')^m [(2\alpha_1 + \alpha_2)(-w')^2 \mathbf{e}_r \otimes \mathbf{e}_r - \mu(-w') (\mathbf{e}_r \otimes \mathbf{e}_z \\ &\quad + \mathbf{e}_z \otimes \mathbf{e}_r) + \alpha_2 (-w')^2 \mathbf{e}_z \otimes \mathbf{e}_z]. \end{aligned} \tag{6.2.8}$$

Since the flow is assumed to be steady, it may be shown that

$$\dot{\mathbf{v}} = \mathbf{0}$$

and the balance equation of linear momentum is simplified to

$$\begin{aligned}
 & \partial p / \partial r = \partial [(2\alpha_1 + \alpha_2)(-w')^2] / \partial r + (2\alpha_1 + \alpha_2)(-w')^2 / r, \\
 \text{(I)} \quad & \partial p / \partial \phi = 0, \\
 & \partial p / \partial z + \partial [\mu r (-w')^{m+1}] / \partial r / r = 0,
 \end{aligned} \tag{6.2.9}$$

$$\begin{aligned}
 & \partial p / \partial r = \partial [(2\alpha_1 + \alpha_2)(-w')^{m+2}] / \partial r + (2\alpha_1 + \alpha_2)(-w')^{m+2} / r, \\
 \text{(II)} \quad & \partial p / \partial \phi = 0, \\
 & \partial p / \partial z + \partial [\mu r (-w')^{m+1}] / \partial r / r = 0
 \end{aligned} \tag{6.2.10}$$

when the body force is neglected. Since the pressure gradient  $k$  is constant in the fluid, i.e.

$$-\partial p / \partial z = \partial T_{zz} / \partial z = k,$$

the velocity profile can be solved from the equation

$$\begin{aligned}
 \text{(I, II)} \quad & \partial [\mu r (-w')^{m+1}] / \partial r = rk \\
 \text{or} \\
 \text{(I, II)} \quad & w'(r) = -[kr / (2\mu(\theta))]^{1/(m(\theta)+1)},
 \end{aligned} \tag{6.2.11}$$

where we have used the symmetric condition  $w'(0) = 0$ .

Next we proceed to deal with the equation of heat conduction which will be derived from the balance of energy. It is known from the theory of continuum mechanics (Gurtin, 1972) that the first law of thermodynamics is given in local form as follows:

$$\rho D\mathcal{E} / Dt = \mathbf{T} \cdot \mathbf{L} - \text{div} \mathbf{q} + \rho \gamma; \tag{6.2.12}$$

here  $\mathcal{E}$  is the internal energy,  $\gamma$  the radiant heat supply per

unit mass,  $\mathbf{T}$  the Cauchy stress tensor,  $\mathbf{L}$  the velocity gradient,  $\mathbf{q}$  the heat flux, and  $\rho$  the density.

In general, the specific internal energy  $\varepsilon$  for the Rivlin-Ericksen fluid of complexity 2 can be written as

$$\varepsilon = \varepsilon(\Theta, \mathbf{A}_1, \mathbf{A}_2).$$

For the present problem where  $\mathbf{A}_1$  and  $\mathbf{A}_2$  are given in the form (6.2.5), the function  $\varepsilon$  is specialized to

$$\varepsilon = \bar{\varepsilon}(\Theta, w').$$

But  $\varepsilon$  and  $w'$  are only dependent on  $r$  from (6.2.3) and (6.2.4). Thus

$$D\varepsilon/Dt = 0. \quad (6.2.13)$$

Suppose the constitutive relation of the heat flux can be characterized by Fourier's law

$$(I, II) \quad \mathbf{q} = -K(\Theta)\text{grad}\Theta.$$

Then in the present problem

$$(I, II) \quad \text{div}\mathbf{q} = -d[rK(\Theta)d\Theta/dr]/dr/r. \quad (6.2.14)$$

It may be easily shown that

$$\mathbf{T} \cdot \mathbf{L} = \mathbf{T} \cdot \mathbf{A}_1 / 2 = \mu(\Theta) (-w')^{m(\Theta)+2}. \quad (6.2.15)$$

Suppose there is no radiant heat supply, i.e.  $\gamma = 0$ . Hence by substituting (6.2.14) and (6.2.15) into (6.2.12) and keeping (6.2.11) in mind, we obtain the temperature and velocity field equations for models (I) and (II):

$$\mu(\Theta) (-w')^{m(\Theta)+2} + d[rK(\Theta)\Theta'] / dr / r = 0, \quad (6.2.16)$$

$$w' + [kr / (2\mu(\Theta))]^{1/(m(\Theta)+1)} = 0 \quad (6.2.17)$$

with the boundary conditions:

$$\begin{aligned} w(R) &= w_\phi, \\ \Theta(R) &= \Theta_\phi \end{aligned} \quad (6.2.18)$$

and the symmetric condition:

$$\Theta'(0) = 0, \quad (6.2.19)$$

where  $w_\phi$  and  $\Theta_\phi$  are the given constants, and  $\Theta' \equiv d\Theta/dr$ . Since (6.2.16) and (6.2.17) with (6.2.18) and (6.2.19) are two-point boundary value problems, their numerical solution may be found by the finite-difference method (Walsh, 1981, Kubicek & Hlavacek, 1983) as long as the functions  $\mu(\Theta)$  and  $m(\Theta)$  are specified.

To find the difference between non-Newtonian and Newtonian fluids in the heat and mass transfer problem, Szeri and Rajagopal (1985) applied the third grade fluid model to steady shearing flows between two fixed and heated plates. Using Reynold's and Vogel's models as viscosity coefficients, they found that if the fluid is even slightly non-Newtonian, variable viscosity solutions are not too distant from constant viscosity solutions in contrast with Newtonian fluid. Basing on their results, we may approximately assume that the viscosity in models (I) and (II) is independent of temperature. For simplicity in further analysis, we only consider the case in which the heat conductivity  $K$  and  $m$ , the exponent in models (I) and (II), are also constants. Then (6.2.16) and (6.2.18) reduce to:

$$(I, II) \quad \mu(-w')^{m+2} + Kd(r\theta')/dr/r = 0, \quad (6.2.20)$$

$$(I, II) \quad w' + (kr/2/\mu)^{1/(m+1)} = 0, \quad (6.2.21)$$

which show that in the present case, the velocity  $w$  is independent of temperature but the temperature  $\theta$  depends on the velocity through (6.2.20).

A straightforward integration of (6.2.20) and (6.2.21) yields

$$w(r) - w_0 = \frac{m+1}{m+2} \left( \frac{k}{2\mu} \right)^{1/(m+1)} R^{\frac{m+2}{m+1}} [1 - (r/R)^{\frac{m+2}{m+1}}], \quad (6.2.22)$$

$$\Theta(r) - \Theta_0 = \left( \frac{m+2}{m+1} + 2 \right)^2 \frac{\mu}{K} \left( \frac{kR}{2\mu} \right)^{\frac{m+2}{m+1}} R^2 [1 - (r/R)^{\frac{m+2}{m+1}+2}], \quad (6.2.23)$$

where the conditions (6.2.18) and (6.2.19) have been used.

## CONCLUSION

The main theoretical results presented in this thesis are the thermodynamic constitutive restrictions on models (I) and (II) derived under the assumptions that (1) the motion of fluids characterized by models (I) and (II) is slow; (2) the free energy has a minimum at the rest state and is convex in  $A_1$  in a neighbourhood of  $A_1 = 0$ . Furthermore, it is shown that if  $A_1$  remains in the respective constitutive domain of the two models, and models (I) and (II) are (not) consistent with the constitutive restrictions, cannister flows and triaxial homogeneous flows are (not) asymptotically stable. It remains as further work to study the Lyapunov stability of the rest state and various motions of fluids (I) and (II).

When models (I) and (II) are applied to fit the creep data of pressuremeter and triaxial tests, it is found that the two models can adequately describe both the primary and the secondary creep of polycrystalline ice. This finding will be important in the endeavour to predict the long-term creep behaviour of ice by using the two models to fit short-term creep data. The values of the material parameters of models (I) and (II) estimated from the data of Kjartanson and Jones corroborate the derived thermodynamic restrictions. The fitting process is essentially based on a nonlinear optimization method by the use of the computer.

The techniques to evaluate the material parameters of models (I) and (II) by fitting creep data are described in detail in this thesis. As for the problem to devise a short-term in-situ pressuremeter test which will delineate the long-term creep behaviour of ice, it is found that the experimental data of a single-stage pressuremeter creep test are not enough to evaluate all the relevant material parameters in the two models. To solve this problem, doing short-term multistage tests may be worthwhile to provide sufficient data for the applications of the two models.

## APPENDICES

## A.1 Least squares fitting with constraints

Let

$$(x_j, Y_j), \quad j=1, 2, \dots, m,$$

be a set of given data points. The problem at issue is to use a polynomial

$$f(x) = \sum_{i=1}^n c_i x^{i-1} \quad (\text{A.1.1})$$

to fit the points  $(x_{k+1}, Y_{k+1}), \dots, (x_m, Y_m)$  under the constraints that

$$f(x_j) = Y_j, \quad j=1, 2, \dots, k < m. \quad (\text{A.1.2})$$

More precisely, we seek coefficients  $c_i$  in (A.1.1) that minimize

$$\sum_{j=k+1}^m [f(x_j) - Y_j]^2 \quad (\text{A.1.3})$$

and satisfy

$$f(x_j) = Y_j, \quad j=1, 2, \dots, k < m.$$

This problem can be solved by the method of Lagrange

multipliers. Let

$$F(\mathbf{c}, \mathbf{b}) = \sum_{j=k+1}^m \left[ \left( \sum_{i=1}^n c_i x_j^{i-1} - y_j \right)^2 \right] + \sum_{j=1}^k \lambda_j \left( \sum_{i=1}^n c_i x_j^{i-1} - y_j \right), \quad (\text{A.1.4})$$

where  $\mathbf{c}$  and  $\mathbf{b}$  are the transpose of  $(c_1, c_2, \dots, c_m)$  and  $(\lambda_1, \lambda_2, \dots, \lambda_k)$ , respectively;  $\mathbf{b}$  is the as yet undetermined Lagrange multiplier vector.

When  $F$  is at a minimum,

$$\partial F / \partial \mathbf{c} = \mathbf{0}, \quad \text{and} \quad \partial F / \partial \mathbf{b} = \mathbf{0},$$

or in detail

$$\sum_{j=k+1}^m \left( \sum_{h=1}^n c_h x_j^{h-1} - y_j \right) x_j^{i-1} + \sum_{j=1}^k \lambda_j x_j^{i-1} = 0, \quad i=1, 2, \dots, n,$$

$$\sum_{i=1}^n (c_j x_j^{i-1} - y_j) = 0, \quad j=1, 2, \dots, k. \quad (\text{A.1.5})$$

(A.1.5) can be recasted compactly as

$$\mathbf{AW} = \mathbf{B}, \quad (\text{A.1.6})$$

where  $\mathbf{A}$  is a square matrix of order  $(n+k)$  defined by

$$A_{j,i} = x_j^{i-1}, \quad i=1, 2, \dots, n, \quad j=1, 2, \dots, k$$

$$A_{i,j+n} = 0, \quad i, j, = 1, 2, \dots, k$$

$$A_{i+k,h} = 2 \sum_{j=k+1}^m x_j^{h+i-2}, \quad h, i = 1, 2, \dots, n,$$

$$A_{i+k,j+n} = x_j^{i-1}, \quad i = 1, 2, \dots, n, \quad j = 1, 2, \dots, k,$$

B is an  $(n+k)$  vector defined by

$$B_j = Y_j, \quad j = 1, 2, \dots, k,$$

$$B_{i+k} = 2 \sum_{j=k+1}^m Y_j x_j^{i-1}, \quad i = 1, 2, \dots, n,$$

(A.1.7)

and  $W = (c, b)$  is the unknown  $(n+k)$  vector to be determined. The matrices  $A$  and  $B$  can be evaluated from the given data. The unknown coefficients  $c$  and  $b$  can be easily determined by solving the linear algebraic equations (A.1.6).

## A.2 Nonlinear least squares optimization by the Levenberg-Marquardt method

Statement of the problem: let  $\mathbf{y} = (y_1, y_2, \dots, y_n) = (y(t_1), y(t_2), \dots, y(t_n))$  be the  $n$ -observations of the dependent variable  $\mathbf{y}$ ,  $\mathbf{x} = (x_1, x_2, \dots, x_m)$  the vector of  $m$  parameters,  $f(\mathbf{x}, t)$  the predicted solution, and

$$f_i = f(\mathbf{x}, t_i), \quad i = 1, 2, \dots, n. \quad (\text{A.2.1})$$

The objective is to find an  $\mathbf{x}$  such that

$$F = \sum_i (y_i - f_i)^2 = \min, \quad (\text{A.2.2})$$

locally, where  $F$  is called the objective function.

The Gauss-Newton method for the iteration of parameters is as follows. Suppose one has got  $\mathbf{x}^{(k)}$  after  $(k - 1)^{\text{th}}$  step of iteration. Then next step is to find an increment vector

$$\delta \mathbf{x} \quad \text{such that} \quad F(\mathbf{x}^{(k)} + \delta \mathbf{x}^{(k)}) = \min \quad (\text{A.2.3})$$

locally. Since

$$F(\mathbf{x}^{(k)} + \delta \mathbf{x}^{(k)}) \approx \sum_i [y_i - f_i(\mathbf{x}^{(k)}) - (\partial f_i / \partial \mathbf{x}^{(k)})^T \delta \mathbf{x}^{(k)}]^2 \quad (\text{A.2.4})$$

by the Taylor expansion, then one must have

$$\partial F(\mathbf{x}^{(k)} + \mathbf{w}) / \partial \mathbf{w} = \mathbf{0} \quad \text{at} \quad \mathbf{w}^{(k)} = \delta \mathbf{x} \quad (\text{A.2.5})$$

which with (A.2.4) leads to

$$\sum_i [Y_i - f_i - (\partial f_i / \partial \mathbf{x}^{(k)})^T \delta \mathbf{x}^{(k)}] \partial f_i / \partial \mathbf{x}^{(k)} = \mathbf{0}. \quad (\text{A.2.6})$$

By defining

$$\mathbf{g}^{(k)} = \sum_i (Y_i - f_i) \partial f_i / \partial \mathbf{x}^{(k)}, \quad (\text{A.2.7})$$

$$J_{ij}^{(k)} = \partial f_i / \partial x_j^{(k)}, \quad j = 1, 2, \dots, m \quad (\text{A.2.8})$$

$$\mathbf{A}^{(k)} = \mathbf{J}^{(k)T} \mathbf{J}^{(k)}, \quad (\text{A.2.9})$$

(A.2.4) can be represented in the neat form

$$\mathbf{g}^{(k)} = \mathbf{A}^{(k)} \delta \mathbf{x}^{(k)} \quad (\text{A.2.10})$$

from which,  $\delta \mathbf{x}^{(k)}$  can be solved by

$$\delta \mathbf{x}^{(k)} = (\mathbf{A}^{(k)})^{-1} \mathbf{g}^{(k)}. \quad (\text{A.2.11})$$

Since (A.2.4) is approximately valid,

$$F(\mathbf{x}^{(k)} + \delta \mathbf{x}^{(k)})$$

would not exactly arrive at a minimum when the increment vector solved from (A.2.11) is substituted into (A.2.3). The further iteration given by

$$\mathbf{x}^{(k+1)} = \mathbf{x}^{(k)} + (\mathbf{A}^{(k)})^{-1} \mathbf{g}^{(k)} \quad (\text{A.2.12})$$

is needed until the assigned convergent conditions are satisfied. The matrix  $\mathbf{J}$  defined by (A.2.8) can be computed either analytically if there exists an explicit expression of  $\partial f / \partial \mathbf{x}$  or numerically by the finite-difference method.

To avoid interruption of the iteration when  $\mathbf{A}$  is singular and to accelerate the iteration, Levenberg(1944) and Marquardt(1963) independently proposed to replace (A.2.12) by the superior formula

$$\mathbf{x}^{(k+1)} = \mathbf{x}^{(k)} + (\lambda^{(k)} \mathbf{I} + \mathbf{A}^{(k)})^{-1} \mathbf{g}^{(k)}, \quad (\text{A.2.13})$$

where  $\lambda$  is a positive real number and  $\mathbf{I}$  the unit matrix. In addition, Marquardt(1963) proved the convergence of the iteration (A.2.13) for any  $\lambda \geq 0$  and showed the strategy to choose  $\lambda$  at each step  $k$ . As another contribution to the method, Marquardt showed that the iteration (A.2.13) approaches the gradient or steepest descent method when  $\lambda \rightarrow \infty$ . Consequently, (A.2.13) shares both the merits of the Gauss-Newton and gradient methods.

The Fortran computer program of the Levenberg-Marquardt method called ZXSSQ is issued by IMSL.

### A.3 Procedure of fitting creep data of ice by nonlinear optimization

In the subroutine ZXSSQ issued by IMSL, which gives a least squares estimation of the material parameters, it is necessary to start with an initial guess of the parameters. For models (I) and (II), we can determine a reasonable "guess" by using the method introduced in Sec. 4.2 for triaxial tests and in Sec. 5.2 for pressuremeter tests of ice, respectively. In what follows we shall assume that an initial "guess" of the material parameters has been determined.

When the estimate satisfies one of the following convergence criteria, the iteration will stop. The first criterion is denoted by NSIG, an integer. This convergence criterion is satisfied if on two successive iterations the estimated values of the parameters agree to NSIG digits. The second is denoted by EPS, a small real number. This convergence criterion is satisfied if on two successive iterations the sum of squared residuals has a difference whose absolute value is less than or equal to EPS. The third is denoted by DELTA, a small real number. This convergence criterion is satisfied if the Euclidean norm of the approximate gradient is less than or equal to DELTA. For further details, cf. the description that accompanies subroutine ZXSSQ issued by IMSL.

The major steps in using models (I) and (II) to fit the creep data of polycrystalline ice are as follows:

1. Read the creep data and pressure of the test.
2. Choose a function to fit the first several data-points to determine the initial conditions of the creep equation in question. If the creep data have the same value during some time interval, only the middle point in the interval will be used for the fitting.
3. Choose the time interval over which the fitting will be done and set the time at which prediction of creep will be terminated.
4. Give an initial guess of the material parameters.
5. Set the values of the convergence criteria: NSIG, EPS and DELTA.
6. Enter the subroutine ZXSSQ for the iterative estimation of the material parameters.
7. Compute the numerical solution of the creep equation that corresponds to a given estimate of the material parameters by the fifth-order Runge-Kutta-Nyström algorithm.
8. Interpolate the predicted creep at the time nodes where experimental data are measured.
9. Compute the value of the objective function and its gradient with respect to the material parameters by a finite difference method.
10. Examine the convergence criteria. If one of them is satisfied, then jump to step 12; otherwise, go to the next

step.

11. The values of the parameters are modified by the subroutine ZXSSQ. Then go back to step 7.

12. Print out the values of the optimized parameters and the final value of the objective function.

13. Compute the statistical errors of the optimized parameters.

14. Compare the predicted creep with the experimental data and compute the predicted creep rate.

15. Stop.

In the preceding program, the fifth-order Runge-Kutta-Nyström method is used to integrate numerically the creep equation in question. For the initial value problem

$$y' = f(t, y; c), \quad y(t_0) = y_0, \quad (\text{A.3.1})$$

where  $c$  denotes the parameters,  $t_0$  the initial time,  $y_0$  the initial value of  $y$ , a numerical solution of (A.3.1) is computed from the following recursion formulae:

$$Y_{n+1} - Y_n = h(23k_1 + 125k_2 - 81k_3 + 125k_4)/192,$$

$$k_1 = f(t_n, Y_n; c),$$

$$k_2 = f(t_n + h/3, Y_n + hk_1/3; c),$$

$$k_3 = f(t_n + 2h/3, Y_n + h(4k_1 + 6k_2)/25; c),$$

$$\begin{aligned}
k_4 &= f(t_n + h, y_n + h(k_1 - 12k_2 + 15k_3)/4; c), \\
k_5 &= f(t_n + 2h/3, y_n + h(6k_1 + 90k_2 - 50k_3 + 8k_4)/81; c), \\
k_6 &= f(t_n + 4h/5, y_n + h(6k_1 + 36k_2 + 10k_3 + 8k_4)/75; c);
\end{aligned}
\tag{A.3.2}$$

here  $h$  is the step length.

As for the interpolation step 8, the Lagrange method for three points with different distance is employed:

$$y(x) = \sum_{k=i}^{i+2} \left( \prod_{\substack{j=i \\ j \neq k}}^{i+2} \frac{(x - x_j)}{(x_k - x_j)} \right) Y_k, \tag{A.3.3}$$

where

$$\begin{aligned}
i &= j - 1, \text{ if } x < (x_j + x_{j+1})/2, \quad j = 2, 3, \dots, n - 2, \\
i &= n - 2, \text{ if } x \geq (x_{n-2} + x_{n-1})/2.
\end{aligned}
\tag{A.3.4}$$

## REFERENCES

- Ashby, M.F. 1985. "The creep of polycrystalline ice". Cold Reg. Sci. Tech., Vol. 11, p. 285-300.
- Baguelin, F., Jezequel, J.F. & Shields, D.H. 1978. **The pressuremeter and foundation engineering**. Tran Tech Pub. Clausthal, Germany.
- Coleman, B.D. & Noll, W. 1959. "On the thermostatics of continuous media", Arch. Rat. Mech. Anal., Vol. 4, p. 97-128.
- Coleman, B.D. & Noll, W. 1960. "An approximation theorem for functionals, with application in continuum mechanics". Arch. Rat. Mech. Anal., Vol. 6, p. 355-370.
- Coleman, B.D. & Noll, W. 1963. "The thermodynamics of elastic materials with heat conduction and viscosity", Arch. Rat. Mech. Anal., Vol. 13, p. 245-261.
- Coleman, B.D. & Markovitz, H. 1964. "Normal stress effects in second-order fluids". J. Appl. Physics, Vol. 35, p. 1-19.
- Coleman, B.D., Duffin, R.J. & Mizel, V. 1965. "Instability, uniqueness, and nonexistence theorems for the equation  $u_{t-t} - u_{xx} - u_{xtx} = 0$  on a strip". Arch. Rat. Mech. Anal., Vol. 19, p. 100-116.
- Coleman, B.D., Markovitz, H. & Noll, W. 1966. **Viscomeric flows of non-Newtonian fluids**. Springer-Verlag, New York.
- Coleman, B.D. & Mizel, V. 1966. "Breakdown of laminar shearing flows for second-order fluids in channels of critical width". ZAMM, Vol. 46, p. 445-448.
- Dunn, J.E. & Fosdick, R.L. 1974. "Thermodynamic, stability, and boundedness of fluids of complexity 2 and fluids of second grade". Arch. Rat. Mech. Anal., Vol. 56, p. 191-252.
- Dunn, J.E. 1982. "On the free energy and stability of nonlinear fluids". Journal of Rheology, Vol. 26, No.1, p. 43-68.
- Fosdick, R.L. & Rajagopal, K.R. 1979. "Anomalous features in the model of 'second order fluids". Arch. Rat. Mech. Anal., Vol. 70, p. 145-152.
- Fosdick, R.L. & Rajagopal, K.R. 1980. "Thermodynamics and

stability of fluids of third grade". Proc. Roy. Soc. London, A. 339, p. 351-377.

Glen, J.W. 1952. "Experiments on the deformed ice". J. of Glaciology, Vol. 2, No.12, p. 111-114.

Glen, J.W. 1955. "The creep of polycrystalline ice". Proc. Roy. Soc. London, A. Vol. 228, No.1175, p. 519-538.

Glen, J.W. 1958. "The flow of ice". IASH, AISH Publ. Vol. 47, p. 171-183.

Gurtin, M.E. 1972. **Modern continuum thermodynamics.** Mechanics Today. Pergamon, New York.

Gurtin, M.E. 1981. **An introduction to continuum mechanics.** Academic Press, New York.

Hewitt, E. & Stromberg, K. 1965. **Real & abstract analysis.** Spring-Verlag, New York Inc.

Hooke, R.L. 1981. "Flow law for polycrystalline ice in glaciers: comparison of theoretical predictions, laboratory data, and field measurements". Review of Geophysics and Space Physics, Vol. 9, No.4, p. 664-672.

Huilgol, R.R. & Phan-Thien, N. 1986. "Recent advances in the continuum mechanics of viscoelastic liquids". Int. J. Eng. Sci., Vol. 24, No.2, p.161-251.

Hutter, K. 1983. **Theoretical glaciology.** D. Reidel Pub., Holland.

Jacka, T.H. 1984. "The time and strain required for development of minimum strain rate". Cold Reg. Sci. Tech., Vol. 8, p. 261-268.

Jones, S.J. & Glen, J.W. 1969. "The mechanical properties of single crystals of pure ice". J. of Glaciology, Vol. 8, No.54, p. 463-474.

Joseph, D. 1981. "Instability of the rest state of fluids of arbitrary grade greater than one". Arch. Rat. Mech. Anal., Vol. 75, p. 251-256.

Kjartanson, B. 1986. "Pressuremeter creep testing in laboratory ice". Ph.D thesis. The University of Manitoba, Canada.

Kubicek, M. & Hlavacek, V. 1983. **Numerical solution of nonlinear boundary value problem with application.** Prentice-

Hall, New Jersey.

Ladanyi, B. & Johnston, G.H. 1973. "Evaluation of in situ creep properties of frozen soils with pressuremeter". Permafrost: The North American contribution to the Second Int. Conf.

Ladyzhenskaya, O.A. 1969. **The mathematical theory of viscous incompressible fluid.** Gordon & Breach, New York.

Lambert, J.D. 1972. **Computational methods in ordinary differential equations.** John Wiley & Sons, London.

Levenberg, K. 1944. "A method for the solution of certain non-linear problems in least squares". Quart. Appl. Math., Vol. 2, p. 164-168.

Man, C.-S. 1984. Private communication.

Man, C.-S., Shields, D.H. Kjartanson, B. & Sun, Q.-X. 1985. "Creep of ice as a fluid of complexity 2: the pressuremeter problem". Proc. 10th. Canadian Cong. Appl. Mech. London, Canada, Vol 1, p. A347-348. Complete paper in preparation.

Man, C.-S. & Sun, Q.-X. 1986. "On the significance of normal stress effects in the flow of glaciers". Submitted to J. of Glaciology.

Markovitz, H. & Coleman, B.D. 1964. "Nonsteady helical flows of second order fluids". Physics of Fluids, Vol. 7, p. 833-841.

Marquardt, D.W. 1963. "An algorithm for least-squares estimation of nonlinear parameters". J. SIAM., Vol. 11, No.2, p. 431-440.

McTigue, D.F., Passman, S.L. & Jones, S.J. 1985. "Normal stress effects in the creep of ice". J. of Glaciology, Vol. 31, No.108, p. 120-126.

Mellor, M. & Cole, D.M. 1983. "stress/strain/time relations for ice under uniaxial compression". Cold Reg. Sci. Tech. Vol. 6, p. 207-230.

Michel, B. 1978. **Ice mechanics.** Laval Univ. Press, Quebec.

Morland, L.W. & Spring, U. 1981. "Viscoelastic fluid relation for the deformation of ice". Cold Reg. Sci. Tech., Vol. 4, No. 3, p. 255-268.

Norton, F.H. 1929. **The creep of steel at high temperature.**

McGraw-Hill, New York.

Nye, J.F. 1952. "The mechanics of glacier flow". J. of Glaciology, Vol. 2, No.12, p. 82-93.

Nye, J.F. 1957. "The distribution of stress and velocity in glaciers and ice-sheets". Proc. Roy. Soc. London, A. 239, No.1216, p.113-133.

Odqvist, F.K.G. 1966. **Mathematical theory of creep and creep rupture**. Oxford, Clarendon.

Passman, S.L. 1982. "Creep of a second-order fluid". J. of Rheology, Vol. 26, No. 4, p. 373-385.

Rektorys, K. 1975. **Variational methods in mathematics, science and engineering**. D. Reidel Pub., Holland.

Rivlin, R.S. & Ericksen, J.L. 1955. "Stress-deformation relations for isotropic materials". J. Rat. Mech. Anal., Vol. 4, p. 323-425.

Schowalter, W.R. 1978. **Mechanics of non-Newtonian fluids**. Pergamon, Oxford.

Spring, U. & Morland, W. 1982. "Viscoelastic solid relations for the deformation of ice". Cold Reg. Sci. Tech., Vol. 5, p. 221-234.

Spring, U. & Morland, W. 1983. "Integral representations for the viscoelastic deformation of ice". Cold Reg. Sci. Tech., Vol. 6, p. 185-193.

Szeri, A.Z. & Rajagopal, K.R. 1985. "Flow of non-Newtonian fluid between heated parallel plates". Int. J. Non-linear Mechanics, Vol. 20, No.2, p. 91-101.

Truesdell, C. 1954. **The kinematics of vorticity**. Indiana Univ. Press, Bloomington.

Truesdell, C. 1965. "Fluids of the second grade regarded as fluids of convected elasticity". The Physics of Fluids, Vol. 8, No.11, p. 1936-1938.

Truesdell, C. 1969. **Rational thermodynamics**. McGraw-Hill, Yew York.

Truesdell, C. & Noll, W. 1965. **The non-linear field theories of mechanics**. Flugge's Handbuch der Physik, Vol. III/3, Springer-Verlag, Berlin etc.

Walsh, J.E. 1981. **The numerical solution of nonlinear problems.** Ed. C.T. H. Baker & C. Phillips, Oxford Univ. Press, etc.

## Computer programs

```

10. // JOB ',,T=5'
20. // EXEC FORTXCLG,OPT=2,SIZE=512K
30. // FORT.SYSIN DD *
40. C      This program is used to evaluate the material parameters
50. C      mu and m at the time when ddr/dtt=0.
60. C      Program name---MUM
70. C      -----
80.      EXTERNAL OBJFUN
90.      DIMENSION PARM(4),XJAC(22,2),XJTJ(3),WORK(100),F(50),AA(22),X(2
100. &      ,Y(2,2),DX(2),DXPROB(2),WORK1(4),S(2),AINV(2,2),B(2,2),
110. &      ALN(22),PLN(22),AALN(22)
120.      COMMON/C1/A(22),P(22)/C2/B1,B2
130.      WRITE(6,100)
140. 100  FORMAT(//////////50X,'Table A',/50X,'-----')
150.      WRITE(6,120)
160. 120  FORMAT(//5X,'Determination of mu and m from the secondary'
170. &      , ' creep rates by nonlinear regression',//5X,'Notaton:',/5X,
180. &      'P---cavity pressure; b---rate of secondary creep; ',
190. &      'bb---predicted values of b;',/5X,'residual---b(i)-bb(i);',
200. &      ' Objfun---sum of squared residuals;',/5X,
210. &      'er1=100.*(b(i)-bb(i))/b(i); er2=100.*(Ln(b(i))-Ln(bb(i)))',
220. &      ' /(-Ln(b(i))).',/5X,'Units:',/5X,'P in KPa;',
230. &      ' b and bb in 1./min; mu in KPa.min**(1.+m);',
240. &      ' m is a real number.')
250.      M=22
260.      N=2
270.      A(1)=.3692E-5
280.      A(2)=.7111E-5
290.      A(3)=.1052E-4
300.      A(4)=.105E-4
310.      A(5)=.120E-4
320.      A(6)=.134E-4
330.      A(7)=.180E-4
340.      A(8)=.204E-4
350.      A(9)=.210E-4
360.      A(10)=.2227E-4
370.      A(11)=.310E-4
380.      A(12)=.3147E-4
390.      A(13)=.3171E-4
400.      A(14)=.342E-4
410.      A(15)=.345E-4
420.      A(16)=.4582E-4
430.      A(17)=.540E-4
440.      A(18)=.540E-4
450.      A(19)=.545E-4
460.      A(20)=.780E-4
470.      A(21)=.8125E-4
480.      A(22)=.840E-4
490.      P(1)=1000.
500.      P(2)=1250.
510.      P(3)=1500.
520.      P(4)=1500.
530.      P(5)=1500.
540.      P(6)=1500.
550.      P(7)=1750.
560.      P(8)=1750.
570.      P(9)=1750.
580.      P(10)=1750.
590.      P(11)=2000.
600.      P(12)=2000.
610.      P(13)=2000.
620.      P(14)=2000.
630.      P(15)=2000.
640.      P(16)=2250.

```

```

650.      P(17)=2250.
660.      P(18)=2250.
670.      P(19)=2250.
680.      P(20)=2500.
690.      P(21)=2500.
700.      P(22)=2500.
710.      WRITE(6,230)
720. 230  FORMAT(/3X,'mu:',14X,'m:',15X,'Objfun:  in iteration')
730.      X(1)=9006.
740.      X(2)=-0.7132
750.      B1=1.
760.      B2=1.
770.      X(1)=X(1)*B1
780.      X(2)=X(2)*B2
790.      NSIG=3
800.      MAXFN=100
810.      IXJAC=M
820.      EPS=1.E-8
830.      DELTA=1.E-15
840.      IOPT=2
850.      PARM(1)=0.5
860.      PARM(2)=5.
870.      PARM(3)=120.
880.      PARM(4)=1.E-4
890.      CALL ZXSSQ(OBJFUN,M,N,NSIG,EPS,DELTA,MAXFN,IOPT,PARM,X,SSQ,
900.      & F,XJAC,IXJAC,XJTJ,WORK,INFER,IER)
910.      X(1)=X(1)/B1
920.      X(2)=X(2)/B2
930.      WRITE(6,200) X(1),X(2),SSQ,INFER
940. 200  FORMAT(/5X,'Least square estimates: mu=',F15.5,5X,'m=',
950.      & F12.5,5X,'Objfun=',E10.5,5X,'Convergence criterion=',I2)
960.      WRITE(6,380)
970. 380  FORMAT(/5X,'XJAC, gradient of residuals w.r.t. mu and m',
980.      & ' at the least square estimates.',5X,'Residuals:')
990. 390  FORMAT(5X,E15.6,10X,E15.6,38X,E12.5)
1000.     DO 90 I=1,M
1010.     XJAC(I,1)=XJAC(I,1)*B1
1020.     XJAC(I,2)=XJAC(I,2)*B2
1030. 90  WRITE(6,390) XJAC(I,1),XJAC(I,2),F(I)
1040.     TOL=0.0
1050.     IA=N
1060.     IAINV=N
1070.     BBB=1.
1080.     DO 50 K=1,N
1090.     DO 60 J=1,N
1100.     DO 30 I=1,M
1110. 30  Y(J,K)=Y(J,K)+XJAC(I,J)*XJAC(I,K)/BBB
1120.     B(J,K)=Y(J,K)*BBB
1130. 60  CONTINUE
1140. 50  CONTINUE
1150.     WRITE(6,410)
1160. 410  FORMAT(/9X,'Matrix XJACT*XJAC',40X,'Inverse of XJACT*XJACT')
1170.     DO 70 J=1,N
1180.     DET=B(1,1)*B(2,2)-B(1,2)*B(2,1)
1190.     AINV(1,1)=B(2,2)/DET
1200.     AINV(2,2)=B(1,1)/DET
1210.     AINV(1,2)=-B(2,1)/DET
1220.     AINV(2,1)=-B(1,2)/DET
1230. 250  FORMAT(5X,E15.6,5X,E15.6,20X,E15.6,5X,E15.6)
1240. 70  WRITE(6,250) B(J,1),B(J,2),AINV(J,1),AINV(J,2)
1250.     SS=(SSQ/FLOAT(M-N))**(0.5)
1260.     DO 80 I=1,N
1270.     DX(I)=AINV(I,I)**(0.5)*SS
1280. 80  DXPROB(I)=2.086*DX(I)

```

```

1290.      ZU1=X(1)-DXPROB(1)
1300.      ZU2=X(1)+DXPROB(1)
1310.      ZU3=X(1)-2.4231*DX(1)
1320.      ZU4=X(1)+2.4231*DX(1)
1330.      Z1=X(2)-DXPROB(2)
1340.      Z2=X(2)+DXPROB(2)
1350.      Z3=X(2)-2.4231*DX(2)
1360.      Z4=X(2)+2.4231*DX(2)
1370.      WRITE(6,430) DX(1),DX(2),ZU1,ZU2,Z1,Z2,
1380.      & ZU3,ZU4,Z3,Z4
1390. 430  FORMAT(//5X,'SE(mu)=' ,F12.3,5X,'SE(m)=' ,F11.7, /5X,
1400.      & '95% confidence interval of mu: [' ,F7.1,' , ',F7.1,']' ,5X,
1410.      & '95% confidence interval of m: [' ,F7.5,' , ',F7.5,']' , /5X,
1420.      & '95% Bonferroni joint confidence interval of mu: [' ,F7.1,' , ',
1430.      & F7.1,']' ,5X,'of m: [' ,F7.5,' , ',F7.5,']')
1440.      WRITE(6,130)
1450. 130  FORMAT(//8X,'P:' ,12X,'b:' ,12X,'bb:' ,12X,'er1%:' ,8X,'Ln(P):' ,
1460.      & 8X,'Ln(b):' ,8X,'Ln(bb):' ,7X,'er2%:')
1470.      DO 110 I=1,M
1480.      AA(I)=((1.+X(2))*P(I)/X(1))*((1./(1.+X(2))))/2.
1490.      PLN(I)=ALOG(P(I))
1500.      ALN(I)=ALOG(A(I))
1510.      ZZZ=P(I)*(1.+X(2))/X(1)
1520.      AALN(I)=ALOG(ZZZ)/(1.+X(2))-ALOG(2.)
1530.      ER2=-100.*(ALN(I)-AALN(I))/ALN(I)
1540.      ER1=100.*(A(I)-AA(I))/A(I)
1550.      WRITE(09,*)P(I),A(I),AA(I),PLN(I),ALN(I),AALN(I)
1560. 110  WRITE(6,500) P(I),A(I),AA(I),ER1,PLN(I),ALN(I),AALN(I),ER2
1570. 500  FORMAT(5X,8(E10.4,4X))
1580.      STOP
1590.      END
1600. C
1610. C      Evaluate the objective function
1620.      SUBROUTINE OBJFUN(X,M,N,OBJ)
1630.      DIMENSION AA(22),X(N),OBJ(M)
1640.      COMMON/C1/A(22),P(22)/C2/B1,B2
1650.      X(1)=X(1)/B1
1660.      X(2)=X(2)/B2
1670.      OBJJ=0.0
1680.      DO 10 I=1,22
1690.      AA(I)=((1.+X(2))*P(I)/X(1))*((1./(1.+X(2))))/2.
1700.      OBJ(I)=A(I)-AA(I)
1710. 10  OBJJ=OBJJ+OBJ(I)**2
1720.      WRITE(6,*) X,OBJJ
1730.      X(1)=X(1)*B1
1740.      X(2)=X(2)*B2
1750.      RETURN
1760.      END
1770. /*
1780. //GO.FT09F001 DD DSN=QSUN.PA,DISP=OLD

```

```

10. // JOB ',,T=15',CLASS=A
20. // EXEC PASSWORD
30. //SYSIN DD *
40. QSUN.ICE26 DAVID
50. // EXEC FORTXCLG,OPT=2,SIZE=512K
60. //FORT.SYSIN DD *
70. C      Program name---ALPHA1, Estimate alpha1 by fitting r(t)
80. C      -----
90.      DIMENSION XJAC(100,3),XJTJ(20),WORK(200),F(100)
100.     COMMON/C8/T(1000),R(1000)/C25/TI(10),PI(10)/C16/NN,L,I0,LI,LRR
110. C      NN---NUMBER OF PRESSURES IN MULTISTAGE TEST
120. C      L---TOTAL NUMBER OF TIME NODES
130. C      I0---BEGAINING POINT IN EXPERIMENTAL DATA FOR ANALYSIS
140. C      LI---NUMBER OF POINTS USED FOR OBJECTIVE FUNCTION
150. C      LRR---TERMINATING TIME OF PREDICTION TT=LRR**2*0.01/2. MIMUTES
160. C      T---ARRAY OF TIME NODES IN EXPERIMENT
170. C      R---ARRAY OF RADIUS FROM EXPERIMENT
180. C      TI & PI ARE ILLUSTRATED BY THE FORMULA:
190. C      PRESSURE ON CAVITY P=PI(I) WHEN TI(I-1)<T<TI(I),WHERE TI(0)=0.
200.     WRITE(6,100)
210.     100 FORMAT(/5X,'This program is used to evaluate alpha1 when ',
220.     + 'mu & m are fixed and compare predicted radius with radius ',
230.     + /5X,'from pressuremeter test for Model 1  TEST#3',//)
240.     NN=1
250.     L=185
260.     I0=5
270.     LI=30
280.     FCT1=2.064
290.     NP=1
300.     LRR=1200
310.     DO 14 I=1,L
320.     14 READ(01,*) T(I),R(I)
330.     DO 15 I=1,NN
340.     READ(02,*) TI(I),PI(I)
350.     TII=TI(I-1)+1.
360.     15 WRITE(6,120) TII,TI(I),PI(I)
370.     120 FORMAT(5X,'When time is from',F8.0,' MIN to',F8.0,
380.     + 'MIN the pressure on cavity=',F5.0,' KPA in the experiment')
390.     NW=5*NP+2*LI+(NP+1)*NP/2
400.     NXJ=(NP+1)*NP/2
410.     CALL ICE(FCT1,NW,NXJ,NP,XJAC,XJTJ,WORK,F)
420.     STOP
430.     END
440. C
450. C      THIS SUBROUTINE IS USED TO ESTIMATE ALPHA1 WHEN M,MU ARE FIXED,
460. C      COMPARE THE PREDICT RADIUS WITH RADIUS FROM PRESSUREMETER TEST
470. C      SUBROUTINE ICE(FAC,NW,NXJ,NP,XJAC,XJTJ,WORK,F)
480. C      EXTERNAL OBJFUN
490. C      DIMENSION PARM(4),XJAC(LI,NP),XJTJ(NXJ),WORK(NW),F(LI)
500. C      + ,TT(1200),RR(1200),DDR(1200),X(1),
510. C      + DR(1000),ALPHA(1000)
520. C      COMMON/C1/T0,R0,DR0/C6/L0,LR/C10/XX(3)/C16/NN,L,I0,LI,LRR
530. C      + /C25/TTI(10),PI(10)/C8/T(1000),R(1000)/C12/B1,B2,B3
540. C      FOLLOWING CALL IS TO FIND R(T0),DR(T0)/DT
550. C      CALL INITIL(80,T,R,I0,14,3,T0,R0,DR0)
560.     DO 111 K=1,L
570.     IF (T(K).GE.T0) GO TO 115
580.     111 CONTINUE
590.     115 T0=T(K)
600.     L0=K
610.     LR=L0+LI-1
620.     TL=T(LR)
630.     XX(1)=9114.
640.     XX(2)=0.1E+10

```

```

650.      XX(3)=-0.7111
660.      B1=1.
670.      B2=1.
680.      B3=1.
690.      WRITE(6,106) T0,TL,LI,R0,DR0,XX,B1,B2,B3
700. 106  FORMAT(/5X,16HInitial time t0=,
710.      + F10.3,5X,20HTerminating time t1=,F6.1,5X,'LI,number of points',
720.      + ' for fitting=',I2,/5X,'Initial radius r0=',
730.      + F8.4,5X,'Initial velocity of r,dr(t0)/dt=',E11.4,/5X,
740.      + 'Initial parameters in iteration x=',3E13.5,/5X,
750.      + 'where X1,X2,X3---',
760.      + 'mu,alpha1,m',/5X,'Multipliers for x, b1,b2,b3=',
770.      + E11.3,,3X,E11.3,3X,E11.3,/11X)
780.      XX(1)=XX(1)*B1
790.      XX(2)=XX(2)*B2
800.      XX(3)=XX(3)*B3
810.      X(1)=XX(2)
820.      N=1
830.      NSIG=3
840.      MAXFN=500
850.      M=LI
860.      IXJAC=M
870.      EPS=0.1E-4
880.      DELTA=0.1E-10
890.      IOPT=2
900.      PARM(1)=0.01
910.      PARM(2)=2.0
920.      PARM(3)=1200.
930.      PARM(4)=0.001
940.      WRITE(6,170) NSIG,EPS,DELTA,IOPT,PARM
950. 170  FORMAT(/5X,'Given parameters in subroutine ZXSSQ:',
960.      & ' NSIG=',I1,3X,'EPS=',E7.1,3X,'DELTA=',E7.1,/5X,
970.      & ' IOPT=',I1,3X,'PARM(1)=' ,4(F12.4,3X))
980.      WRITE(6,118)
990. 118  FORMAT(/2X,' mu:',14X,'alpha1:',11X,'m:',14X,
1000.     + 'Objfun: in iteration')
1010. C   FOLLOWING CALL IS FOR ITERATION IN OPTIMIZATION
1020.     CALL ZXSSQ(OBJFUN,M,N,NSIG,EPS,DELTA,MAXFN,IOPT,
1030.     + PARM,X,SSQ,F,XJAC,IXJAC,XJTJ,WORK,INFER,IER)
1040.     WRITE(6,190) INFER,IER
1050. 190  FORMAT(/5X,'Convergence criterion INFER=',I1,
1060.     & 5X,'error parameter IER=',I3)
1070.     XX(2)=X(1)
1080.     XX(1)=XX(1)/B1
1090.     XX(2)=XX(2)/B2
1100.     XX(3)=XX(3)/B3
1110.     WRITE(6,117) XX(1),XX(2),XX(3),SSQ
1120. 117  FORMAT(/5X,'After iteration,the material moduli mu=',
1130.     + F8.1,3X,'alpha1=',E10.4,3X,'m=',F10.6,3X,'Objfun=',E10.4,
1140.     + /5X)
1150.     WRITE(6,222)
1160. 222  FORMAT(/5X,'The first five elements of array WORK:')
1170.     WRITE(6,*) WORK(1),WORK(2),WORK(3),WORK(4),WORK(5)
1180.     WRITE(6,210)
1190. 210  FORMAT(/5X,'XJAC',15X,'Residuals:')
1200.     DO 30 I=1,LI
1210.         XJAC(I,1)=XJAC(I,1)*B2
1220.         SU=SU+XJAC(I,1)**2
1230.         WRITE(6,*) XJAC(I,1),F(I)
1240. 30    CONTINUE
1250.         SUINV=1./SU
1260.         DA=(SSQ*SUINV/FLOAT(LI-1))**(0.5)
1270.         PDA=FAC*DA
1280.         WRITE(6,230) SU,SUINV,DA,PDA

```

```

1290. 230  FORMAT(/5X,'XJAC+2=',E10.4,5X,'XJAC-2=',E10.4,5X,
1300.  + 'Standard error=',E10.4,5X,'Probability error=',E10.4)
1310.  DA1=XX(2)-DA
1320.  DA2=XX(2)+DA
1330.  PDA1=XX(2)-PDA
1340.  PDA2=XX(2)+PDA
1350.  WRITE(6,355) DA1,DA2,PDA1,PDA2,FAC
1360. 355  FORMAT(/5X,'Standard rang of alpha1:',E10.4,3X,E10.4,5X,
1370.  & 'probability rang of alpha1:',E10.4,3X,E10.4,
1380.  & /5X,'Probability factor=',F10.3,/)
1390. C    COMPARING THE EXPERIMENTAL AND PREDICTED CREEP
1400.  WRITE(6,108)
1410. 108  FORMAT(/5X,10HNOTATIONS:,/5X,8Ht---Time,5X,
1420.  + 'r---Experimental radius',5X,'rr---Predicted radius',/5X,
1430.  + 'alpha---drr/dt/rr',5X,'error---100*(r-rr)/(r-r0)',
1440.  + /5X,'Residual=r(i)-rr(i)  Objfun=sum of residuals',
1450.  + /./4X,2Ht:,7X,2Hr:,13X,3Hrr:,12X,
1460.  + 7Hdrr/dt:,11X,6Halpha:,11X,'error:%')
1470.  CALL RNUM(LRR,XX,TT,RR,DDR)
1480.  L01=L0+1
1490.  DO 20 I=L01,L
1500.  TI=T(I)
1510.  CALL LAG(TT,RR,LRR,TI,Y1)
1520.  CALL LAG(TT,DDR,LRR,TI,Y2)
1530.  YY=Y2/Y1
1540.  ER1=100.*(R(I)-Y1)/(R(I)-R0)
1550.  WRITE(04,*) T(I),YY
1560. 109  FORMAT(F10.3,3X,E12.6,3X,E12.6,3X,E12.6,3X,
1570.  + 3X,E12.6,3X,F8.4)
1580. 20  WRITE(6,109) T(I),R(I),Y1,Y2,YY,ER1
1590.  WRITE(6,200) TT(LRR)
1600. 200 FORMAT(/5X,'TERMINATING TIME OF PREDICTION',F10.2)
1610.  RETURN
1620.  END
1630. C
1640. C
1650. C    To calculate numerical solution of a set of diff. eqs by
1660. C    Runge-Kutta method
1670.  SUBROUTINE CMLAMB(N,H,L,Y,DY,YC,YK,XX)
1680.  DIMENSION Y(N),DY(N),YC(N),YK(5,N),B(4),A(4,4),XX(3)
1690.  DATA B/0.11979166666,0.0,0.6510416666,0.0/,A/0.3333333333,
1700.  + 0.16,0.25,0.0740740740,0.0,0.24,-3.0,1.1111111111,0.0,
1710.  + 0.0,3.75,-0.6172839506,0.0,0.0,0.0,0.098765432/
1720.  IF(L) 12,10,12
1730. 10  DO 1 I=1,N
1740. 1  YK(5,I)=Y(I)
1750.  CALL DIFUN(N,Y,DY,XX)
1760.  RETURN
1770. 12  DO 3 K=1,4
1780.  DO 2 I=1,N
1790.  YK(K,I)=DY(I)
1800.  YC(I)=YK(5,I)+H*(A(K,1)*YK(1,I)+A(K,2)*YK(2,I)+
1810.  + A(K,3)*YK(3,I)+A(K,4)*YK(4,I))
1820. 2  Y(I)=Y(I)+H*B(K)*YK(K,I)
1830. 3  CALL DIFUN(N,YC,DY,XX)
1840.  DO 7 I=1,N
1850.  YC(I)=YK(5,I)+H*(0.08*YK(1,I)+0.48*YK(2,I)+
1860.  + 0.1333333333*YK(3,I)+0.1066666666666666*YK(4,I))
1870. 7  Y(I)=Y(I)-H*0.421875*DY(I)
1880.  CALL DIFUN(N,YC,DY,XX)
1890.  DO 8 I=1,N
1900. 8  Y(I)=Y(I)+H*0.6510416666*DY(I)
1910.  GO TO 10
1920.  END

```

```

1930. C
1940. C      To calculate function on right side of a set of diff. eqs.
1950.      SUBROUTINE DIFUN(N,Y,DY,X)
1960.      DIMENSION Y(N),DY(N),X(3)
1970.      COMMON/C25/TI(10),PI(10)
1980.      DO 60 I=1,10
1990.      IF (Y(1).LT.TI(I)) GO TO 70
2000.      GO TO 60
2010.      70 P=PI(I)
2020.      GO TO 100
2030.      60 CONTINUE
2040.      100 DY(1)=1.
2050.      DY(2)=Y(3)
2060.      YY=(Y(3)/Y(2))*2
2070.      DY(3)=Y(2)*0.5*(P-X(1)*YY*(1.+X(3))/(1.+X(3)))/X(2)
2080.      RETURN
2090.      END
2100. C
2110. C      To calculate numerical solution R,DR/DT
2120.      SUBROUTINE RNUM(K,XX,TT,RR,DDR)
2130.      DIMENSION XX(3),Y(3),DY(3),YC(3),YK(5,3),TT(K),RR(K),DDR(K)
2140.      COMMON/C1/T0,R0,DRO
2150.      Y(1)=T0
2160.      Y(2)=R0
2170.      Y(3)=DRO
2180.      CALL CMLAMB(3,0.001,0,Y,DY,YC,YK;XX)
2190.      TT(1)=T0
2200.      RR(1)=R0
2210.      DDR(1)=DRO
2220.      DO 10 I=2,K
2230.      H=0.01*FLOAT(I)
2240.      CALL CMLAMB(3,H,1,Y,DY,YC,YK,XX)
2250.      TT(I)=Y(1)
2260.      RR(I)=Y(2)
2270.      10 DDR(I)=Y(3)
2280.      RETURN
2290.      END
2300. C
2310. C
2320. C      Lagrange's interpolation for variable distance by three points
2330.      SUBROUTINE LAG(X0,Y0,N,X,Y)
2340.      DIMENSION X0(N),Y0(N)
2350.      I=1
2360.      10 IF(X.LT.0.5*(X0(I+1)+X0(I+2))) GO TO 30
2370.      IF(X.GE.0.5*(X0(N-2)+X0(N-1))) GO TO 20
2380.      I=I+1
2390.      GO TO 10
2400.      20 I=N-2
2410.      30 M=I+2
2420.      Y=0.0
2430.      DO 60 J=I,M
2440.      P=1.0
2450.      DO 50 K=I,M
2460.      IF(J-K) 40,50,40
2470.      40 P=P*(X-X0(K))/(X0(J)-X0(K))
2480.      50 CONTINUE
2490.      60 Y=Y+P*Y0(J)
2500.      RETURN
2510.      END
2520. C
2530. C      Fitting experimental data to find R,DR/DT at some time t. Befor
2540. C      fitting, some points with repeat value are taken off according
2550. C      certain rule.
2560.      SUBROUTINE INITIL(NN,T,R,IO,N,M,T0,R0,DRO)

```

```

2570.      DIMENSION T(NN),R(NN),RR(100),TT(100),AA(30,30),B(30)
2580. C    NN---NUMBER OF POINTS TAKEN FROM DATA FOR TREATMENT
2590. C    T---TIME NODES
2600. C    R---EXPERIMENTAL RADIUS AT T
2610. C    I0---FIRST POINT OF TREATMENT
2620. C    N---NUMBER OF POINTS FOR FITTING
2630. C    M-1---POWER OF POLYNOMIAL FOR FITTING
2640. C    T0---AT THIS TIME,R & DR/DT ARE CALCULATED
2650. C    R0---RADIUS AT TIME T0
2660. C    DR0--- VELOCITY DR/DT AT T0
2670. C    K---ORDERTH OF T0 IN TT
2680. C    TT---TIME NODES AFTER TREATMENT
2690.      KK=1
2700.      J=1
2710.      RR(1)=R(I0)
2720.      TT(1)=T(I0)
2730.      NNN=NN-1
2740.      DO 10 I=I0,NNN
2750.      IF (R(I+1).GT.R(I)) GO TO 20
2760.      KK=KK+1
2770.      GO TO 10
2780. 20    J=J+1
2790.      RR(J)=R(I+1)
2800.      TT(J)=T(I+1)
2810.      IF (KK.GT.1.AND.I.GE.I0+1) TT(J-1)=(T(I)+T(I-KK+1))/2.0
2820.      KK=1
2830. 10    CONTINUE
2840.      DO 40 K=1,N
2850.      IF (K.GT.3.AND.FLOAT(INT(TT(K))).EQ.TT(K)) GO TO 50
2860. 40    CONTINUE
2870. 50    T0=TT(K)
2880. C    FOLLOWING CALL IS TO FIT EXPERIMENTAL POINTS
2890.      CALL MXCVFT(N,TT,RR,M,B,AA,K,T0,R0,DR0)
2900.      RETURN
2910.      END
2920. C
2930. C    Least-squares fitting
2940.      SUBROUTINE MXCVFT(M,X,Y,N,B,AA,K,T0,R0,DR0)
2950.      DIMENSION X(M),Y(M),B(N),AA(N,N),R(50),DR(50)
2960.      DO 10 I=1,N
2970.      B(I)=0.0
2980.      DO 20 J=1,M
2990. 20    B(I)=B(I)+Y(J)*X(J)**(I-1)
3000.      DO 30 L=1,N
3010.      AA(I,L)=0.0
3020.      DO 40 J=1,M
3030. 40    AA(I,L)=AA(I,L)+X(J)**(L+I-2)
3040. 30    CONTINUE
3050. 10    CONTINUE
3060.      CALL GAUSS(N,AA,B,1.E-10,ISW)
3070.      DO 50 I=1,M
3080.      R(I)=0.0
3090.      DR(I)=0.0
3100.      DO 60 J=1,N
3110. 60    R(I)=R(I)+B(J)*(X(I)**(J-1))
3120.      DO 70 J=2,N
3130. 70    DR(I)=DR(I)+B(J)*(X(I)**(J-2))*FLOAT(J-1)
3140.      EE=(Y(I)-R(I))/(Y(I)-Y(1)+0.1)
3150. 50    CONTINUE
3160.      T0=X(K)
3170.      R0=R(K)
3180.      DR0=DR(K)
3190.      RETURN
3200.      END

```

```

3210. C
3220. C      To calculate solution of a system of linear algebra eqs.
3230.      SUBROUTINE GAUSS(N,A,B,EPS,ISW)
3240.      DIMENSION A(N,N),B(N)
3250.      NM1=N-1
3260.      DO 10 K=1,NM1
3270.      C=0.0
3280.      DO 2 I=K,N
3290.      IF (ABS(A(I,K)) .LE.ABS(C)) GO TO 2
3300.      C=A(I,K)
3310.      I0=I
3320.      2 CONTINUE
3330.      IF (ABS(C).GE.EPS) GO TO 3
3340.      ISW=0
3350.      GO TO 100
3360.      3 IF (I0.EQ.K) GO TO 6
3370.      DO 4 J=K,N
3380.      T=A(K,J)
3390.      A(K,J)=A(I0,J)
3400.      4 A(I0,J)=T
3410.      T=B(K)
3420.      B(K)=B(I0)
3430.      B(I0)=T
3440.      6 KP1=K+1
3450.      C=1.0/C
3460.      B(K)=B(K)*C
3470.      DO 10 J=KP1,N
3480.      A(K,J)=A(K,J)*C
3490.      DO 20 I=KP1,N
3500.      20 A(I,J)=A(I,J)-A(I,K)*A(K,J)
3510.      10 B(J)=B(J)-A(J,K)*B(K)
3520.      B(N)=B(N)/A(N,N)
3530.      DO 40 K=1,NM1
3540.      I=N-K
3550.      C=0.0
3560.      IP1=I+1
3570.      DO 50 J=IP1,N
3580.      50 C=C+A(I,J)*B(J)
3590.      40 B(I)=B(I)-C
3600.      ISW=1
3610.      100 RETURN
3620.      END
3630. C
3640. C      Calculate the value of objective function
3650.      SUBROUTINE OBJFUN(X,M,N,RX)
3660.      DIMENSION X(N),RX(M),TT(300),RR(300),DDR(300)
3670.      COMMON/C6/L0,LR/C10/XX(3)
3680.      + /C8/T(1000),R(1000)/C12/B1,B2,B3
3690.      XX(2)=X(1)
3700.      XX(1)=XX(1)/B1
3710.      XX(2)=XX(2)/B2
3720.      XX(3)=XX(3)/B3
3730.      CALL RNUM(300,XX,TT,RR,DDR)
3740.      RXR=0.0
3750.      DO 10 I=L0,LR
3760.      TI=T(I)
3770.      CALL LAG(TT,RR,300,TI,Y1)
3780.      RX(I-L0+1)=(R(I)-Y1)
3790.      10 RXR=RXR+RX(I-L0+1)**2
3800.      WRITE(6,*) XX,RXR
3810.      XX(1)=XX(1)*B1
3820.      XX(2)=XX(2)*B2
3830.      XX(3)=XX(3)*B3
3840.      RETURN

```

3850.            END  
3860.    /\*  
3870.    ///GO.FT01F001 DD DSN=QSUN.ICE26,DISP=OLD  
3880.    ///GO.FT02F001 DD DSN=QSUN.TIPI6,DISP=OLD  
3890.    ///GO.FT04F001 DD DSN=QSUN.ICE6,DISP=OLD

```

10. // JOB ',,T=15',CLASS=A
20. // EXEC FORTXCLG,OPT=2,SIZE=512K
30. // FORT.SYSIN DD *
40. C FIND VALUES OF MATERIAL PARAMETERS BASED ON DATA FORM TRIAXIAL
50. C TESTS OF ICE
60. C Program---X31, Estimate mu,alpha1 by fitting r(t) MODEL 1
70. C -----
80. C when m=-2/3 is fixed.
90. C EXTERNAL OBJFUN
100. DIMENSION W(9),PARM(4),XJAC(17,2),XJTJ(6),X(2),
110. & WORK(47),F(17),DDA(1000),D(2),PD(2),AINV(2,2),Y(2,2),YY(2,2)
120. DIMENSION TT(1000),AA(1000),S(4,50),WX(17),WY(17),B(5),C(5,5)
130. COMMON/C1/T0,A0,DA0/C2/LI,LRR/C3/P/CB/T(50),A(50)/C12/B1,B2,B3
140. & /C5/X3
150. K=4
160. LI=17
170. LR=23
180. FCT1=2.131
190. FCT2=2.490
200. LRR=700
210. DO 10 I=1,37
220. READ(13,*) T(I),S(1,I),S(2,I),S(3,I),S(4,I)
230. 10 A(I)=1.-S(K,I)/100.
240. P=S(K,37)
250. N=12
260. DO 20 I=1,N
270. WX(I)=T(I)
280. 20 WY(I)=A(I)
290. CALL MXCVFT(N,WX,WY,4,B,C,1,T0,A0,DA0)
300. WRITE(6,500)
310. 500 FORMAT(//5X,'Compute the values of material parameters based',
320. & ' on the data from the triaxial tests of polycrystalline ice',
330. & /5X,'when m=-.71 is fixed. MODEL 1 TEST#4')
340. WRITE(6,510) S(K,35),S(K,36),S(K,37),T(1),T(LR),A(1),DA0,LI
350. 510 FORMAT(//5X,'Experimental temperature T=',F5.1,'C, Homogen',
360. & 'eous pressure v=',F8.0,'KPa, Axial stress sigma=',F6.0,'KPa',
370. & /5X,'Initial time t0=',F5.1,' day, Terminate time t1=',F5.1,
380. & ' day',/5X,'Initial stretch a(t0)=',F10.5,
390. & ' Initial stretching da(t0)/dt=',F10.6,' 1/day',
400. & /5X,'Number of points for fitting=',I2)
410. X(1)=2000.
420. X(2)=2.E+5
430. X3=-.71
440. B1=1.
450. B2=1.
460. B3=1.
470. WRITE(6,520) X,B1,B2
480. 520 FORMAT(//5X,'Initial values of material parameters X=',2E15.5,
490. & /5X,'where x1,x2---mu,alpha1',/5X,'Multipliers for X B1,',
500. & 'B2=',2E11.3)
510. N=2
520. NSIG=3
530. MAXFN=500
540. M=LI
550. IXJAC=M
560. EPS=0.1E-8
570. DELTA=0.1E-8
580. IOPT=2
590. PARM(1)=0.0001
600. PARM(2)=1.5
610. PARM(3)=120.
620. PARM(4)=1.E-7
630. WRITE(6,170) NSIG,EPS,DELTA,IOPT,PARM
640. 170 FORMAT(/5X,'Given parameters in subroutine ZXSSQ:',

```

```

650.      & ' NISG=',I1,3X,'EPS=',E7.1,3X,'DELTA=',E7.1,/5X,
660.      & ' IOPT=',I1,3X,' PARM(1)=' ,4(E10.4,3X))
670.      WRITE(6,118)
680.      118  FORMAT(/5X,' MU:',14X,'ALPHA1:',8X,
690.      + 'OBJECTIVE FUNCTION F: IN ITERATION')
700. C      FOLLOWING CALL IS FOR ITERATION IN OPTIMIZATION
710.      CALL ZXSSQ(OBJFUN,M,N,NSIG,EPS,DELTA,MAXFN,IOPT,
720.      + PARM,X,SSQ,F,XJAC,IXJAC,XJTJ,WORK,INFER,IER)
730.      WRITE(6,190) INFER,IER
740.      190  FORMAT(/5X,'Convergence criterion INFER=',I1,
750.      & 5X,'error parameter IER=',I3)
760.      WRITE(6,117) X(1),X(2),SSQ
770.      117  FORMAT(/5X,'After iteration,the material moduli mu=',
780.      + E10.4,3X,'alpha1=',E10.4,3X,'Objfun=',E10.4)
790.      WRITE(6,222)
800.      222  FORMAT(/5X,'The first five elements of array WORK:')
810.      WRITE(6,*) WORK(1),WORK(2),WORK(3),WORK(4),WORK(5)
820.      WRITE(6,210)
830.      210  FORMAT(/5X,'XJAC,Gradient of Residuals w.r.t. X',18X,'Residuals
840.      DO 60 I=1,L1
850.      WRITE(6,260) XJAC(I,1),XJAC(I,2),F(I)
860.      XJAC(I,1)=XJAC(I,1)*B1
870.      XJAC(I,2)=XJAC(I,2)*B2
880.      60   XJAC(I,2)=XJAC(I,2)*B2
890.      260  FORMAT(5X,2(E11.4,5X),20X,E10.4)
900.      DO 30 I=1,N
910.      DO 40 J=1,N
920.      DO 50 II=1,L1
930.      50   Y(I,J)=Y(I,J)+XJAC(II,I)*XJAC(II,J)
940.      40   YY(I,J)=Y(I,J)
950.      30   CONTINUE
960.      TOL=0.0
970.      IA=N
980.      IAINV=N
990.      CALL GJ(Y,SSS,N,EP)
1000.     WRITE(6,270)
1010.     270  FORMAT(/5X,'Matrix XJACT*XJAC',20X,'Inverse of XJACT*XJAC')
1020.     DO 80 I=1,N
1030.     80   WRITE(6,280) YY(I,1),YY(I,2),Y(I,1),Y(I,2)
1040.     280  FORMAT(5X,2(E10.4,3X),10X,2(E10.4,3X))
1050.     DO 90 I=1,N
1060.     D(I)=(SSQ*Y(I,1)/FLOAT(L1-2))**(0.5)
1070.     90   PD(I)=2.046*D(I)
1080.     G11=X(1)-FCT1*D(1)
1090.     G12=X(1)+FCT1*D(1)
1100.     G21=X(2)-FCT1*D(2)
1110.     G22=X(2)+FCT1*D(2)
1120.     H11=X(1)-FCT2*D(1)
1130.     H12=X(1)+FCT2*D(1)
1140.     H21=X(2)-FCT2*D(2)
1150.     H22=X(2)+FCT2*D(2)
1160.     WRITE(6,290) D(1),D(2),G11,G12,G21,G22,H11,H12,H21,
1170.     & H22,FCT1,FCT2
1180.     290  FORMAT(/5X,'SE(mu)=' ,E10.4,5X,'SE(alpha1)=' ,E10.4,5X,
1190.     & /5X,'95% confidence interval of mu: [' ,
1200.     & E10.4,' , ' ,E10.4,']',/5X,'of alpha1: [' ,E10.4,' , ' ,E10.4,']',
1210.     & 5X,/5X,'Bonferroni confidence'
1220.     & ' interval of mu: [' ,E10.4,' , ' ,E10.4,']',/5X,'of alpha1: [' ,
1230.     & E10.4,' , ' ,E10.4,']',/5X,
1240.     & '95% factor=' ,F6.3,5X,'Bonferroni factor=' ,F6.3)
1250.     WRITE(6,570)
1260.     570  FORMAT(/5X,'NOTATION:      a---Experimental value of l(t)/L',
1270.     & ' aa---Predicted value of l(t)/L',',      Error---100*(a-aa)/a')
1280.     CALL RNUM(LRR,X,TT,AA,DDA)

```

```

1290.      WRITE(6,540)
1300. 540  FORMAT(//6X,'Time (Day):',8X,'a:',15X,'aa:',13X,'daa/dt:',
1310.      & '(1/day):',5X,'daa/dt/aa (1/day):',6X,'Error (%):')
1320.      DO 44 I=1,LR
1330.      TI=T(I)
1340.      CALL LAG(TT,AA,LRR,TI,Y1)
1350.      CALL LAG(TT,DDA,LRR,TI,Y2)
1360.      ZZ=Y2/Y1
1370.      C1=1-A(I)
1380.      C2=1-Y1
1390.      WRITE(09,*) T(I),C1,C2
1400.      ER=100.*(A(I)-Y1)/A(I)
1410.      WRITE(6,560) T(I),A(I),Y1,Y2,ZZ,ER
1420. 560  FORMAT(10X,F5.1,5X,F10.5,8X,F10.5,10X,F10.7,10X,F10.7,12X,F10.5
1430.      44  CONTINUE
1440.      STOP
1450.      END
1460. C
1470. C
1480. C      To calculate numerical solution of set of diff. eqs.
1490.      SUBROUTINE CMLAMB(N,H,L,Y,DY,YC,YK,XX)
1500.      DIMENSION Y(N),DY(N),YC(N),YK(5,N),B(4),A(4,4),XX(3)
1510.      DATA B/0.11979166666,0.0,0.6510416666,0.0/,A/0.3333333333,
1520.      + 0.16,0.25,0.0740740740,0.0,0.24,-3.0,1.1111111111,0.0,
1530.      + 0.0,3.75,-0.6172839506,0.0,0.0,0.0,0.098765432/
1540.      IF(L) 12,10,12
1550.      10  DO 1 I=1,N
1560.      1   YK(5,I)=Y(I)
1570.      CALL DIFUN(N,Y,DY,XX)
1580.      RETURN
1590.      12  DO 3 K=1,4
1600.      DO 2 I=1,N
1610.      YK(K,I)=DY(I)
1620.      YC(I)=YK(5,I)+H*(A(K,1)*YK(1,I)+A(K,2)*YK(2,I)+
1630.      + A(K,3)*YK(3,I)+A(K,4)*YK(4,I))
1640.      2   Y(I)=Y(I)+H*B(K)*YK(K,I)
1650.      3   CALL DIFUN(N,YC,DY,XX)
1660.      DO 7 I=1,N
1670.      YC(I)=YK(5,I)+H*(0.08*YK(1,I)+0.48*YK(2,I)+
1680.      + 0.1333333333*YK(3,I)+0.1066666666*YK(4,I))
1690.      7   Y(I)=Y(I)-H*0.421875*DY(I)
1700.      CALL DIFUN(N,YC,DY,XX)
1710.      DO 8 I=1,N
1720.      8   Y(I)=Y(I)+H*0.6510416666*DY(I)
1730.      GO TO 10
1740.      END
1750. C
1760. C      To calculate function on right side of a set of diff. eqs.
1770.      SUBROUTINE DIFUN(N,Y,DY,X)
1780.      DIMENSION Y(N),DY(N),X(2)
1790.      COMMON/C3/P/C5/X3
1800.      DY(1)=1.
1810.      DY(2)=Y(3)
1820.      YY=-Y(3)/Y(2)
1830.      DY(3)=Y(2)*((P/3.+3.*(X3/2.)*X(1)*YY*(1.+X3))/X(2)
1840.      & +YY**2)
1850.      RETURN
1860.      END
1870. C
1880. C      To calculate numerical solution R,DR/DT
1890.      SUBROUTINE RNUM(K,XX,TT,RR,DDR)
1900.      DIMENSION XX(3),Y(3),DY(3),YC(3),YK(5,3),TT(K),RR(K),DDR(K)
1910.      COMMON/C1/T0,R0,DR0
1920.      Y(1)=T0

```

```

1930.      Y(2)=R0
1940.      Y(3)=DR0
1950.      CALL CMLAMB(3,0.001,0,Y,DY,YC,YK,XX)
1960.      TT(1)=T0
1970.      RR(1)=R0
1980.      DDR(1)=DR0
1990.      DO 10 I=2,K
2000.      H=0.05
2010.      CALL CMLAMB(3,H,1,Y,DY,YC,YK,XX)
2020. C     WRITE(6,*) Y
2030.      TT(I)=Y(1)
2040.      RR(I)=Y(2)
2050.      10  DDR(I)=Y(3)
2060.      RETURN
2070.      END
2080. C
2090. C
2100. C     Lagrange's interpolation for variable distance by three points
2110.      SUBROUTINE LAG(X0,Y0,N,X,Y)
2120.      DIMENSION X0(N),Y0(N)
2130.      I=1
2140.      10  IF(X.LT.0.5*(X0(I+1)+X0(I+2))) GO TO 30
2150.      IF(X.GE.0.5*(X0(N-2)+X0(N-1))) GO TO 20
2160.      I=I+1
2170.      GO TO 10
2180.      20  I=N-2
2190.      30  M=I+2
2200.      Y=0.0
2210.      DO 60 J=I,M
2220.      P=1.0
2230.      DO 50 K=I,M
2240.      IF(J-K) 40,50,40
2250.      40  P=P*(X-X0(K))/(X0(J)-X0(K))
2260.      50  CONTINUE
2270.      60  Y=Y+P*Y0(J)
2280.      RETURN
2290.      END
2300. C
2310.      SUBROUTINE MXCVFT(M,X,Y,N,B,AA,K,T0,R0,DR0)
2320.      DIMENSION X(M),Y(M),B(N),AA(N,N),R(50),DR(50)
2330.      DO 10 I=1,N
2340.      B(I)=0.0
2350.      DO 20 J=1,M
2360.      20  B(I)=B(I)+Y(J)*X(J)**(I-1)
2370.      DO 30 L=1,N
2380.      AA(I,L)=0.0
2390.      DO 40 J=1,M
2400.      40  AA(I,L)=AA(I,L)+X(J)**(L+I-2)
2410.      30  CONTINUE
2420.      10  CONTINUE
2430.      CALL GAUSS(N,AA,B,1.E-10,ISW)
2440.      DO 50 I=1,M
2450.      R(I)=0.0
2460.      DR(I)=0.0
2470.      DO 60 J=1,N
2480.      60  R(I)=R(I)+B(J)*(X(I)**(J-1))
2490.      DO 70 J=2,N
2500.      70  DR(I)=DR(I)+B(J)*(X(I)**(J-2))*FLOAT(J-1)
2510.      EE=(Y(I)-R(I))/(Y(I)-Y(1)+0.1)
2520.      50  CONTINUE
2530.      T0=X(K)
2540.      R0=R(K)
2550.      DR0=DR(K)
2560.      RETURN

```

```

2570.      END
2580. C
2590. C      Find solution of a system of linear algebra eqs.
2600.      SUBROUTINE GAUSS(N,A,B,EPS,ISW)
2610.      DIMENSION A(N,N),B(N)
2620.      NM1=N-1
2630.      DO 10 K=1,NM1
2640.      C=0.0
2650.      DO 2 I=K,N
2660.      IF (ABS(A(I,K)) .LE.ABS(C)) GO TO 2
2670.      C=A(I,K)
2680.      IO=I
2690.      2 CONTINUE
2700.      IF (ABS(C).GE.EPS) GO TO 3
2710.      ISW=0
2720.      GO TO 100
2730.      3 IF (IO.EQ.K) GO TO 6
2740.      DO 4 J=K,N
2750.      T=A(K,J)
2760.      A(K,J)=A(IO,J)
2770.      4 A(IO,J)=T
2780.      T=B(K)
2790.      B(K)=B(IO)
2800.      B(IO)=T
2810.      6 KP1=K+1
2820.      C=1.0/C
2830.      B(K)=B(K)*C
2840.      DO 10 J=KP1,N
2850.      A(K,J)=A(K,J)*C
2860.      DO 20 I=KP1,N
2870.      A(I,J)=A(I,J)-A(I,K)*A(K,J)
2880.      10 B(J)=B(J)-A(J,K)*B(K)
2890.      B(N)=B(N)/A(N,N)
2900.      DO 40 K=1,NM1
2910.      I=N-K
2920.      C=0.0
2930.      IP1=I+1
2940.      DO 50 J=IP1,N
2950.      50 C=C+A(I,J)*B(J)
2960.      40 B(I)=B(I)-C
2970.      ISW=1
2980.      100 RETURN
2990.      END
3000. C
3010. C      Inverse of symmetric positive definite matrix
3020.      SUBROUTINE GJ(A,B,N,EP)
3030.      DIMENSION A(N,N),B(N)
3040.      EP=1.
3050.      DO 10 K=1,N
3060.      KK=N-K+1
3070.      W=A(1,1)
3080.      IF(W.LE.0.) GO TO 30
3090.      DO 20 I=2,N
3100.      G=A(I,1)
3110.      IF(I-KK) 2,2,3
3120.      3 B(I)=G/W
3130.      GO TO 4
3140.      2 B(I)=-G/W
3150.      4 DO 20 J=2,I
3160.      20 A(I-1,J-1)=A(I,J)+G*B(J)
3170.      A(N,N)=1./W
3180.      DO 10 I=2,N
3190.      10 A(N,I-1)=B(I)
3200.      RETURN

```

```
3210.    30    EP=-EP
3220.        RETURN
3230.        END
3240. C
3250. C      Calculate the value of objective function
3260.        SUBROUTINE OBJFUN(X,M,N,RX)
3270.        DIMENSION X(N),RX(M),TT(1000),AA(1000),DDA(1000)
3280.        COMMON/C2/LI,LRR
3290.        + /CB/T(50),A(50)
3300.        CALL RNUM(LRR,X,TT,AA,DDA)
3310.        RXR=0.0
3320.        DO 10 I=1,LI
3330.        TI=T(I)
3340.        CALL LAG(TT,AA,LRR,TI,Y1)
3350.        RX(I)=A(I)-Y1
3360.    10    RXR=RXR+RX(I)**2
3370.        WRITE(6,*) X,RXR
3380.        RETURN
3390.        END
3400. /*
3410. //GO.FT13F001 DD DSN=QSUN.X3,DISP=OLD
3420. //GO.FT09F001 DD DSN=QSUN.X34,DISP=OLD
```